The School of Biosciences/Physical Sciences

Synthesis of Thiourea and Guanidine Derivatives and Testing for Biological Activity

Samuel Thomas
Masters of Science by Research
January 2019

Abstract:

Thiourea and guanidine derivatives are versatile compounds that have previously been synthesised for use in a variety of industries from materials manufacturing to medical research. It is this versatility which interests us in new possible pathways for these compounds, with the focus being the potential for advanced oncology research. This thesis discusses a single project in two halves, the first synthesising thiourea and guanidine derivatives, whilst the second half looks at the biological activity of those target molecules on three different ovarian cancer cell lines. Once synthesised, the derivative compounds were fully characterised by ^{1}H NMR, ^{13}C NMR, elemental analysis, mass spectrometry and melting point analysis. Four additional compounds were included for biological testing, which comprise of thiourea and guanidine iridium complexes with alternative uses in OLED technology, whose ligand environment may also provide biological activity in mammalian cell cultures. There were no specific biological targets in which we were attempting to challenge but treated this research as a 'fishing trip', to understand how well these thiourea and guanidine derivatives could perform as potential anticancer drugs.

A panel of ovarian cancer cells consisting of adherent cell lines EFO-21 and EFO-27 followed by a suspension cell line (COLO-704) were investigated. Parental and cisplatin resistant sublines of these cells were used to observe effects of the thiourea and guanidine derivatives against cisplatin resistance. These cell lines were then dosed with each derivative from the compound library and their biological activity examined through MTT viability. Cisplatin resistant cell lines were the focus due to the broad extent in which the anticancer drug has been researched, but also due to resistant mechanisms it has produced in human cancer cells.

The investigated compounds showed promising results and displayed notable differences in their effects on reducing the viability of ovarian cancer cell lines, with the data collected potentially providing a start to new therapeutic pathways in the battle against cancer resistant cell lines.

Table of Contents

List of Abbreviations:

ACN - Acetonitrile

CC - Column Chromatography

+CDDP - Cisplatin Resistant

^{13}C NMR - Carbon-13 Nuclear Magnetic Resonance

DCM - Dichloromethane

DF - Dilution Factor

DMF - Dimethylformamide

4-DMAP - 4-(Dimethylamino)pyridine

DMSO - Dimethyl sulfoxide

EA - Elemental Analysis

EI-MS *m/z* - Electron Impact Mass Spectrometry *Mass/Charge Number of Ions*

Equiv - Equivalent

FBS - Fetal Bovine Serum

IC50 - 50% inhibitory concentration of cells

IMDM - Iscove's Modified Dulbecco's Medium

IR - Infrared Spectroscopy

MeOH - Methanol

$MgSO_4$ - Magnesium Sulphate

MP - Melting Point Analysis

MS - Mass Spectrometry

MTT - 3-(4,5-Dimethylthiazol-2-yl)-2,5-diphenyltetrazolium bromide

N_2 - Nitrogen

$NaHCO_3$ - Sodium Bicarbonate

NaOH - Sodium Hydroxide

^{1}H NMR - Proton Nuclear Magnetic Resonance/Hydrogen-1 Nuclear Magnetic Resonance

NMR - Nuclear Magnetic Resonance Spectroscopy

PBS - Phosphate-Buffered Saline

Pen Strep - Antibiotic penicillin 100 IU/ml and Streptomycin 100mg/ml)

PTL - Parental

RF - Retardation Factor

RT - Room Temperature

SDS - Sodium Dodecyl Sulphate

TCDI - 1,1'-Thiocarbonyldiimidazole

TLC – Thin Layer Chromatography

Acknowledgements:

Firstly, I would like to thank SACO AEI Polymers UK for supporting me in funding this research project and all the colleagues who have supported me through the past two years.

I would also like to thank my three supervisors at The University of Kent who have encouraged me with support and words of wisdom throughout my MSc. Dr Barry Blight who gave me the understanding I needed to grasp the complexities of Organic Chemistry and helped to motivate and spark my ideas, Dr Christopher Serpell for his continuing support throughout my final year and Dr Martin Michaelis for introducing me to the wonderful world of MTT assays along with his continuing support throughout my year in The School of Biosciences.

I extend this thanks to all my friends in Lab 310 for their encouragement and laughter, especially Barbora Balonova who went out of her way to teach me the organic chemistry knowledge I had previously lacked. Also, to my friends in Lab 414, especially Hannah Onafuye, Joanna Bird and Evie Rogers for supporting me during many MTT assays, when balancing a full-time research career with a part time research degree proves to be a strenuous task.

Finally, I would like to thank all my family for their unconditional support through all the stress, long days and late nights, with an extra big thank you to my Fiancé Sophie for always having faith in me.

Chapter 1: Introduction

Organic and inorganic chemical synthesis is a fundamental component of the continuing research efforts which tackle the ever-challenging subject of cancer prevention. Evidence of cancer research pre-dates the 20th century with early surgical procedures carried out to remove tumours cell mass in a variety of cancers.[57] Although it was not until the late 20th century when research into cancers bloomed, with the first major discovery in 1975 by Harold Varmus and J. Michael Bishop observing that normal cells are susceptible to alterations resulting in cancer.[55] Since then, oncological technologies have continuously been explored with notable diversity of novel therapeutics and cellular pathways discovered in the first decade of the 21st century.[56] Within these recent advances of novel therapeutics are two organic structures thiourea and guanidine, which have shown promise as potential anticancer agents.

Thiourea, guanidine, and their derivatives are versatile compounds which have previously been synthesised in a variety of industries from materials/textile manufacturing to medical research.[1] In their simplest form thiourea and guanidine are structurally similar as seen in Figure 1 although the properties between the two are significantly different.

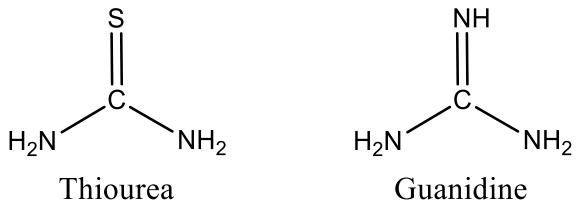

Figure 1. Structures of thiourea and guanidine in their basic form.

The idea for this project sparked from initial research into organic light-emitting diode (OLED) technologies by Dr Barry Blight and Barbora Balonova (The Blight Chemistry Group, University of New Brunswick, Canada), where by derivatives of thiourea and guanidine were synthesised and incorporated into iridium complexes observed in Figure 2.[82] The versatility of these structures spurred this research project to synthesise a variety of thiourea and guanidine derivatives and test them for

biological activity in human ovarian cancer cell lines. There were no specific biological targets in which we were attempting to challenge but treated this research as a 'fishing trip' to understand how well these thiourea and guanidine derivatives could perform as potential anticancer drugs.

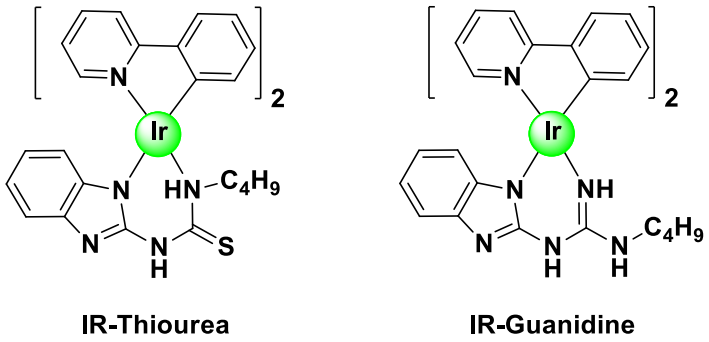

Figure 2. Structures of iridium centred complexes incorporating butyl-thiourea and butyl-guanidine derivatives.

1.1 Thioureas and their applications:

Ureas are widely used amide compounds with its neutral structure observed in Figure 3. While urea plays a role in the regulation of pH balance in humans,[5] the structure has also been synthetically modified into a large array of derivatives for many industrial applications.[2,4] Heavily used in the cosmetics industry, urea aids the rehydration of skin to combat dermatological conditions such as dermatitis in emollient treatments,[2] with derivatives of urea also having successes in the treatment of cancers with positive inhibitory effects observed in rodent and human cancer models.[6] These derivatives of urea include a variety of thiourea and guanidine compounds which will further discussed in this research project.

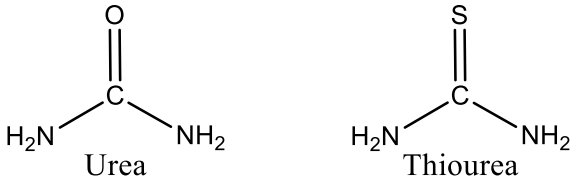

Figure 3. Structures of urea in its neutral form and thiourea.

While our attempts were to synthesis successful thiourea derivatives for ovarian cancer screening, there have been various derivatives of these synthesised with a wide array of targets in mind.[3,4,7,8] These include successes observed in the potency of non-nucleoside inhibitors of HIV-1 reverse transcriptase enzyme with effective doses exhibited in the nanomolar range,[3] but research for thioureas also extends to insecticidal growth regulators,[7] anti-inflammatory drugs,[7] anticancer and antiviral effects,[8] anti-thyroid properties[1] and a more industrial materials application of thioureas being synthesised to aid the ozonolysis of olefin polymers.[4]

Thioureas show promise of being successful anticancer candidates partly due to its sulfur group,[38] with sulfur itself being a versatile and biologically important element to all living organisms.[33] Sulfur has many forms including a variety of oxides and dioxide known for toxicity effects contributing to environmental concerns,[34] but also within biotechnology sulfur has been incorporated into structures which have presented responses when screened for anti-inflammatory effects, and the inhibition of tumour growth.[36] Sulfur is also favoured in a variety of biochemical applications, due to its versatility in the movement of electron pairs, being electrophilic or nucleophilic depending on its stereochemistry.[33,35]

Previous sulfur based compounds for the application of ovarian cancer studies include sulofenur, a diarylsulfonylurea compound which in clinical trials was observed to have modest anticancer activity, against those treated previously with cisplatin.[9] Although anticancer activity was observed, toxicity was also noted with patients suffering from anaemia and irregular liver functions,[10] with similar toxicity alongside resistances observed throughout a variety of clinical trials.[25]

In more recent studies, non-metal containing thiourea derivatives have been synthesised with an assortment of partnering organic structures, and screened via MTT cell viability assays against an array of human cell lines including breast and lung cancer lines, with promising IC50 values observed as low as 7-20 μM[37] in some studies. Included in the diverse array of non-metal synthesis are a series of phosphonate thiourea derivatives which when screened against human breast, pancreatic and

prostate cancer cell lines, in an *in vitro* study achieved promising responses in IC50 values between 3-14 µM.[39] Achievable low-dose responses like these show promise for early research in to thiourea derivatives, while similar values to the above can be recognised across a further range of derivatives, including bis-thiourea structures for the application of human leukaemia cell lines with IC50 values as low as 1.50 µM[40], but also in more aromatic derivatives of thiourea, synthesised with indole and adamantane compounds achieving a variety of positive IC50 values below 20 µM in breast, liver and lung cancers.[41] This insight into derivatives of thiourea is just a fraction of research which has been completed over the past few years, as thioureas have become a popular focal point during the past decade. With low-dose responses achieved using a plethora of derivatives, it gives us confidence in the derivatives synthesised in this research project to achieve positive anticancer effects throughout the cell lines selected for screening.

1.2 Guanidine's and their applications:

Sharing a similar structure to thiourea with the replacement of the sulfur ion with an NH group as seen in Figure 4, guanidine and its derivatives have great versatility throughout a variety of industries. The differing heteroatom in the structure lends guanidine a pKa of 13.6 making it a rather strong organic base,[42] facilitating water solubility when protonated and known to exhibit strong interactions with DNA bases.[44,43]

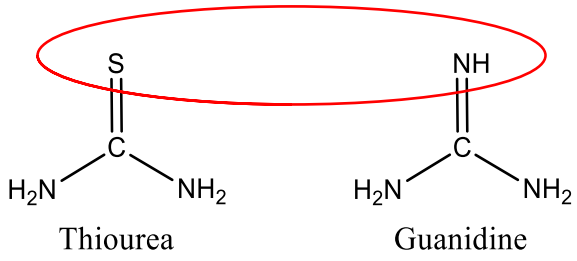

Figure 4. Highlighting the structural differences of thiourea and guanidine.

These compounds have been observed with successes in catalytic synthesis for advances in green chemistry,[29] antiviral responses observed in poliovirus,[30] adhesive promotors in the materials

industry,[31] synthesised derivatives with positive anticancer activity,[32] but are also found in more natural sources like the human body, being mainly present in urine.[27,28] Like ureas and thiourea groups, guanidines functionality has shown vast promise in the past decade, with advances in research leading to an array of derivatives with a main focal point being antimicrobial and anticancer properties, including successful observations in ovarian, lung and breast cancer cell lines achieved,[26,32] further raising our interests as to the potentials which new synthesised derivatives could achieve and highlighting their biological importance.

When examining the anticancer properties of various metal and non-metal guanidine derivatives we observe a similar pattern as seen in thioureas, being the success of low IC50 values achieved within *in vitro* studies throughout various human cancer cell lines.[45] These include more heavily aromatic guanidine derivatives incorporating a ketone group 'chalcones' which have achieved IC50 values as low as 0.09 μM in human breast cancer cells,[46] but also platinum centred derivatives assayed against ovarian and colorectal cancer cell lines achieving IC50 values below 5 μM in several synthesised variants.[47] Successes like these support advances in synthesising further derivatives of guanidine compounds to target new areas of cancer therapeutics, and further proving the biological importance of these somewhat simple and easily manipulatable structures.

Researching structures of the thiourea and guanidine derivatives synthesised in this research project was somewhat challenging. Whilst some of the compounds have previously been used for various biological purposes, there are limiting amounts of literature for the majority. When referencing all the derivative structures through SciFinder (Chemical Abstracts Service (CAS)) database it was observed at the time of synthesis that compounds **2**, **4**, **7** and **8** had no direct structural matches, thus suggesting these compounds which were synthesised are novel.

1.3 Iridium Complex Compounds:

The Iridium complexes used in this research project were synthesised and characterised by Barbora Balonova of The University of Kent/University of New Brunswick under the supervision of Dr Barry

Blight.[82] The compounds and methods were prepared by Barbora as part of her research towards advancing organic light-emitting diode (OLED) technologies with curiosities leading to the potential observations of anticancer effects. These interests arose when discussing several observations around the research into these complexes; from a practical point of view, if these compounds were to be used in OLED screen technologies there is a risk of possible cytotoxic effects to the user if a screen were to break, resulting in contact with the compounds in question. From a research point of view due to successes in cancer therapeutics involving metal ion containing complexes,[45,47] we would expect to observe a positive anticancer response from these iridium compounds. These compounds also have the advantage of long luminescence lifetimes when exposed to ultraviolet (UV) light, giving the opportunity to further be used in live cell imaging, without having to synthetically modify the compounds to accept fluorescent cellular probes like BODIPY.

Luminescence is the excitation of molecules when exposed to UV light, which vibrate to a state whereby emission of light occurs at a longer wavelength then the absorbed light,[59] making the luminescence properties visible to the human eye.

Fluorescence and phosphorescence are both modes of luminescence but differ in their excitation lifetimes. Longer excitation lifetimes are acknowledged as phosphorescence and are defined by the ability of a compound to continue its emission properties even when the excitation promotor such as UV light has been terminated.[66] The occurrence of phosphorescence is due to the excitation of an electron state known as a triplet state.[68] A triplet state causes a lower but more stable energy state, giving a slower release of light emission and the effect of prolonged emission on removal of the excitation source.[69] Shorter excitation lifetimes occur in fluorescence due to a singlet electron state, which has a higher and more unstable balance of energy acting as a fast and short-lived release of light emission, once the excitation source has been withdrawn the emission will cease.[66] These two processes of excitation and emission are displayed through the Jablonski diagram in Figure 5.[86]

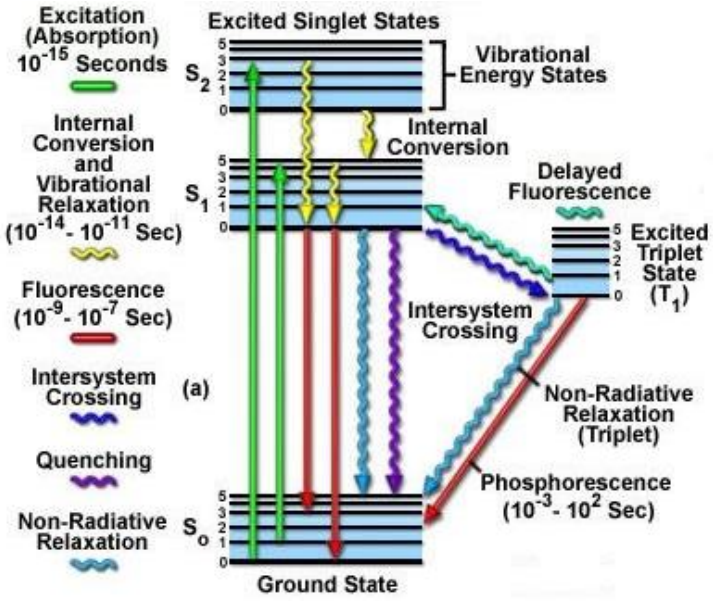

Figure 5. Jablonski Diagram of the electronic states of a molecule. Adapted from reference 86.[86]

Whilst the market for fluorescent probes is vastly populated, one of the more commonly used probes includes BODIPY (Figure 6) which has become an ever-popular choice throughout the past two decades.[60] Fluorescent probes like BODIPY allow structures which do not promote natural luminescence to be synthesised with the BODIPY compound attached.[61] This gives an advantage within *in vitro* cell screening assays, allowing the structure to be traced throughout the cell under techniques such as confocal microscopy, demonstrated in Figure 7.[85]

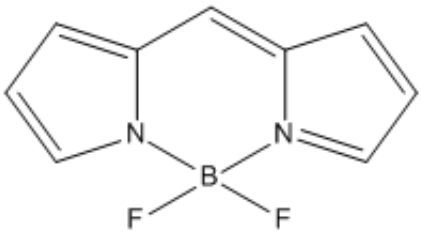

Figure 6. Chemical structure of BODIPY.

Derivatives of BODIPY have had successes in a variety of screening applications, including monitoring the regulation of amino acid uptake to differentiate between ovarian cancer cells and non-cancerous cells through fluorescence uptake,[62] and prove a useful tool within oncology research due to its robustness in a variety of structures and solutions.[63]

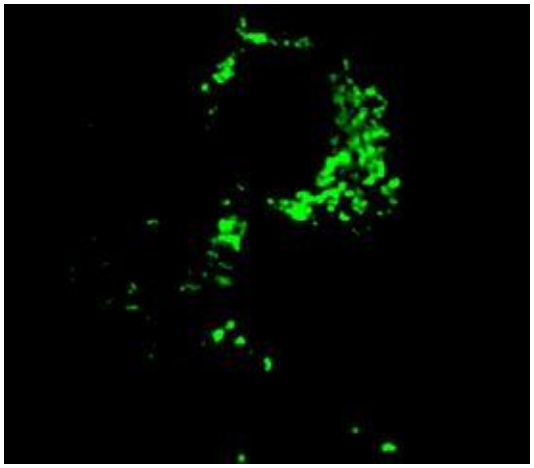

Figure 7. Confocal image of SKOV-3 human ovarian cancer cells dosed with a BODIPY derivative, adapted from reference 85.[85]

The iridium complexes have the advantage of being phosphorescent as demonstrated in Figure 8,[82] which provides a useful tool within research as compounds with these properties are used throughout numerous applications as effective biological probes for live cell imaging.[58] The effectiveness of these complexes comes down to the emission properties, with iridium complexes in general exhibiting intense emission periods with high efficiency and long lifetimes.[64] This establishment of highly efficient luminescence properties from iridium complexes has seen a surge in the need of these compounds for the development of high resolution OLED screen technologies,[67] and biological probes with longer luminescence lifetimes when compared against traditional dyes such as BODIPY.[68]

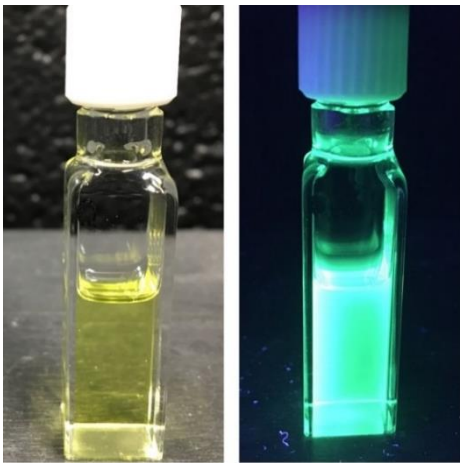

Figure 8. Image of an Iridium centred complex exposed to ambient light (left) and UV light (365nm) (right). Adapted from reference 82.[82]

It is expected the iridium complexes will be promising candidates for potency against ovarian cancer cells, due to a variety of metal ion containing compounds being heavily studied and proving their anticancer activity since the introduction of cisplatin in the 1960's.[25,84] Previous studies with iridium complexes have shown high potency towards cancer cells, with great potential due to a variety of abilities including adaptations of ligand bonding to alter their effectiveness and properties in biological systems,[22] but also due to the fact iridium compounds are often associated with high cytotoxicity through the targeting and binding of DNA.[24] This includes synthesis of iridium complexes for the application of ovarian cancer cells, where studies have observed promising IC50 values being obtained as low as 10.8 μM, when dosing human A2780 cell lines with an iridium centred complex.[23]

With iridium-based complexes, derivatives of thioureas, and guanidines exhibiting positive effects during previous *in vitro* studies as potential anticancer agents, we posit that through synthesising a pair of derivatives incorporated in an iridium complex may further promote efficient low-dose responses, when screening these complexes against a panel of ovarian cancer cell lines.

1.4 Ovarian cell lines in cancer:

Ovarian cancer is an epithelial disease which is the sixth most common cancer in women across the globe,[19] but also has the highest mortality rate within all gynaecological cancers.[20] Current treatments include surgical procedures to remove tumour mass and chemotherapy's which include platinum-based and multiagent drugs,[21] although whilst initial responses appear promising the cancer is known to persist in showing resistance 6-12 months post therapy completion.[21] This aggressiveness of the disease has highlighted itself as a focal point for oncology developments, and the reason for this research project to potentially break resistant mechanisms which are regularly seen in clinical drugs such as cisplatin.

Six human ovarian cancer cell lines were used for this research, where parental lines and cisplatin-adapted resistant sublines were both screened to observe whether the resistant mechanisms would hinder toxicity effects of the synthesised compounds. The morphology of these cells visually followed

suit for what is expected of these ovarian cell lines from lab cultures seen in Figure 9. Although stress factors were not tested on these cells pre/post screening, there are a variety of techniques which have been carried out to observe stress factors on ovarian cancer cells. Stresses on tumorous ovarian cells have been shown to lead to a variety of outcomes including density, morphology and proliferation changes being altered by upregulation and downregulation of signalling pathways,[48] whilst through mechanical analysis of cancer cells, it is possible to reveal that morphological changes are more likely to occur due to lower stiffness levels within the cells cytoskeleton.[49,50]

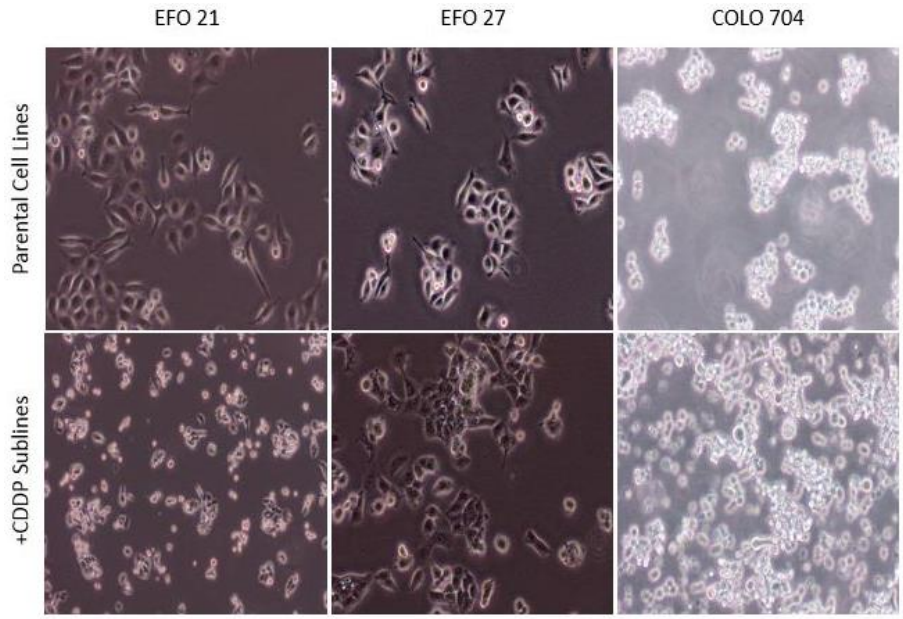

Figure 9. Light microscope images of the 6 ovarian cell lines screened.

1.4.1 Tackling resistance of Cisplatin in Ovarian cancer:

Cisplatin is a successful platinum based anticancer drug widely used in the treatment of a variety of cancers including lung, bladder, testicular and ovarian cancers to name a few.[11] Its developments began in 1845 when the initial structure of cisplatin was first synthesised by Michel Peyrone,[12] (Figure 10) although it was not until the 1960's before the anticancer effects of cisplatin were discovered.[12] The mode of action for the success of cisplatin involves disrupting DNA repair mechanisms of cancer cells though purine bases crosslinking with cisplatin, inhibiting cellular replication finally resulting in

apoptotic cell death.[13] Whilst initial patient responses to cisplatin are positive throughout several cancer types including ovarian cancers,[16] there are negatives to the anticancer drug which include the development of resistant mechanisms and side effects such as immunosuppression, vomiting and nausea,[15] alongside more severe side effects including nephrotoxicity, neurotoxicity and cardiotoxicity.[14,15] Mechanisms of cisplatin resistance have become a dominant problem, particularly in ovarian cancers thus rapidly limiting its effectiveness in clinical environments.[17]

It has been observed that resistance from cisplatin in ovarian cancers occurs after the initial treatment of screening therapeutic drugs, with a relapse in growth of tumour cells noted and known as acquired resistance.[52] Other cancer types such as non-small celled lung cancers are intrinsically resistant to cisplatin.[18] Acquired resistance can arise due to naturally occurring immune responses within the body causing reduced sensitivity to the therapeutic drug in use, thus diminishing the response rate,[51,52] while intrinsic resistance can occur due to complete failure of an anti-tumour response being promoted within the body.[51]

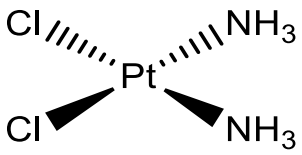

Figure 10. Structure of Cisplatin

While resistant mechanisms of cisplatin prove problematic, there have been a plethora of attempts to overcome this with new therapeutics aimed at cisplatin resistant ovarian cancer cells. Some of which include early *in vitro* studies which have identified areas of controlling metabolic enzyme regulation to be potential novel targets,[53] but also through technological advances into liposomes being used as carriers of cisplatin, exhibiting positive *in vitro* progress with prolonged exposure of platinum levels observed within cells when comparing with a normally dosed cell.[54]

1.5 Thesis Statement

The aim of this thesis is to synthesis a selection of organic thiourea and guanidine derivatives and test their effects on the viability of ovarian cancer cells. Included are several iridium complexes incorporating thiourea and guanidine based ligands, synthesised by Barbora Balonova of The University of Kent/University of New Brunswick under supervision of Dr Barry Blight.[82]

The decision to focus our research on thiourea, guanidine and iridium complexes, was due to the great diversity of research areas in which these compounds have been applied to, alongside positive data generated from early *in vitro* screening assays into anticancer properties.[4,22,30,38] Due to this previous research we decided the compounds presented, have promise to be screened against a panel of human ovarian cancer cell lines. Anticancer activity will be observed through an MTT cell viability assay to determine the compounds *in vitro* effectiveness, while comparing parental cell lines against cisplatin resistant sublines. Human ovarian cell lines were selected due to the aggressiveness of the disease and resistant mechanism, anticipating that our compounds could challenge these mechanisms.

Ovarian cancer cells will be imaged once dosed with the iridium complexes due to the luminescent properties which these structures exhibit. We expect to observe correlations between the uptake of the compound in a cell and its effectiveness during the MTT assay.

With the data collected through these experiments, we aim to identify derivatives of thiourea and guanidine which may be relevant with regards to the identification of new lead structures for drug discovery, but may also provide data on the toxicology of the compounds.

Chapter 2: Synthesis and characterisation of Thiourea/Guanidine Derivatives and Iridium Complex Compounds as Potential Anticancer Drugs.

2.1 Introduction

To formulate our thiourea and guanidine derivatives, three known methods were used throughout the synthesis. The starting compound (**1**) was synthesised following methods from recent research into hydrogen bonding,[70] whilst the thiourea derivatives were derived from this starting compound using the methods of Rakesh et al.,[3] from research into the use of thiourea derivatives for HIV reverse transcriptase therapies. Once all thioureas were produced it was then possible to synthesise their guanidine substructures using the method of Blight et al.[71] While these methods were followed, some of the synthesis steps were amended for the reaction times.

2.2 Materials and Apparatus

All solvents and starting materials were purchased from Fisher Scientific, Sigma-Aldrich, Arcos Organics and Alfa Aesar. These materials were used as received from the supplier without any further purification methods carried out unless otherwise stated. All compound reactions were carried out under nitrogen atmosphere unless stated otherwise.

NMR: ^{1}H NMR (400MHz) and ^{13}C NMR (125MHz) spectra's were recorded on a JEOL ECS 400 NMR spectrometer with deuterated solvents DMSO-d_6 and chloroform-d used. Chemical shifts are recorded in ppm and peaks referred to as singlet (s), doublet (d), triplet (t), quartet (q) or multiplet (m).

MS: Mass Spectra were recorded on a Bruker micrOTOF-Q Mass Spectrometer with a mass accuracy of 1-2 ppm. Peaks are referred to in mass to charge ratio *(m/z)*.

EA: Tested by Stephen Boyer at London Metropolitan University. Data is shown in percentage (%).

MP: Data was collected using a Stuart-Melting Point-SMP10 and all temperatures recorded in degrees celsius (°C).

CC: Completed using silica gel 60, 0.060-0.2mm (70-230 mesh) supplied by Alfa Aesar and fine sand supplied by Fisher Scientific and general-purpose cotton wool.

TLC: Completed using pre-coated silica gel plates supplied by Macherey-Nagel (silica gel 60 with fluorescent indicator UV).

2.3 Methods

2.3 Thioureas

2.3.1 Compound 1

***N*-(1*H*-benzo[*d*]imidazole-2-yl)-1*H*-imidazole-1-carbothioamide**

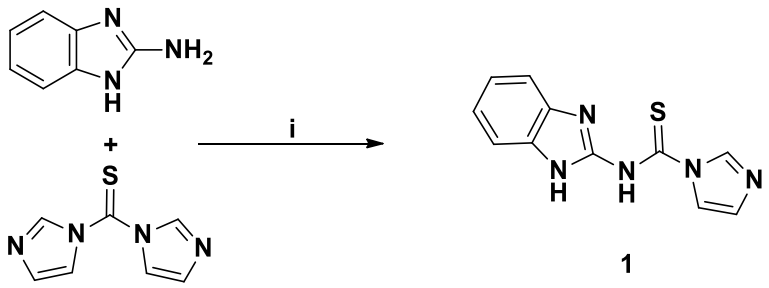

Reagents and Conditions: (i) 2-aminobenzimidazol, TCDI (1.3equiv) (1,1'-thiocarbonyldiimidazole), acetonitrile, 50°C, 18 h.

To a solution of 2-aminobenzimidazol (0.600 g, 4.506×10^{-3} mol) in acetonitrile (20 mL), thiocarbonyldiimidazole (1.043g, 5.858×10^{-3} mol) was added in 4 parts. The flask was sealed and placed in a 50°C oil bath for 18 h under a N_2 atmosphere. The formed precipitate was collected via suction filtration and additional acetonitrile used to wash the precipitate (3x30 mL) then dried via vacuum oven (40°C, overnight). Final product: pale yellow powder (0.654 g, 59% yield).

^{1}H NMR: (400MHz, DMSO -d_6): δ 8.54 (t, J = 1.0 Hz, 1H), 7.92 (t, J = 1.3 Hz, 1H), 7.60 (dd, J = 6.0, 3.2 Hz, 2H), 7.33 (dd, J = 6.0, 3.2 Hz, 2H), 7.00 – 6.98 (m, 1H). **^{13}C NMR:** (125MHz, DMSO): δ 179.34, 152.71,

136.71, 135.51, 129.77, 129.37, 124.34, 121.81, 118.32, 112.99. **EA for $C_{11}H_9N_5$:** Calculated: C; 54.31%, H; 3.73%, N; 28.79%, Obtained: C; 54.19%, H; 3.54%, N; 28.52%. **MP:** 188°C - 190°C.

2.3.2 Compound 2

1-(1*H*-benzo[*d*]imidazole-2-yl)-3-propylthiourea

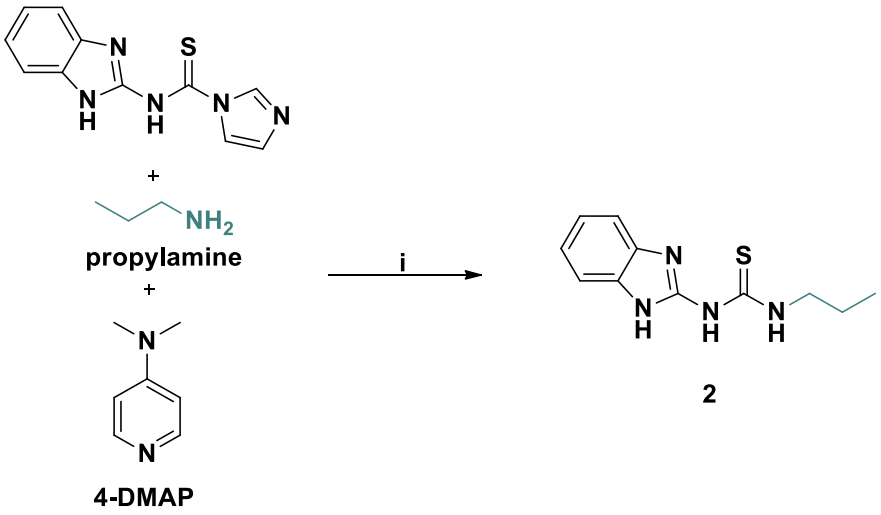

Reagents and Conditions: (i) DMF, propylamine (1.1equiv), 4-DMAP (*N,N*-dimethylpyridin-4-amine) (0.1equiv), 100°C, 15 h.

To a solution of compound **1** (0.500 g, 2.055×10^{-3} mol) in DMF (15 mL), 4-DMAP (0.025 g 2.055×10^{-4} mol) and propylamine (0.185 mL, 2.260×10^{-3} mol) were slowly added while stirring. The flask was sealed and placed in a 100°C oil bath for 18 h under N_2 atmosphere. The solution was then poured into a beaker of icy water (75 mL) and stirred until precipitation formed (1.5 - 2 h). The precipitate was collected via suction filtration then dried in a vacuum oven (40°C, overnight). TLC was carried out dissolving the sample in DCM and using a 1:3 ratio of ethyl acetate to hexane showing one sample trace with an RF value of 0.236. Final product: pale yellow powder (0.303 g, 63% yield).

^{1}H NMR: (400MHz, DMSO -d_6): δ 11.18 (d, J = 60.2 Hz, 3H), 7.42 (dt, J = 6.7, 3.4 Hz, 2H), 7.13 – 7.07 (m, 2H), 3.58 (dd, J = 12.5, 6.7 Hz, 2H), 1.71 – 1.57 (m, 2H), 1.03 – 0.89 (m, 3H). **^{13}C NMR:** (125MHz, chloroform-*d*): δ 178.34, 148.35, 122.72, 111.30, 78.40, 76.84, 47.26, 22.22, 11.66. **EA for $C_{11}H_{14}N_4$:**

Calculated: C; 56.38%, H; 6.02%, N; 23.91%, Obtained: C; 56.49%, H; 6.11%, N; 23.86%. **EI-MS *m/z*:** Calculated: 234.32. Actual: 235.0997 **[M+]. MP:** 165°C - 170°C.

2.3.3 Compound 3

1-(1*H*-benzo[*d*]imidazole-2-yl)-3-butylthiourea

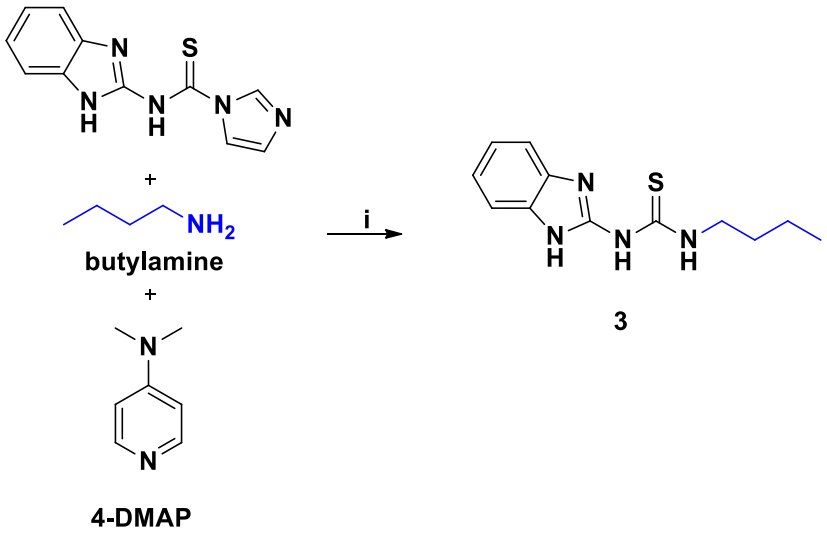

Reagents and Conditions: (i) DMF, butylamine (1.1equiv), 4-DMAP (*N,N*-dimethylpyridin-4-amine) (0.1equiv), 100°C, 15 h.

To a solution of compound **1** (0.500g, 2.055×10^{-3} mol) in DMF (18 mL), 4-DMAP (0.025 g, 2.055×10^{-4} mol) and butylamine (0.223 mL, 2.260×10^{-3} mol) were slowly added. The flask was sealed and placed in a 100°C oil bath for 18 h under a N_2 atmosphere. The solution was then poured into a beaker of icy water (75 mL) and stirred until precipitation formed (0.5 - 1 h). The precipitate was collected via suction filtration then dried in a vacuum oven (40°C, overnight). Final product: White powder (0.372 g, 73% yield). TLC was carried out dissolving sample in DCM and using a 1:3 ratio of ethyl acetate to hexane showing one sample trace with an RF value of 0.270. CC was carried out dissolving the 342 mg sample in DCM and using an eluent system of 1:3 ethyl acetate to hexane. Final product: white powder 192 mg post CC giving a 56.14% column efficiency.

^{1}H NMR: (400MHz, DMSO -d_6): δ 11.15 (s, 2.26H), 7.26 (d, J = 129.4 Hz, 3.51H), 3.63 (s, 1.95H), 1.50 (d, J = 93.6 Hz, 4H), 0.93 (s, 3H). **EA for $C_{12}H_{16}N_4$:** Calculated: C; 58.04%, H; 6.79%, N; 22.56%, Obtained: C; 57.95%, H; 6.32%, N; 22.7%. **EI-MS *m/z*:** calculated: 248.35. Actual: 249.1176 **[M+]. MP:** 165°C - 170°C.

2.3.4 Compound 4

1-(1*H*-benzo[*d*]imidazole-2-yl)-3-hexylthiourea

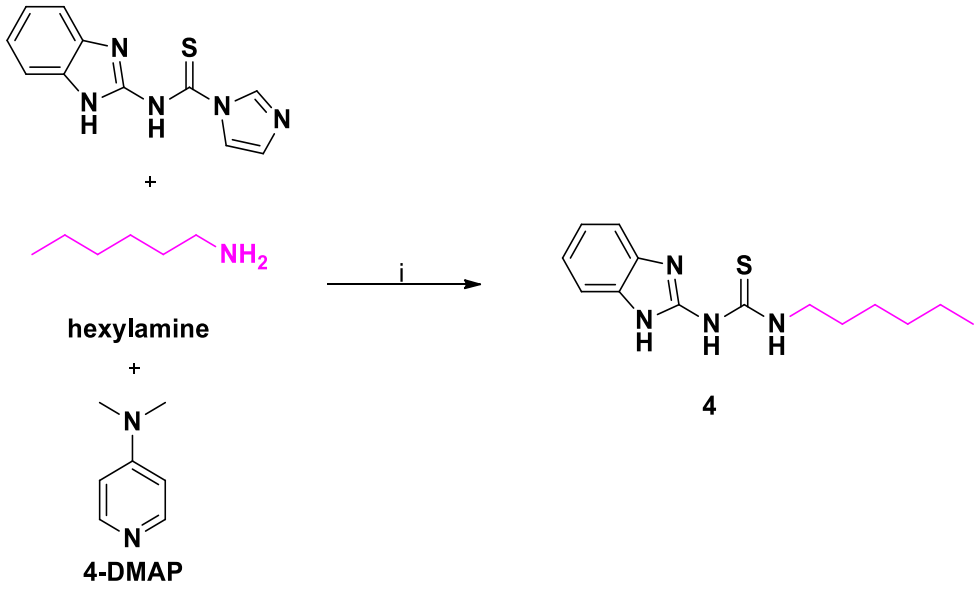

Reagents and Conditions: (i) DMF, hexylamine (1.1equiv), 4-DMAP (*N,N*-dimethylpyridin-4-amine) (0.1equiv), 100°C, 15 h.

To a solution of compound **1** (0.500 g, 2.055x10^{-3} mol) in DMF (15 mL), 4-DMAP (0.025 g, 2.055x10^{-4} mol) hexylamine (0.297 mL, 2.260x10^{-3} mol) were slowly added. The flask was sealed and placed in a 100°C oil bath for 18 h under a N_2 atmosphere. The solution was then poured into a beaker of icy water (75 mL) and stirred until precipitation formed (1 - 2 h). The precipitate was collected via suction filtration then dried in a vacuum oven (40°C, overnight). Final product: off-white powder (0.464 g, 81% yield). TLC was carried out dissolving the sample in DCM and using a 1:3 ratio of ethyl acetate to hexane showing one sample trace with an RF value of 0.342.

^{1}H NMR: (400MHz, DMSO -d_6): δ 11.19 (d, J = 68.3 Hz, 2.20H), 7.78 – 6.67 (m, 3.81H), 3.55 (t, J = 43.6 Hz, 2H), 1.62 (dd, J = 14.4, 7.0 Hz, 2H), 1.42 – 1.21 (m, 6H), 0.88 (t, J = 6.9 Hz, 3H). **^{13}C NMR:** (101 MHz, $CHCL_3$): δ 122.69, 77.48, 77.16, 76.84, 45.63, 31.57, 28.79, 26.79, 22.70, 14.17. **EA for $C_{14}H_{20}N_4$:** Calculated: C; 60.84%, H; 7.29%, N; 20.27%, Obtained: C; 60.93%, H; 7.18%, N; 20.39%. **EI-MS *m/z*:** Calculated: 276.40. Actual: 277.1607 **[M+]. MP:** 117°C - 131°C.

2.3.5 Compound 5

1-(1*H*-benzo[*d*]imidazole-2-yl)-3-benzylthiourea

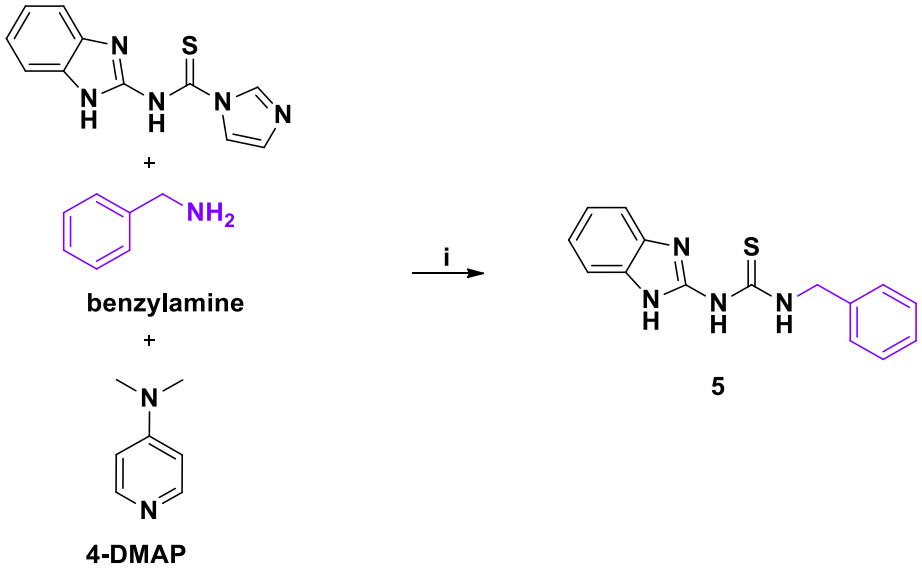

Reagents and Conditions: (i) DMF, benzylamine (1.1equiv), 4-DMAP (*N,N*-dimethylpyridin-4-amine) (0.1equiv), 100°C, 15 h.

To a solution of compound **1** (0.147 g, $6.042x10^{-4}$ mol) in DMF (15 mL), 4-DMAP (0.007 g, $6.042x10^{-5}$ mol) and benzylamine (0.073 mL, $6.646x10^{-4}$ mol) were slowly added. The flask was sealed and placed in a 100°C oil bath for 18 h under a N_2 atmosphere. The solution was then poured into a beaker of icy water (75 mL) and stirred until precipitation formed (6 - 8 h). The precipitate was collected via suction filtration then dried in a vacuum oven (40°C, overnight). Final product: pale yellow powder (0.121 g,

71% yield). TLC was carried out dissolving the sample in DCM and using a 1:2 ratio of ethyl acetate to hexane observing one sample trace with an RF value of 0.235.

^{1}H NMR: (400MHz, DMSO -d_6): δ 11.43 (d, 2.43H), 7.25 (d, 9H), 4.95 (s, 1.77H). **^{13}C NMR:** (101 MHz, DMSO): δ 148.05, 138.15, 128.49, 127.26, 127.13, 126.98, 121.61, 116.34, 110.98, 47.69. **EA for $C_{15}H_{14}N_4$:** Calculated: C; 63.81%, H; 5%, N; 19.89%, Obtained: C; 63.68%, H; 4.93%, N; 19.76%. **EI-MS *m/z*:** Calculated: 282.37. Actual: 283.1017 **[M+]. MP:** 183°C - 192°C.

2.3.6 Compound 6

1,3-bis(5-methylpyridin-2-yl)thiourea

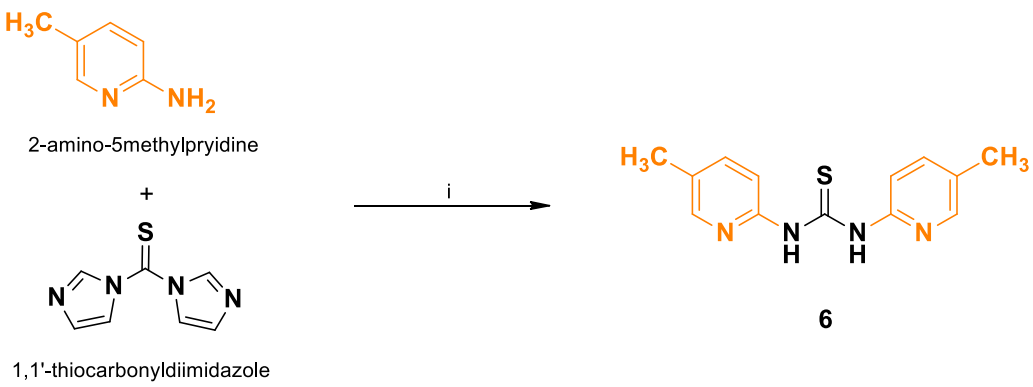

Reagents and Conditions: (i) acetonitrile, 2-amino-5methylpyridine, TCDI (1.3equiv), 50°C, 18 h.

To a solution of 2-amino-5methylpyridine (0.600 g, 5.548×10^{-3} mol) in acetonitrile (15mL), thiocarbonyldiimidazole (1.285 g, 7.212×10^{-3} mol) was added in 4 parts. The flask was sealed and placed in a 50°C oil bath for 18 h under N_2 atmosphere. After 18 h precipitation was not observed, and the reaction was left to cool to room temperature for a further 6 h until precipitation formed. The precipitate was collected via suction filtration and additional acetonitrile used to wash the precipitate (3x30 mL) then dried via vacuum oven (40°C, overnight). Final product: pale orange powder (0.192 g, 15% yield). TLC was carried out dissolving sample in DCM and using a 4:1 ratio of ethyl acetate to hexane observing one sample trace with an RF value of 0.20 and a second trace with an RF value of 0.866. CC was carried out dissolving the 192 mg sample in DCM and using an eluent system of 4:1

ethyl acetate to hexane. 110 mg was collected post CC giving an efficiency of 57.29%. Post CC TLC showed a single sample trace with an RF value of 0.230.

^{1}H NMR: (400MHz, DMSO -d_6): δ 9.08 (s, 1H), 8.39 (d, 0.95H), 7.99 (d, 0.98H), 7.79 (d, 0.99H), 7.32 (d, 1.98H), 2.41-2.28 (m, 6H). **^{13}C NMR:** (101 MHz, $CHCL_3$): δ 179.40, 172.53, 153.45, 150.82, 145.30, 139.91, 134.41, 130.11, 126.25, 124.83, 122.84, 77.48, 77.16, 76.84, 18.50, 18.38. **EA for $C_{13}H_{14}N_4$:** Calculated: C; 60.44%, H; 5.46%, N; 21.69%, Obtained: C; 56.6%, H; 4.20%, N; 18.19%. **EI-MS *m/z*:** Calculated: 258.0939 Actual: 259.1025 **[M+]. MP:** 131°C - 132°C.

2.4 Guanidines

2.4.1 Compound 7

1-(1*H*-benzo[*d*]imidazole-2-yl)-3-propylguanidine

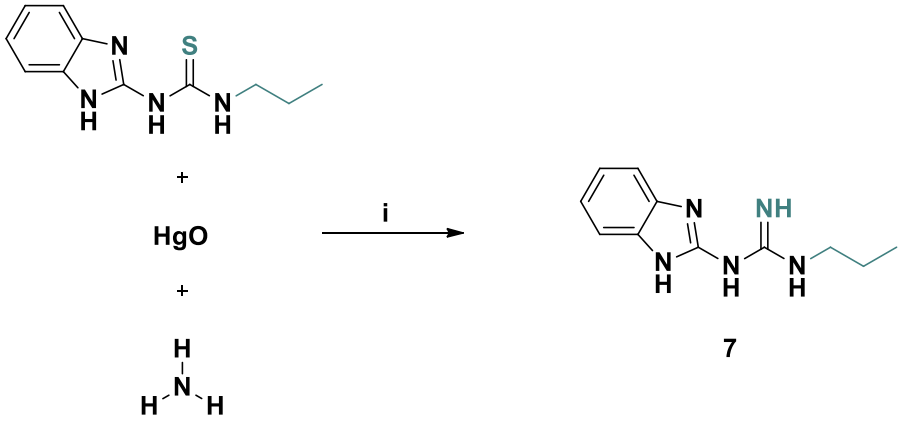

Reagents and Conditions: (i) propylthiourea, $CHCl_3$, HgO (mercury (II) oxide) (1.4equiv), 2 M NH_3/MeOH, RT, 3 h.

To a solution of compound **2** (0.200 g, $8.535x10^{-4}$ mol) in chloroform (20 mL), mercury (II) oxide (0.258 g, $1.194x10^{-3}$ mol) and 2 M ammonia (4 mL) were added. The flask was sealed and stirred at room temperature for 3 h. The reaction solution was filtered through Celite® and washed with additional

chloroform (10 mL) with the solvent then removed under reduced pressure. Physical properties: Filtered solutions pale yellow/gold and pale yellow precipitate.

The precipitate was dissolved in 2 M acetic acid (20 mL) and stirred at room temperature for 1 h. Reaction solution was then filtered through Celite® and adjusted to pH 8.0 by the addition of NaOH (10 M) to provoke precipitation. The formed precipitate was collected via suction filtration and dried in a vacuum oven (40°C, overnight). Final product: pale yellow powder (0.0861g, 46.5% yield). TLC was carried out dissolving the sample in DCM and using a 10:1 ratio of DCM to MeOH showing one sample trace with an RF value of 0.347.

Standard extraction methods were carried out dissolving the 86 mg sample in DCM using saturated $NaHCO_3$. Dried $MgSO_4$ was added to collected organic layer then filtered. Solvent was then removed under reduced pressure. Final product: pale yellow powder (0.035 g, 43.75% extraction efficiency).

^{1}H NMR: (400MHz, DMSO -d_6): δ 11.18 (d, 3H), 7.42 (d, 2H), 7.13 – 7.07 (m, 2H), 3.58 (d, 2H), 1.71 – 1.57 (m, 2H), 1.03 – 0.89 (m, 3H). **^{13}C NMR:** (101 MHz, DMSO -d_6): δ 159.07, 157.71, 132.22, 119.60, 118.99, 114.92, 108.47, 42.14, 22.59, 11.40. **EA for $C_{11}H_{15}N_5$:** Calculated: C; 60.81%, H; 6.96%, N; 32.23%, Obtained: C; 57.64%, H; 6.96%, N; 28.81%. **EI-MS *m/z*:** Expected: 217.2760. Actual: 218.1409 **[M+].** **MP:** 175°C - 178°C.

2.4.2 Compound 8

1-(1*H*-benzo[*d*]imidazole-2-yl)-3-butylguanidine

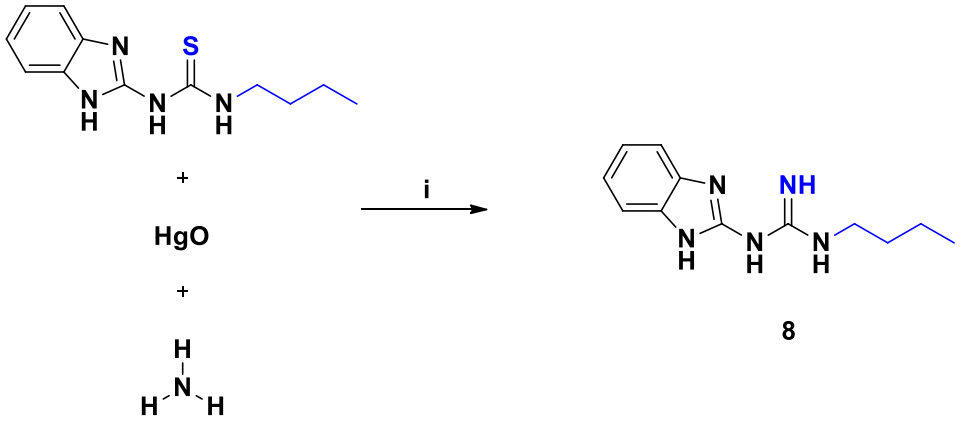

Reagents and Conditions: (i) Butylthiourea, $CHCl_3$, HgO (mercury (II) oxide) (1.4equiv), 2 M NH_3/MeOH, RT, 3 h.

To a solution of compound **3** (0.200 g, 8.053×10^{-4} mol) in chloroform (20 mL), mercury (II) oxide (0.244 g, 1.127×10^{-3} mol) and 2 M ammonia (4 mL) were added. The flask was sealed and stirred at room temperature for 3 h. The reaction solution was filtered through Celite® and washed with additional chloroform (10 mL) with the solvent then being removed under reduced pressure. Physical properties: Filtered solutions pale yellow/gold and yellow precipitate.

The precipitate was dissolved in 2 M acetic acid (20 mL) and stirred at room temperature for 1 h. Reaction solution was then filtered through Celite® and adjusted to pH 8.0 by the addition of NaOH (10 M) to provoke precipitation. The formed precipitate was collected via suction filtration and dried in a vacuum oven (40°C, overnight). TLC was carried out dissolving sample in DCM and using a 10:1 ratio of DCM to MeOH showing one sample trace with an RF value of 0.308. Final product: pale yellow powder (0.0756 g, 40.6% yield).

Standard extraction methods were carried out dissolving the 75 mg sample in DCM using saturated $NaHCO_3$. Dried $MgSO_4$ was added to collected organic layer then filtered. Solvent was then removed under reduced pressure. Final product: pale yellow powder (0.0491 g, 65.4% extraction efficiency).

^{1}H NMR: (400MHz, DMSO -d_6): δ 11.00 (s, 1H), 6.89 (t, 4H), 5.76 (s, 1H), 3.19 (q, 2H), 2.50 (DMSO), 1.49 (m, 2H), 1.36 (m, 2H), 0.91 (t, 3H), 0.07 (s, 3H). **^{13}C NMR:** (101 MHz, $CHCL_3$): δ 157.95, 157.69, 120.76, 77.48, 77.16, 76.84, 41.65, 31.54, 29.87, 20.26, 13.89, 1.93, 1.17. **EA for $C_{12}H_{17}N_5$:** Calculated: C; 62.31%, H; 7.41%, N; 30.28%, Obtained: C; 50.52%, H; 7.33%, N; 18.67%. **EI-MS *m/z*:** Calculated: 231.3030. Actual: 232.1575 **[M+]. MP:** 199°C - 214°C.

2.4.3 Compound 9

1-(1*H*-benzo[*d*]imidazole-2-yl)-3-hexylguanidine

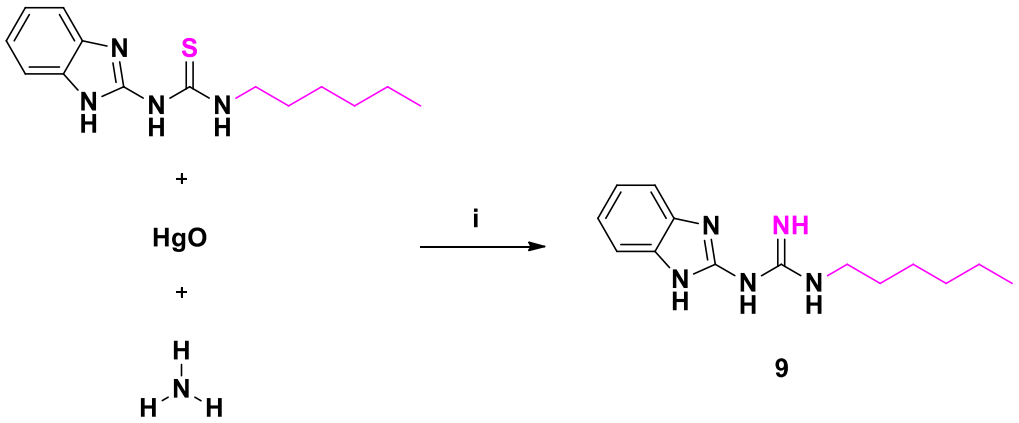

Reagents and Conditions: (i) hexylthiourea, $CHCl_3$, HgO (mercury (ii) oxide) (1.4equiv), 2 M NH_3/MeOH, RT, 3 h.

To a solution of compound **4** (0.210 g, 7.597×10^{-4} mol) in chloroform (25 mL), mercury (II) oxide (0.230 g, 1.063×10^{-3} mol) and 2 M ammonia (4.7 mL) were added. The flask was sealed and stirred at room temperature for 3 h. The reaction solution was filtered through Celite® and washed with additional chloroform (10 mL) with the solvent then removed under reduced pressure. Physical properties: Filtered solutions pale yellow and pale yellow precipitate.

The precipitate was dissolved in 2 M acetic acid (20 mL) and stirred at room temperature for 1 h. Reaction solution then filtered through Celite® and adjusted to pH 8.0 by the addition of NaOH (10 M) to provoke precipitation. The formed precipitate was collected via suction filtration and dried in a vacuum oven (40°C, overnight). TLC was carried out dissolving the sample in DCM and using a 20:1 ratio of DCM to MeOH showing three sample traces with RF values of 0.308, 0.493 and 0.790. Final product: pale yellow powder (0.0812 g, 41.2% yield).

Standard extraction methods were carried out by dissolving the 105 mg sample in DCM and using saturated $NaHCO_3$. Dried $MgSO_4$ added to collected organic layer then filtered. Solvent was then removed under reduced pressure. Post extraction TLC showing one sample trace with an RF value of 0.131. Final product: pale yellow (0.047 g, 44.76% extraction efficiency).

^{1}H NMR: (400MHz, $CHCL_3$): δ 7.41 (s, 1H), 7.26, 7.07 (s, 2H), 5.30, 3.90, 3.24 (t, 3H), 1.67-1.33 (m, 8H), 0.91 (t, 3H), 0.07. **^{13}C NMR:** (101 MHz, DMSO): δ 159.48, 158.10, 119.86, 119.51, 115.35, 108.97, 40.84, 31.53, 29.77, 26.60, 22.59, 14.40. **EA for $C_{14}H_{21}N_5$:** Calculated: C; 64.83%, H; 8.16%, N; 27.00%, Obtained: C; 64.70%, H; 8.27%, N; 26.89%. **EI-MS *m/z*:** Calculated: 259.3570. Actual: 260.1890 **[M+].** **MP:** 159°C - 164°C.

2.4.4 Compound 10

1-(1*H*-benzo[*d*]imidazole-2-yl)-3-benzylguanidine

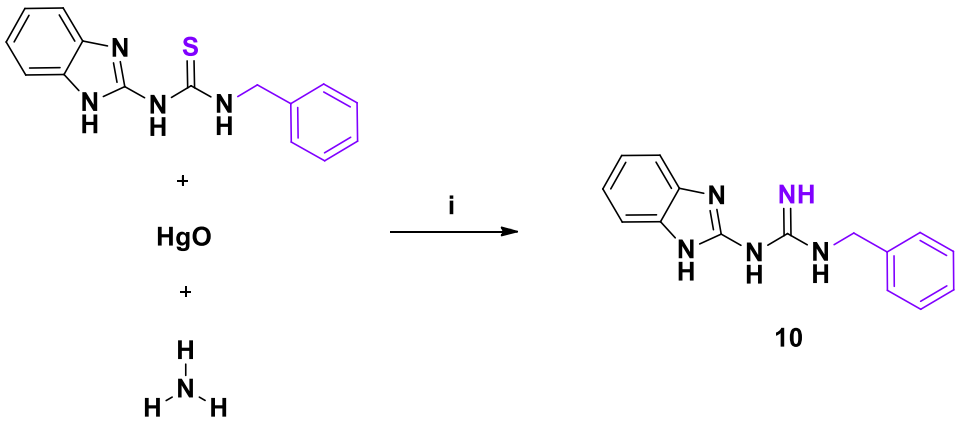

10

Reagents and Conditions: (i) benzylthiourea, $CHCl_3$, HgO (mercury (ii) oxide) (1.4equiv), 2 M NH_3/MeOH, RT, 3 h.

To a solution of compound **5** (0.240 g, $8.499x10^{-4}$ mol) in chloroform (25 mL), mercury (II) oxide (0.257 g, $1.189x10^{-3}$ mol) and 2 M ammonia (5 mL) were added. The flask was sealed and stirred at room temperature for 3 h. The reaction solution was filtered through Celite® and washed with additional chloroform (10 mL) with the solvent then removed under reduced pressure. Physical properties: Filtered solutions pale green/yellow and green oily precipitate.

The precipitate was dissolved in 2 M acetic acid (20 mL) and stirred at room temperature for 1 h. Reaction solution then filtered through Celite® and adjusted to pH 8.0 by the addition of NaOH (10 M) to provoke precipitation. The formed precipitate was then collected via suction filtration and dried in a vacuum oven (40°C, overnight). Final product: pale yellow powder (0.201 g, 78.8% yield). TLC carried out dissolving sample in DCM and using a 20:1 ratio of DCM to MeOH showing one sample trace with an RF value of 0.188.

Standard methods of extraction were carried out dissolving the 201 mg sample in DCM and using saturated $NaHCO_3$. Dried $MgSO_4$ added to collected organic layer then filtered. Solvent was then removed under reduced pressure. Final product: pale yellow (0.040 g, 19.90% extraction efficiency).

^{1}H NMR: (400MHz, $CHCL_3$,): δ 7.37-7.30 (m, 7H), 7.26 ($CHCL_3$), 7.08 (m, 2H), 5.30, 4.50 (s, 2H), 3.89, 1.25, 0.87, 0.07. **^{13}C NMR:** (101 MHz, DMSO): δ 159.25, 157.99, 140.57, 128.77, 127.66, 127.21, 119.97, 115.53, 44.16. **EA for $C_{15}H_{15}N_5$:** Calculated: C; 67.90%, H; 5.70%, N; 26.40%, Obtained: C; 67.75%, H; 5.82%, N; 26.67%. **EI-MS *m/z*:** Expected: 265.3200. Actual: 266.1429 **[M+]. MP:** 141°C - 145°C.

2.4.5 Discussion - Thiourea & Guanidine Derivatives

Five thiourea derivatives were successfully synthesised with yields as high as 81%. We found the most successful route of synthesis was by addition of differing amine chains as seen in compounds **2-5**, using a slight modification of known methods by Rakesh et al.,[3] with compound **1** as the precursor. Compound **6** used an addition of a 2-amino-5methylpryidine which was not successful in its synthesis when using the same methods as compounds **2-5**, even after several attempts in amending reaction and precipitation times. Due to being unsuccessful the methods of Mukherjee et al.,[70] as used in compound **1** were then applied and the 2-aminobenzimidazol structure replaced with a 2-amino-5methylpryidine compound, which whilst achieving a low yield of 15% still demonstrated through analysis that the structure was successfully synthesised.

Once the thioureas had been synthesised and characterised we then carried out the methods of Blight et al.[71] to successfully produce four guanidine derivatives from compounds **2-5** with a mixture of high and low yields. Synthesis was also attempted using compound **6** to gain a further guanidine structure, but after several attempts it was not possible to collect a clean compound with high purity using this method.

During the initial synthesis stages, we attempted to design further thiourea derivatives using both methods from Rakesh et al.,[3] and Mukherjee et al.,[70] with additions of aminopyridine involving methyl and chlorine moieties. Unfortunately, these were unsuccessful in producing clear spectra during NMR analysis even after purification attempts and due to this were disregarded.

2.5 Iridium Complex Compounds

2.5.1 Synthesis Statement

Compounds **11** to **14** were successfully synthesised and characterised by Barbora Balonova during her PhD carried out between the University of Kent, UK and the University of New Brunswick, CA.[82] While her research into these structures continues, all synthesis methods and analysis are correct at the time of this research project.

2.5.2 Precursor to Compound 11 and 12

Ir-chloro-bridged dimer[4]:

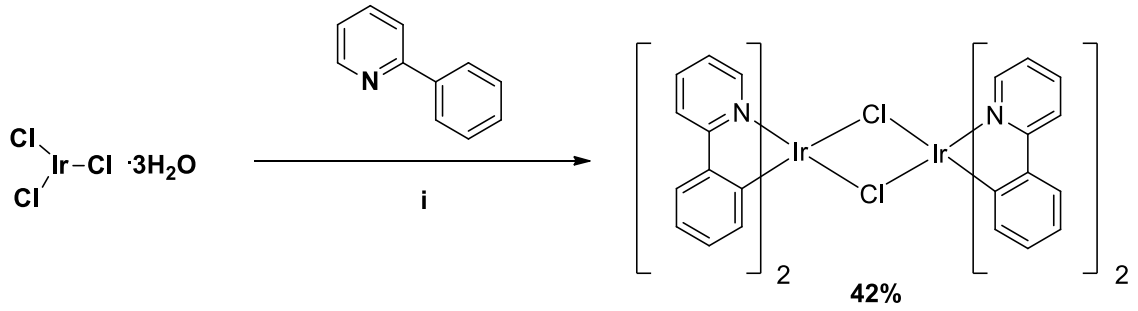

Reagents and Conditions: (i) Iridium(lll) chloride, 2-phenylpyridine, 2-ethoxyethanol : water (3:1), reflux, 24 h.

To a solution of 2-ethoxyethanol (15 mL), 2-phenylpyridine (0.69 mL, 4.85 mmol), iridium (III) chloride trihydrate (0.81 g, 2.31 mmol) were dissolved with an addition of water (5 mL). The flask was sealed and placed in an oil bath for 24 h under a N_2 atmosphere. The flask was left to cool to room temperature, forming a yellow precipitate which was collected via suction filtration and thoroughly washed with additional water (20 mL), ethanol (20 mL) and acetone (20 mL) then dried via vacuum oven (40^{o}C, 24 h). Final product: Canary yellow powder (1.05 g, 84% yield) with no further purification required.

^{1}H NMR: (400MHz, 298K, chloroform-*d*): δ 5.92-5.94 (s, 1H), 6.55-6.58 (t, 1H), 6.73-6.79 (m, 2H), 7.48-7.50 (d, 1H), 7.72-7.76 (t, 1H), 7.86-7.88 (d, 1H), 9.23-9.25 (d, 1H). **^{13}C NMR:** (100MHz, 298K,

chloroform-*d*): δ 168.97, 152.13, 145.79, 144.14, 136.61, 131.03, 129.54, 124.05, 122.57, 121.28, 118.85.

2.5.3 Compound 11

Iridium (ppy)-butyl-thiourea

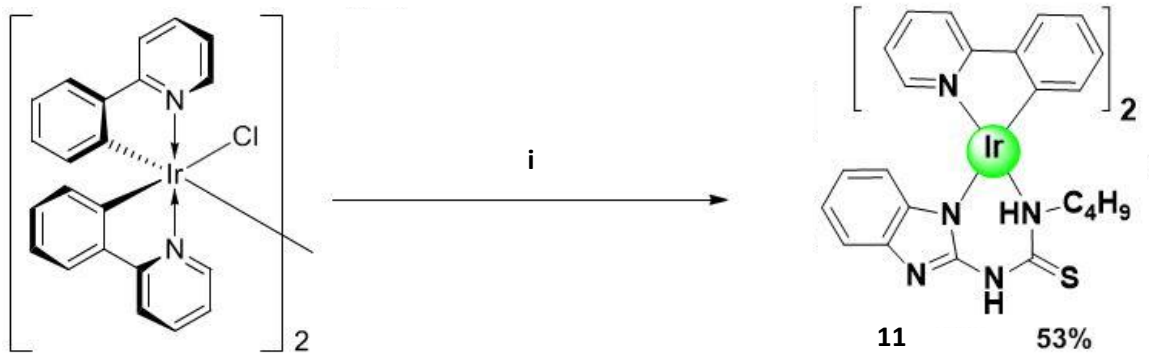

Reagents and Conditions: (i) iridium (ppy)-chloro dimer, butylthiourea, K_2CO_3, toluene, reflux, 22 h.

To a solution of 25 mL dry toluene, Iridium (ppy)-chloro dimer (145 mg, 1.35 x 10^{-4} mol) and butylthiourea (83 mg, 2.5 equiv) were added with potassium carbonate (184 mg). The mixture was stirred for 22 h under N^2 atmosphere resulting in a bright yellow solution. The reaction mixture was cooled to room temperature and diluted with dichloromethane. Extraction with water (2x20 mL) removed the excess base. The organic layers were separated, combined and dried over $MgSO_4$ resulting in a yellow solid which was further purified. Solids were dissolved in chloroform and hexane was added dropwise while stirring, until a precipitate formed. Solids were filtered via suction filtration and dried under vacuum on Schlenk line for 24 h. Final product: bright yellow powder in (53 mg, 53% yield).

EA for $C_{34}H_{31}IrN_6S$: Calculated: C, 54.60; H, 4.18; N, 11.24. Obtained: C, 54.26; H, 4.11; N, 11.22. **EI-MS *m/z*** calculated: 749.2033. Found: 749.2038 **[M+]**.

2.5.4 Compound 12

Iridium (ppy)-butyl-guanidine

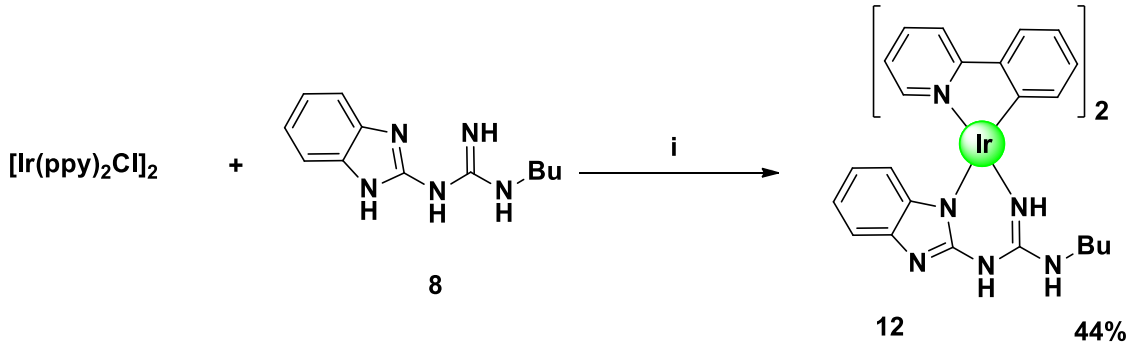

Reagents and Conditions: (i) IR-chloro-bridged dimer[4] ($[Ir(ppy)_2Cl]_2$), butylguanidine, K_2CO_3, toluene, 110°C, 16 h.

To a solution of 12 mL of dry toluene, Iridium dimer $[Ir(ppy)_2CL]_2$ (39.7 mg, 3.70 $x10^{-5}$ mol), 2.5 equivalents of compound **8** and 10 equivalents of potassium carbonate were slowly added. The flask was sealed and placed in a 110°C oil bath with the addition of an N_2 atmosphere and stirred overnight. The solvent was then evaporated under a reduced pressure forming a precipitate. To dissolve the solid, 8-12 mL of dichloromethane was added, then to remove excess base the solution was extracted with water (3x20 mL). The organic layers of the extraction were combined, and the solvent evaporated under a reduced pressure. Column chromatography was carried out to purify the sample using silica gel and an eluent system of 10:0.25 - 10:1 DCM to MeOH. Final product: Bright yellow powder and a 44% yield.

^{1}H NMR (600 MHz, 298 K, chloroform-*d*): δ 8.68 (dd, *J* = 5.9, 0.8 Hz, 1H), 8.15 – 8.04 (m, 1H), 7.88 (d, *J* = 8.1 Hz, 1H), 7.78 (d, *J* = 8.0 Hz, 1H), 7.73 (td, *J* = 8.0, 1.6 Hz, 1H), 7.67 (dd, *J* = 7.4, 1.3 Hz, 1H), 7.60 (d, *J* = 7.8 Hz, 2H), 7.15 (d, *J* = 7.9 Hz, 1H), 7.08 (ddd, *J* = 7.3, 5.9, 1.3 Hz, 1H), 7.01 – 6.87 (m, 4H), 6.79 (dtd, *J* = 20.6, 7.4, 1.3 Hz, 2H), 6.68 – 6.62 (m, 1H), 6.43 (dd, *J* = 7.6, 0.8 Hz, 1H), 6.24 – 6.19 (m, 1H), 6.15 (s, 1H), 6.09 (d, *J* = 8.3 Hz, 1H), 5.72 (s, 1H), 4.56 (s, 1H), 3.04 – 2.78 (m, 2H), 1.41 (ddd, *J* = 14.0, 7.1, 3.5 Hz, 2H), 1.23 (dd, *J* = 14.0, 6.6 Hz, 2H), 0.79 (t, *J* = 7.3 Hz, 3H).

^{13}C NMR (100 MHz, 298K, chloroform-*d*): δ 169.15, 168.17, 153.61, 151.88, 151.57, 150.01, 148.83, 147.52, 144.62, 144.47, 141.20, 136.82, 136.51, 133.05, 132.01, 129.72, 124.57, 124.01, 122.63, 121.84, 121.62, 121.33, 121.08, 118.80, 116.86, 110.65, 77.16, 41.06, 30.85, 20.05, 13.76. **EI-MS** *m/z calculated:* 731.2348 *found:* 732.2450 [M+]. **Anal. calcd. for $C_{12}H_{14}N_5$**: C, 55.87; H, 4.41; N, 13.41. Found: C, 55.96; H, 4.31; N, 13.35.

2.5.5 Compound 13

Pyrimido-isoquinolin-3-amine

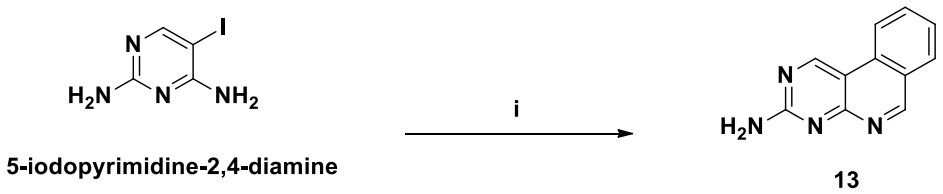

5-iodopyrimidine-2,4-diamine → **13**

Reagents and Conditions: (i) 5-iodopyrimidine-2,4-diamine, 2-formylphenyl boronic acid, K_2CO_3, $Pd(PPh_3)_4$, reflux, 3 h.

To a solution of a 3:1 mixture of dioxane (9 mL) with an addition of water (3 mL), 5-iodopyrimidine-2,4-diamine (197 mg, $8.34x10^{-4}$ mol), 2-formylphenyl boronic acid (182 mg, 1.21 mmol), potassium carbonate (0.461 g, 3.33 mmol) followed by triphenylphosphine palladium (1.4 mg, 0.5 mol%) were all added. The flask was sealed with an addition of a reflux and placed in an oil bath for 3 h under a N_2 atmosphere. The flask was then left to cool to room temperature and submerged in a chilled bath to form precipitate, which from this was filtered then washed with water (2x30 mL). Lastly the precipitate was sonicated in water then dried via vacuum oven (40^{o}C, 24 h). Final product: Bright yellow powder (82 mg, 50% yield).

^{1}H NMR: (400 MHz, 298K, DMSO-d_6,): δ 9.86 (s, 1H), 9.48 (s, 1H), 8.70-8.72 (d, 1H), 8.14-8.16 (d, 1H), 7.88-7.90 (t, 1H), 7.63-7.67 (t, 1H), 7.16 (br, s, 2H, NH_2). **^{13}C NMR:** (100 MHz, 298 K, DMSO-d_6): δ

163.68, 161.43, 158.80, 158.50, 132.58, 132.22, 129.33, 126.43, 124.43, 124.41, 120.35, 107.00. **EI-MS** *m/z calculated:* 196.07 *found:* 197.08 [M+]. **MP:** > 280°C. **EA for $C_{11}H_8N_4$**: Calculated: C, 67.34; H, 4.11; N, 28.55. Obtained: C, 67.19; H, 4.25; N, 28.35.

2.5.6 Compound 14

3, 5-diiodo-2, 6-diaminopyridineamine (Precursor to Compound 14)

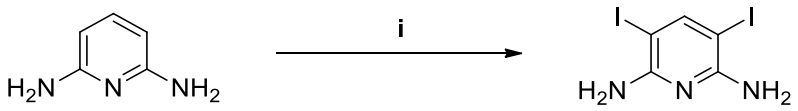

Reagents and Conditions: (i) 2,6-diaminopyridine, N-iodosuccineimide (2.2 equiv), DMF, -30°C, 1 h.

To a solution of DMF (20 mL), 2,6-diaminopyridine (0.99 g, 9.09 mmol) in dry DMF (28 mL) and *N*-iodosuccineimide (4.5 g, 19.9 mmol) were slowly added over 1 h at -30°C in a cooling bath on dry ice. The flask was then raised to cool to room temperature and stirred for a further 1 h with the solution then being poured into a beaker of icy water followed by stirring for 20 mins. The formed precipitate from this was collected via suction filtration and washed with water (2x20 mL) followed by pentane (2x15 mL) before being dried via vacuum oven (40°C, overnight). Final Product: grey solid (3.08 g, 94% yield).

^{1}H NMR: (400 MHz, 298 K, DMSO-d_6): δ 7.73(s, 1H), 5.71(s, 4H) **^{13}C NMR:** (100 MHz, 298K, DMSO-d_6): δ 156.84 (s, C2/6), 153.59(s, C4), 59.96 (s, C3/5).

Compound 14

Benzoisoquinolino-napthypyridine

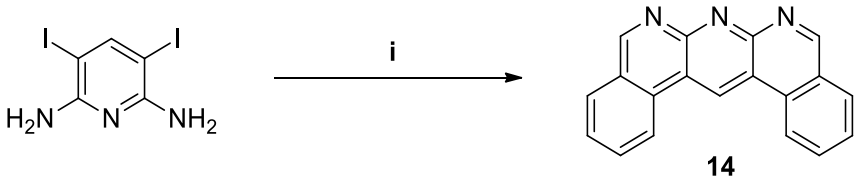

14

Reagents and Conditions: (i) 3,5-diiodo-2,6-pyridinedimine, 2-formylphenylboronic acid, K_2CO_3, $Pd(PPh_3)_4$, dioxane : water (3:1), reflux, 3 h.

To a solution of 3:1 dioxane:water, 3,5-diiodo-2,6-pyridinediamine (0.43 g, 1.21 mmol), 2-formylphenylboronic acid (0.36 g, 2.42 mmol), potassium carbonate (2 g, 0.014 mol) and triphenylphosphine palladium (0.02 g, 1.73 x 10^{-5}mol) were added in a sealed flask with an addition of a reflux and placed in an oil bath for 3 h. The flask was then raised to cool to room temperature and left to stir for 1 h with the formed precipitate then collected via suction filtration and washed with water (2x15 mL) before being dried via vacuum oven (40°C, overnight). Final Product: Yellow powder (98% yield).

^{1}H NMR (400 MHz, 298 K, chloroform-d): δ 7.86-7.90 (t, 2H), 8.03-8.07(t, 2H), 8.21-8.22(d, 2H), 8.90-8.92 (d, 2H), 9.70 (s, 2H), 10.18 (s, 1H). **MP:** > 280^{o}C.

Chapter 3: Analysis of compound anti-cancer activity through MTT cell viability assays

3.1 Introduction

To examine the biological activity of the compounds synthesised in chapter 2, they were tested on the viability of human ovarian cancer cell lines EFO-21, EFO-27 and COLO-704, including their cisplatin-adapted sublines using the 3-(4,5-dimethylthiazol-2-yl)-2,5-diphennyltetrazolium bromide) (MTT) assay. Cisplatin resistant sublines were the focal point due to the broad extent in which the anticancer drug has been used and researched, but also due to resistant mechanisms it has produced in human cancer cells.

When considering the options for cell viability assays there are a variety of techniques used across a wide array of research applications, including MTT, XTT, MTS and Raman Microscopy.[72] The MTT protocol was selected for this cell viability assay due to being one of the most commonly used and robust techniques,[72] whilst allowing for ease of large batch testing with multiple compound types.[73] The assay principle is based on metabolization of the yellow MTT reagent into a purple insoluble formazan compound within the mitochondria of viable cells.[74,75] This colour change from yellow to purple enables for the collection of rapid and coherent cell proliferation data.[65]

3.2 Materials and Apparatus

All compounds were dissolved in DMSO and stored at room temperature prior to the start of the MTT assays.

The cell lines EFO-21, EFO-27 and COLO-704 were purchased from DSMZ (Braunschweig, Germany). The cisplatin-resistant sublines EFO-21^{r}CDDP^{2000} (adapted to 2,000 ng/mL cisplatin), EFO-27^{r}CDDP^{2000}, COLO-704^{r}CDDP^{1000} were obtained from the Resistant Cancer Cell Line (RCCL) collection (https://research.kent.ac.uk/ibc/the-resistant-cancer-cell-line-rccl-collection).

All cell lines were cultured in IMDM (Gibco™ Life Technologies) which was supplemented with 10% (v/v) foetal bovine serum (FBS) (Sigma-Aldrich), 100 IU/mL penicillin (Sigma-Aldrich) and 100 mg/mL

streptomycin (Sigma-Aldrich). PBS tablets (Oxoid Limited) were used to wash all cell lines prior to dissociation. Trypsin (0.25% w/v) (Gibco Life Technologies) was used for dissociation of all adherent cell lines cultured in T25 flasks. MTT (SERVA Electrophoresis – Universal Biologicals) solution was made up in PBS followed by sterile filtering using a vacuum pump. 20% (w/v) SDS (Sigma-Aldrich) solution was prepared using DMF and distilled water in a 1:1 ratio, followed by adjusting the pH to 4.0 using a 1M stock solution of hydrochloric acid (Fisher Scientific). For conducting cell counts, FLUKA Trypan Blue (Sigma-Aldrich) was added to the cells before using a haemocytometer under light microscopy.

A BMG Labtech Fluostar (Omega Plate Reader) was used to read all the assay plates. Multichannel and single tip pipettes were used and purchased from Eppendorf. Clear polystyrene T25cm² tissue culture flasks using a ventilation cap, sterile stripettes and falcon tubes were purchased from Sarstedt. 96 well plates used during all MTT assays were purchased from Greiner Bio-one. Sterile medium reservoirs and drug blocks were used from autoclaved lab supplies.

3.3 Methods

3.3.1 Cell Culture Techniques

All cell lines were cultured in a T25 flask using 10 mL cell culture medium. EFO-21 and EFO-27 cell lines are adherent to surfaces and were passaged as follows; once the T25 flasks had reached around 80% confluence the medium was removed, and the cells were washed with 2 mL PBS. The PBS was then removed and 2 mL of Trypsin (0.25%) was added, followed by the flask being incubated at 37°C/5% CO_2 for around 5 minutes. Once detachment of the cells had been achieved the cells were re-suspended in 8 mL cell culture medium. From this the cells could be used for counting, seeding in 96 well plates or passaging to continue the tissue culture process.

The COLO 704 cells are a suspension cell line and required a modified culture method from the EFO lines. Once the T25 flasks had reached around 80% confluence the cells/medium were transferred to 15 mL falcon tubes followed by centrifuging for 3 minutes at 1000 rpm. Once a pellet of cells had

formed at the base of the falcon the medium was removed, cells dislodged and 2 mL PBS added followed by centrifuging for 3 minutes at 1000 rpm. Once a pellet had reformed the PBS was removed and the cells dislodged followed by adding 1 mL Trypsin (0.25%) and finally adding 9 mL of prepared IMDM medium. From this the cells could be used for counting, seeding in 96 well plates and re-plating in a fresh T25 for continuing the tissue culture process.

3.3.2 MTT colorimetric assay

Medium Setup:

To prevent evaporation of medium in the cell/drug wells, 50 µL of cell culture medium was pipetted into the outer wells of the 96 well plate. Two controls were also set up being 50µl pipetted in row B2-G2 for a positive control and 100 µL pipetted in row B11-G11 for a negative control. For every MTT assay the plates were all initially prepared using this method as seen in Figure 11.

Compound Setup:

All compounds had a starting dose of 50 µM or 20 µM with some using an 8-fold serial dilution of 1:2 or 1:4. These dilutions were made up in a 2 mL drug block with 50 µL of these dilutions being dispensed into the appropriate wells. Two compounds were plated on one 96 well plate for each cell line as seen in Figure 12.

Cell line setup:

Once culturing methods were completed as stated in chapter 3.3.1, 20 µL of re-suspended cells were dispensed into an Eppendorf where a solution of 40 µL Trypan blue and 20µl PBS were added. This cell solution was then viewed under light microscope on a haemocytometer to collect the cell count, then calculating dispensing 7000 cells per 50 µL into each well. 50 µL of cells were dispensed in the positive control (B2-G2) whist 50 µL were dispensed into all the drug wells (B-G/3-10) as seen in Figure 13.

	1	2	3	4	5	6	7	8	9	10	11	12
A	50µl	50µl	50µl	50µl	50µl	50µl	50µl	50µl	50µl	50µl	50µl	50µl
B	50µl	**50µl**									**100µl**	50µl
C	50µl	**50µl**									**100µl**	50µl
D	50µl	**50µl**									**100µl**	50µl
E	50µl	**50µl**									**100µl**	50µl
F	50µl	**50µl**									**100µl**	50µl
G	50µl	**50µl**									**100µl**	50µl
H	50µl	50µl	50µl	50µl	50µl	50µl	50µl	50µl	50µl	50µl	50µl	50µl

Figure 11. Initial IMDM medium setup for MTT cell viability assays.

	1	2	3	4	5	6	7	8	9	10	11	12
A												
B	Compound 1	50µM	25µM	12.5µM	6.25µM	3.125µM	1.562µM	0.781µM	0.390µM	0.195µM		
C		50µM	25µM	12.5µM	6.25µM	3.125µM	1.562µM	0.781µM	0.390µM	0.195µM		
D		50µM	25µM	12.5µM	6.25µM	3.125µM	1.562µM	0.781µM	0.390µM	0.195µM		
E	Compound 2	50µM	25µM	12.5µM	6.25µM	3.125µM	1.562µM	0.781µM	0.390µM	0.195µM		
F		50µM	25µM	12.5µM	6.25µM	3.125µM	1.562µM	0.781µM	0.390µM	0.195µM		
G		50µM	25µM	12.5µM	6.25µM	3.125µM	1.562µM	0.781µM	0.390µM	0.195µM		
H												

Figure 12. Example of a compound layout using a 50 µM concentration with a 1:2 8-fold serial dilution.

	1	2	3	4	5	6	7	8	9	10	11	12
A												
B		**50µl**	50µl	50µl	50µl	50µl	50µl	50µl	50µl	50µl		
C		**50µl**	50µl	50µl	50µl	50µl	50µl	50µl	50µl	50µl		
D		**50µl**	50µl	50µl	50µl	50µl	50µl	50µl	50µl	50µl		
E		**50µl**	50µl	50µl	50µl	50µl	50µl	50µl	50µl	50µl		
F		**50µl**	50µl	50µl	50µl	50µl	50µl	50µl	50µl	50µl		
G		**50µl**	50µl	50µl	50µl	50µl	50µl	50µl	50µl	50µl		
H												

Figure 13. Example of a 96 well plate with cells dispensed in all compound and positive control wells.

Once all cells had been dispensed the plates were incubated at 37°C/5% CO_2 for 5 days before adding 25 µL of MTT solution to each well followed by a 4 hour incubation period at 37°C/5% CO_2 and adding 100 µL of 20% SDS solution to each well followed by a further incubation overnight at 37°C/5% CO_2.

Analysis of MTT plates:

Following overnight incubation, the MTT plates were analysed using an Omega Plate Reader at 600 nm to obtain absorbance values needed for calculating the IC50 values.

3.4 Results: Effects of Thiourea and Guanidine Derivatives Through MTT Analysis.

3.4.1 Compound 1 (carbothiomide) MTT Assay analysis

Of compound **1** a stock solution was worked up in DMSO and a 50 µM start concentration with a 1:4 dilution was plated across all cell lines. Figure 14 displays data from compound **1** with very similar patterns observed between EFO-21 PTL and EFO-27 PTL cell lines whilst greater stability is seen their +CDDP sublines. Whilst averages between the PTL and +CDDP sublines are very similar the margin of error is far higher in both PTL cell lines. COLO-704 PTL is observed to be the least sensitive cell line to this compound whilst its +CDDP subline shares a similar average with EFO-27 +CDDP.

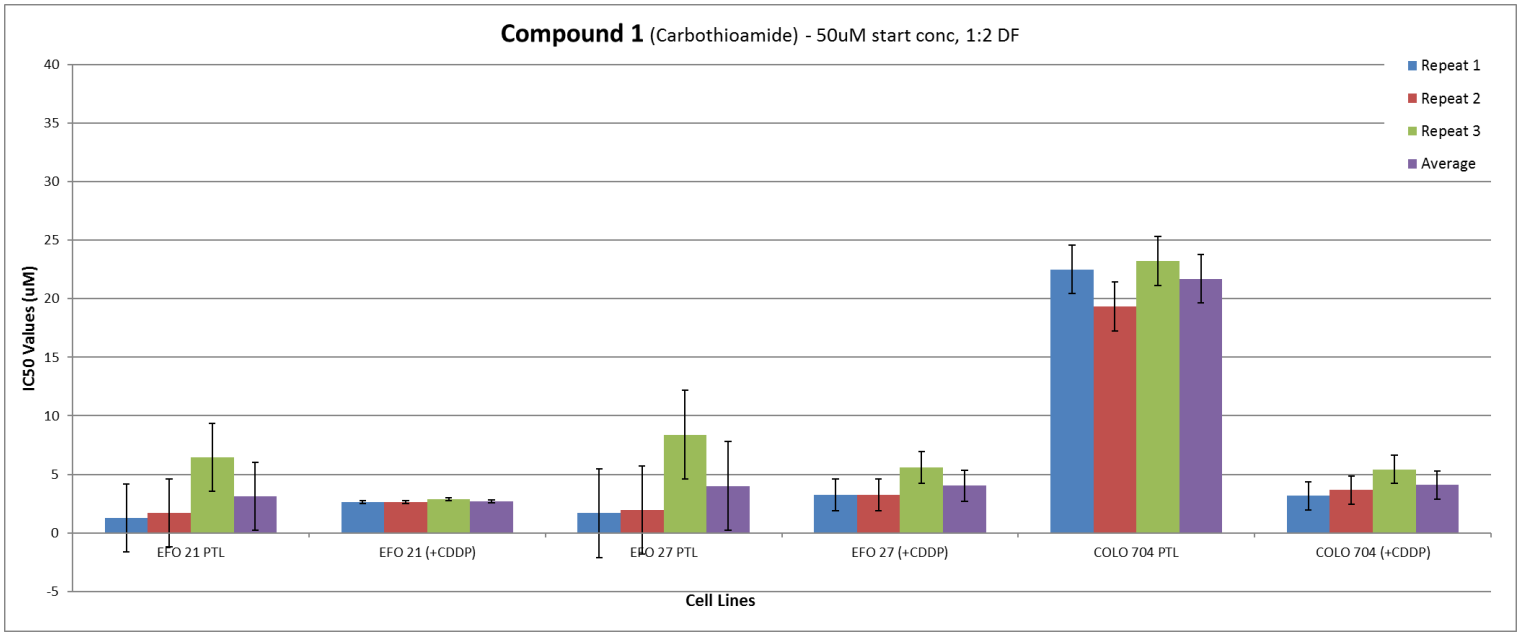

Figure 14. IC50 data of compound 1 against all 6 cell lines. Y-axis represents the concetration of compound needed to achieve the IC50 value in µM. X-axis represents the cell lines used in the assay, with error bars given for the standard deviation of the three repeats.

3.4.2 Compound 2 and 7 (propylamine) MTT Assay analysis

Of compound **2** and compound **7** stock solutions in DMSO were worked up and from this a 50 µM start concentration with a 1:4 dilution was plated across all cell lines. Figure 15 highlights data from the derivatives synthesised with a propylamine chain. Throughout all the cell lines greater sensitivity is observed in the thiourea derivative, compound **2** whilst similar low dose IC50 averages are seen in all

cell lines apart from a slight reduction in sensitivity of EFO-27 +CDDP subline. Throughout the analysis of the guanidine derivative compound **7** the **3** cell lines displayed similar responses with greater resistance seen in their +CDDP sublines although COLO-704 PTL and +CDDP had greater sensitivity overall.

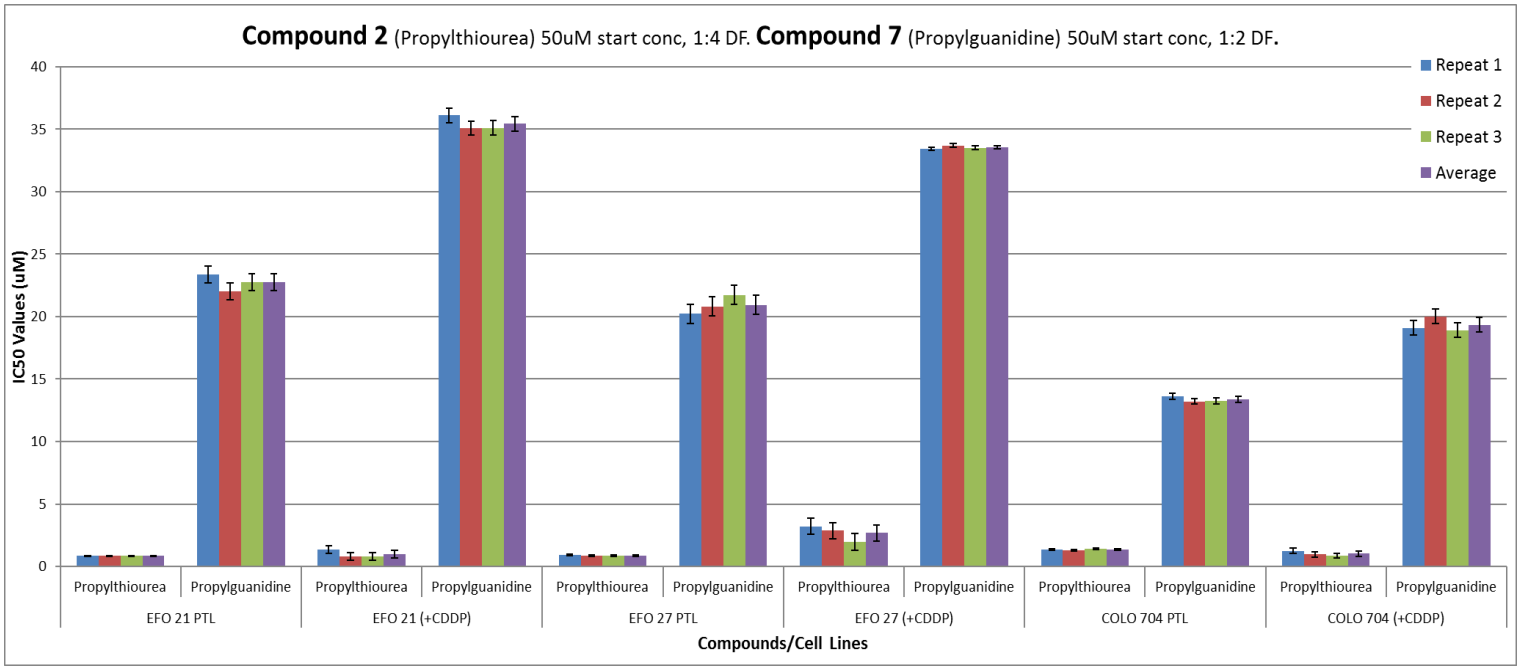

Figure 15. IC50 data of compound 2 and compound 7 against all 6 cell lines. Y-axis represents the concetration of compound needed to achieve the IC50 value in µM. X-axis represents the cell lines used in the assay, with error bars given for the standard deviation of the three repeats.

3.4.3 Compound 3 and 8 (butylamine) MTT Assay analysis

For both compound **3** and compound **8** a stock solution in DMSO was worked up and a 50 µM starting concentration with a 1:2 dilution was plated for compound **3**, whilst a 1:4 dilution was plated across all cell lines for compound **8**. Figure 16 presents IC50 values for the derivatives synthesised using a butylamine chain with cell lines following a similar pattern seen in Figure 15. Greater sensitivity is displayed when the cells are dosed with the thiourea derivative compound **3** whilst similar averages are observed throughout all cell lines.

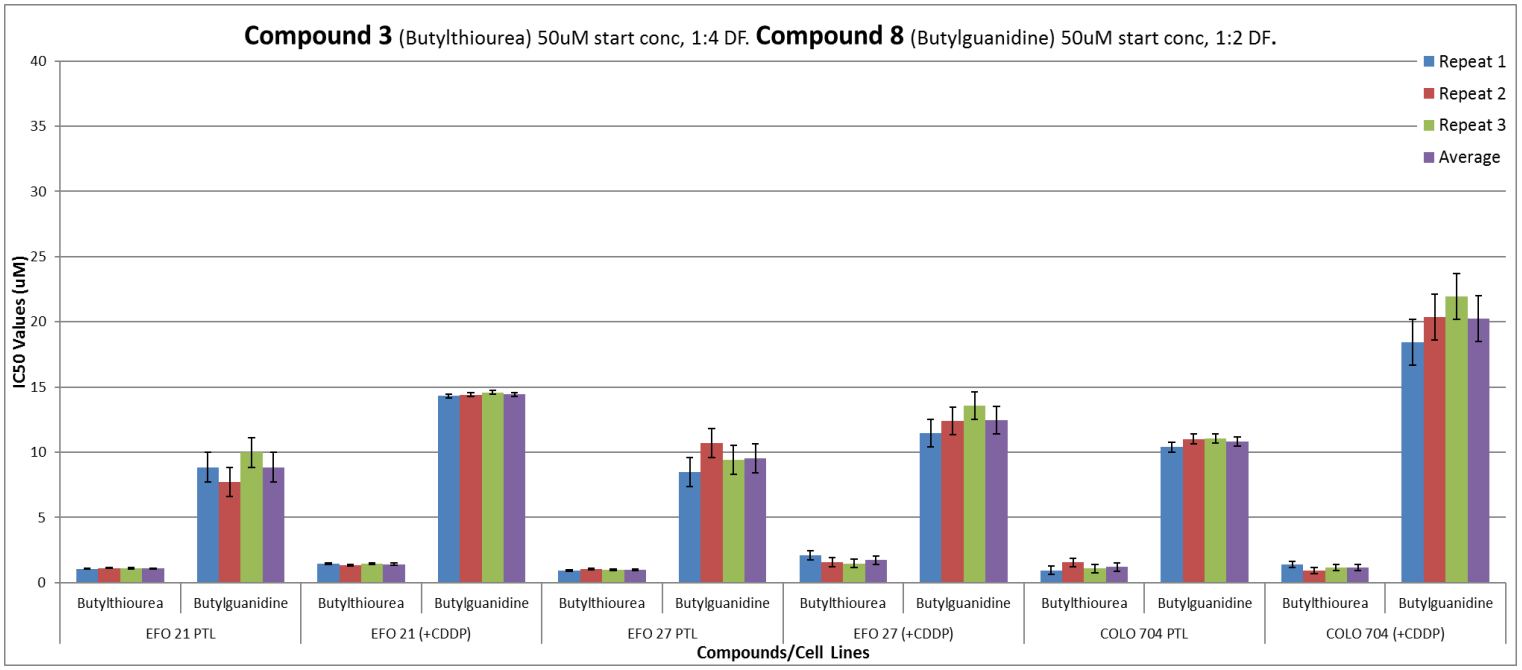

Figure 16. IC50 data of compound 3 and compound 8 against all 6 cell lines. Y-axis represents the concetration of compound needed to achieve the IC50 value in µM. X-axis represents the cell lines used in the assay, with error bars given for the standard deviation of the three repeats.

3.4.4 Compound 4 and 9 (hexylamine) MTT Assay analysis

Figure 17 displays data for the derivatives synthesised with a hexylamine chain, with both compound **4** and compound **9** worked up to a stock solution in DMSO and from this a 50 µM start concentration with a 1:2 dilution was plated across all cell lines. Whilst Figure 15 and Figure 16 select for greater sensitivity in the thiourea derivative compounds, Figure 17 observes greater sensitivity in the guanidine derivative compound **9** throughout all cell lines. A closer examination notes that all PTL cell lines dosed with both derivatives show greater sensitivity when compared to their +CDDP sublines with low error margins produced throughout.

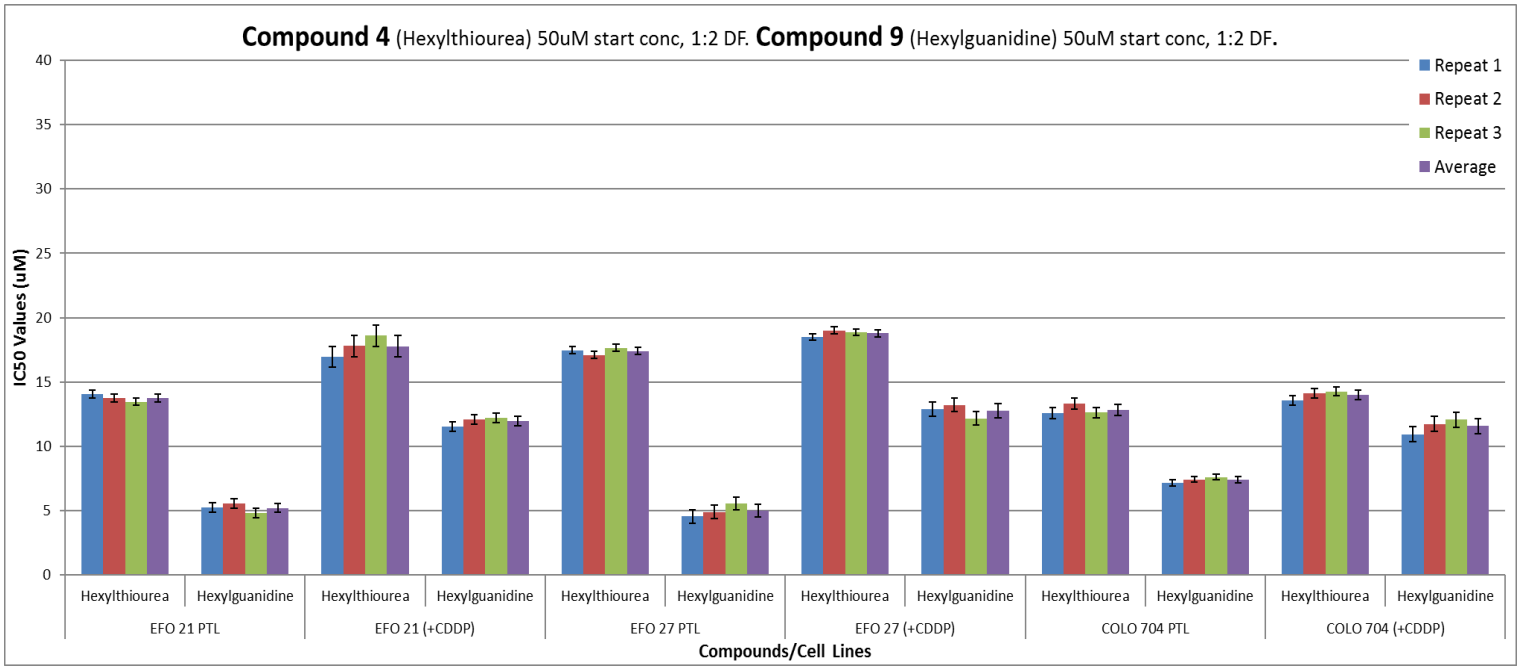

Figure 17. IC50 data of compound 4 and compound 9 against all 6 cell lines. Y-axis represents the concetration of compound needed to achieve the IC50 value in µM. X-axis represents the cell lines used in the assay, with error bars given for the standard deviation of the three repeats.

3.4.5 Compound 5 and 10 (benzylamine) MTT Assay analysis

Of both compound **5** and compound **10** a stock solution in DMSO was worked up and from this a 50 µM start concentration with a 1:2 dilution for the two was plated across all cell lines. Figure 18 depicts analysis of the derivatives synthesised using a benzylamine chain, with greater sensitivity to the thiourea derivative compound **5** observed throughout all cell lines, with EFO-21 and EFO-27 showing greater sensitivity in the PTL cell line. While the majority of data is consistent, there is a high error margin throughout EFO-21 +CDDP, EFO-27 PTL and EFO-27 +CDDP lines although which is not apparent in any other derivatives.

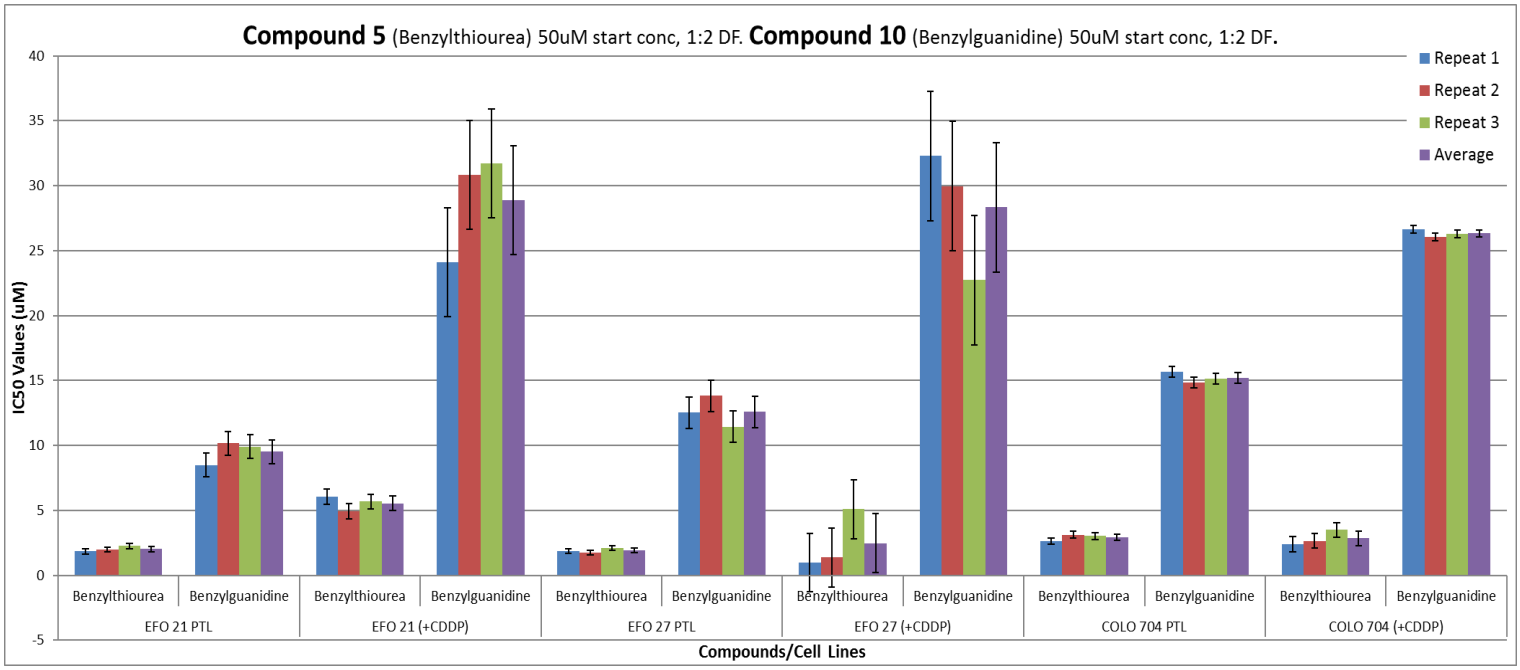

Figure 18. IC50 data of compound 5 and compound 10 against all 6 cell lines. Y-axis represents the concetration of compound needed to achieve the IC50 value in µM. X-axis represents the cell lines used in the assay, with error bars given for the standard deviation of the three repeats.

3.4.6 Compound 6 (methylpyridine) MTT Assay analysis

A stock solution in DMSO was worked up of compound **6** and from this a 50 µM starting concentration was used with a 1:2 dilution plated across the six cell lines. Figure 19 highlights IC50 values from the thiourea derivative compound **6** with a variety of differences noted. Whilst EFO-21 PTL and EFO-27 PTL cell lines were less sensitive to compound **6** then their +CDDP sublines, COLO-704 PTL cells were more sensitive than their +CDDP sublines. COLO-704 PTL and +CDDP sublines are observed to have greater sensitivity overall than both EFO-21 and EFO-27 PTL/+CDDP with a lower dose concentration needed to achieve the IC50 value.

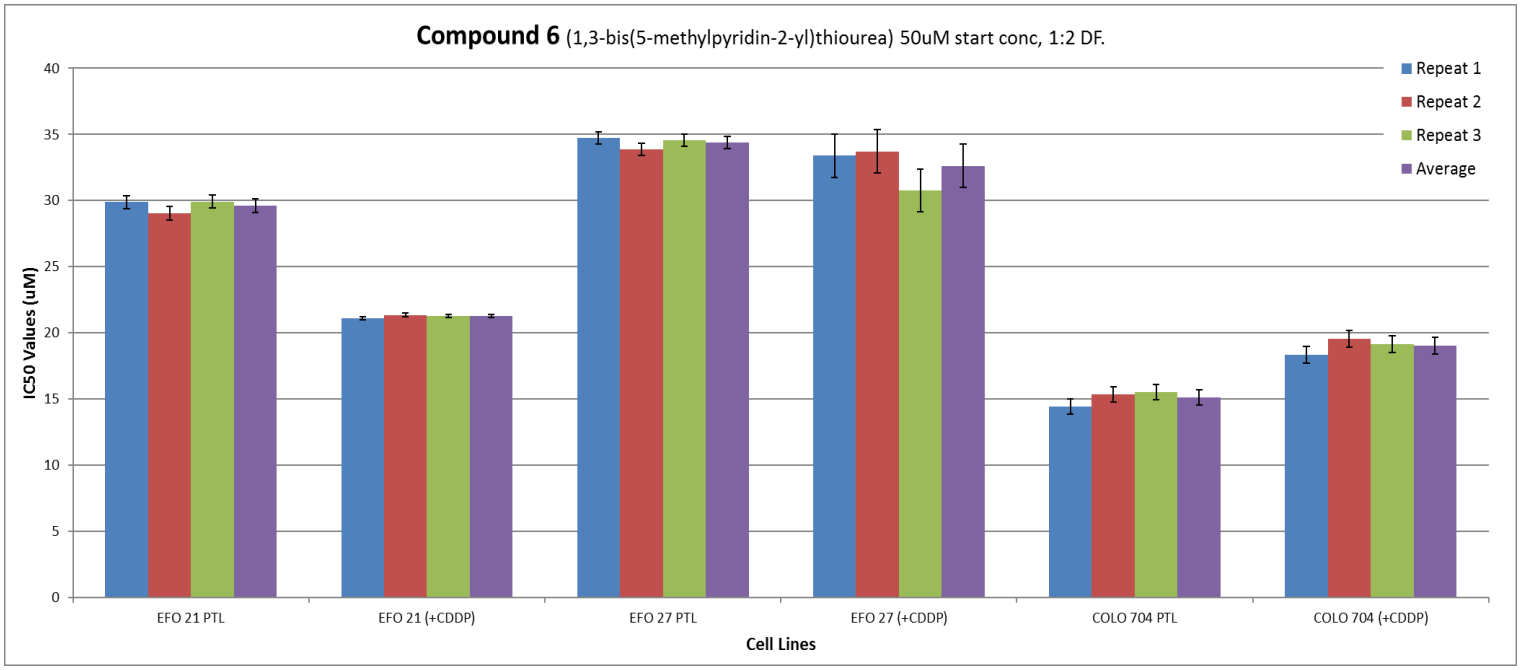

Figure 19. IC50 data of compound 6 against all 6 cell lines. Y-axis represents the concetration of compound needed to achieve the IC50 value in µM. X-axis represents the cell lines used in the assay, with error bars given for the standard deviation of the three repeats.

3.5 MTT analysis: Effects of Iridium Complex Compounds

3.5.1 Compound 11 and 12 (Thiourea/Guanidine IR-Complex's MTT Assay analysis)

Of compound **11** a stock solution in DMSO was worked up with a 50 µM starting concentration used with a 1:4 dilution plated for EFO-21 PTL and EFO-27 PTL cell lines whilst a 1:2 dilution plated for the remaining cell lines. For compound **12** a stock solution in DMSO was worked up and from this a 20 µM starting concentration with a 1:2 dilution was plated across the six cell lines. Figure 20 displays data from the thiourea and guanidine iridium complex's, throughout all cell lines there was an observed sensitivity to the guanidine complex compound **12** with consistent IC50 concentrations noted throughout all PTL and +CDDP sublines when comparing to the thiourea complex compound **11**. Analysis of compound **11** against all cell lines observed all +CDDP sublines to be less sensitive in comparison to all PTL's lines, although COLO-704 PTL and +CDDP sublines were observed to have greater sensitivity out of all the cell lines.

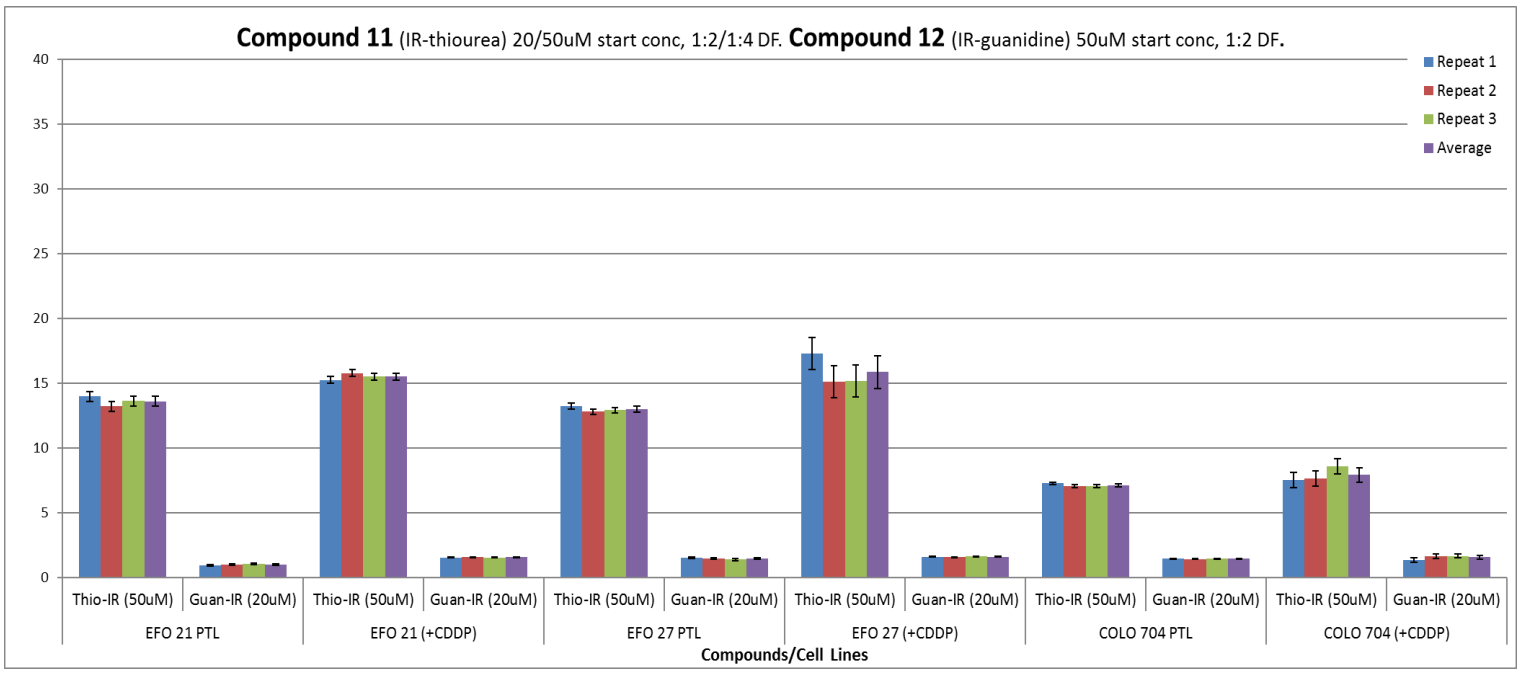

Figure 20. IC50 data of compound 11 and compound 12 against all 6 cell lines. Y-axis represents the concetration of compound needed to achieve the IC50 value in µM. X-axis represents the cell lines used in the assay, with error bars given for the standard deviation of the three repeats.

3.5.2 Compound 13 MTT Assay analysis

A stock solution in DMSO was worked up of compound **13** and from this a 50 µM starting concentration was used with a 1:2 dilution plated across the six cell lines. EFO-21 +CDDP and EFO-27 +CDDP sublines are observed in Figure 21 to have a slightly greater sensitivity then their PTL cell lines, whilst COLO-704 PTL and +CDDP sublines display consistent sensitivity when dosed with compound **13**.

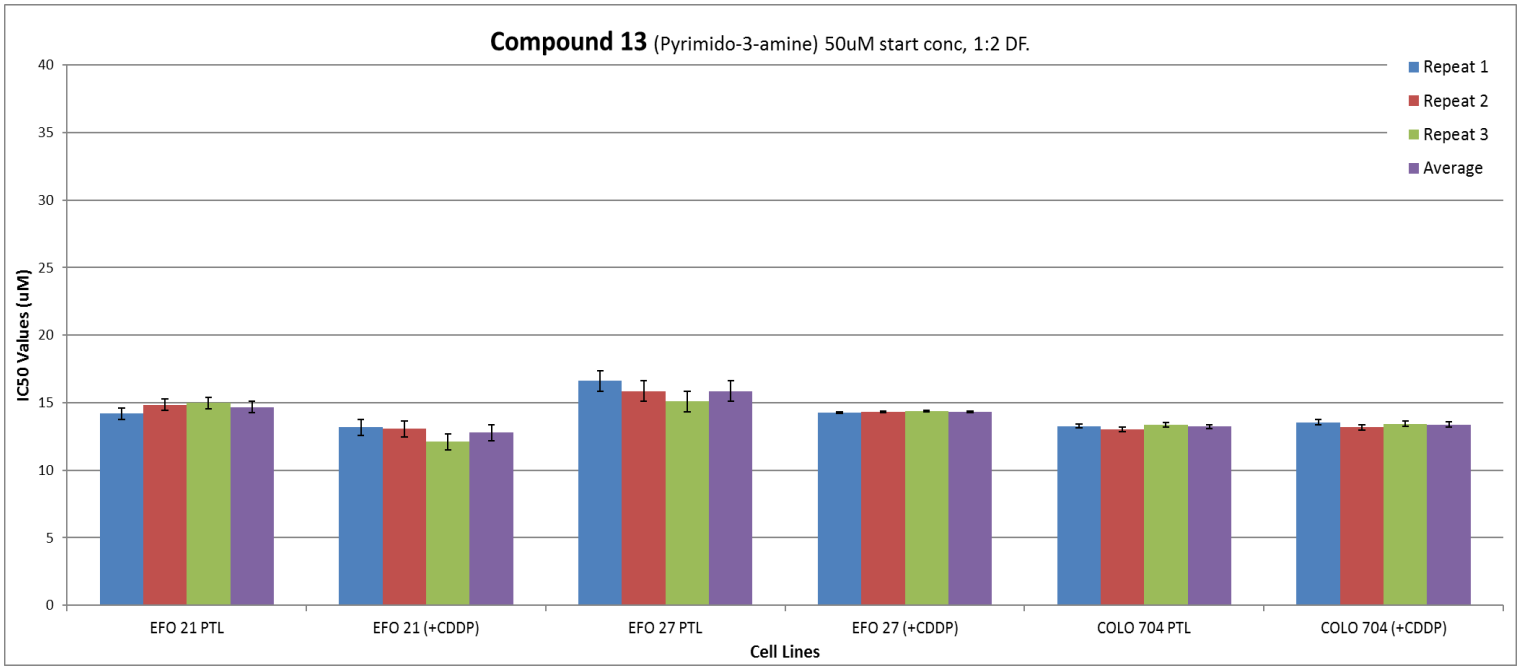

Figure 21. IC50 data of compound 13 against all 6 cell lines. Y-axis represents the concetration of compound needed to achieve the IC50 value in µM. X-axis represents the cell lines used in the assay, with error bars given for the standard deviation of the three repeats.

3.5.3 Compound 14 MTT Assay analysis

Of compound **14** a stock solution in DMSO was worked up with a 50 µM starting concentration used with a 1:2 dilution plated across the six cell lines. Figure 22 exhibits the effects of compound **14** against all cell lines. EFO-21 and EFO-27 PTL cell lines show similar patterns to compound **13** where by their +CDDP subline is observed to show greater sensitivity to compound **14** then both the PTL cell lines. COLO-704 cell lines slightly differ with the PTL cell line showing greater sensitivity then the +CDDP subline but also EFO-21 and EFO-27 PTL cell lines. The COLO-704 +CDDP subline was observed to have the greatest resistance when comparing all resistant lines.

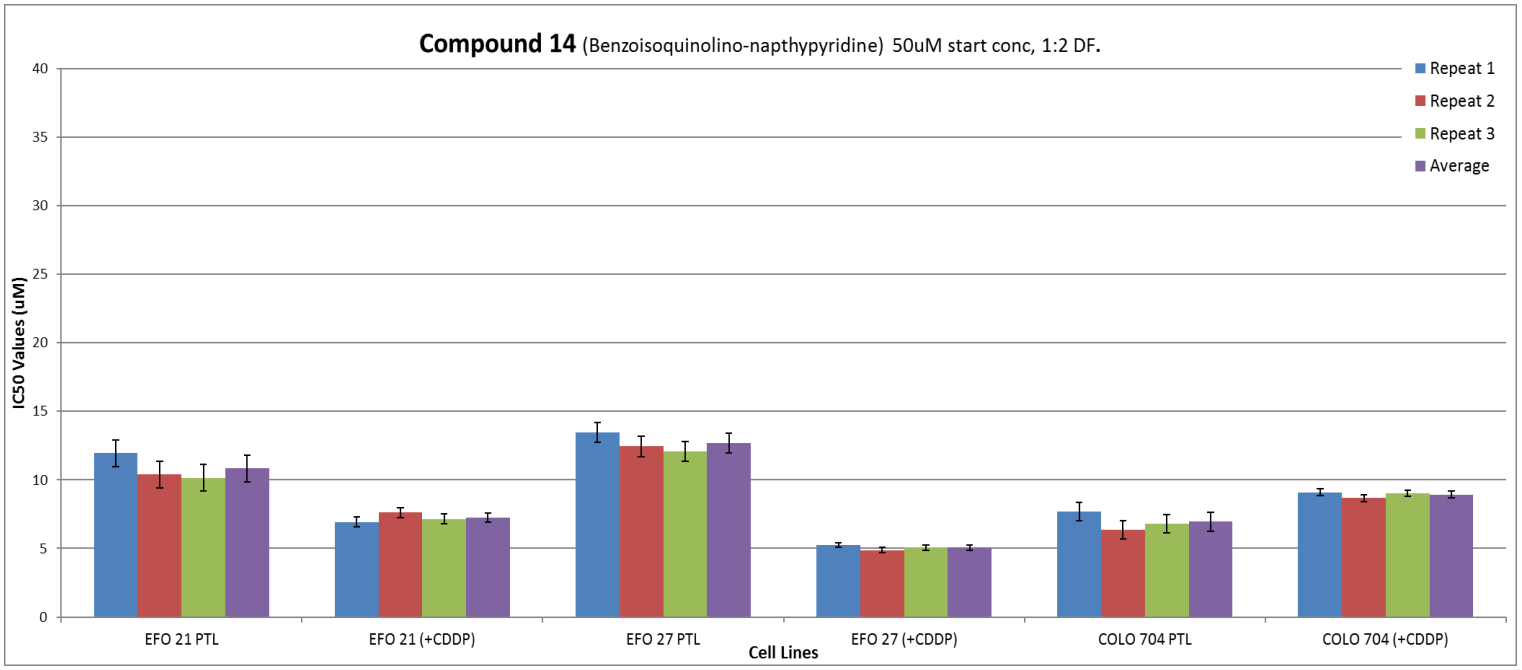

Figure 22. IC50 data of compound 14 against all 6 cell lines. Y-axis represents the concetration of compound needed to achieve an IC50 value in µM. X-axis represents the cell lines used in the assay, with error bars given for the standard deviation of the three repeats.

3.6 Discussion

Evaluation of the MTT cell viability assays reveals a vast array of promising IC50 data ranging between 0.8-35 µM. Throughout compounds **1**-**14** significant differences in toxicities are noted as seen in Figure 23, providing us with a theraputic window observing compounds displaying selectivity rather than killing all cells outright. By calculating the standard deviation of the 3 repeat assays per cell line/compound, we were able to include error margins to figures 14-22.

When comparing the overall effectiveness of the thiourea and guandine derivatives which share the same amine chains, the data collected is varied with no clear indication whether thiourea or guanidine structures are more successful overall (Figure 23/Table 1). The thiourea derivatives synthesised with a propylamine, butylamine and bezylamine chains, compounds **2**, **3** and **5** displayed greater sensitivity to all six cell lines than their guanidine counterparts compound **7**, **8** and **10**. It was expected the thiourea derivative compound **4** (hexylamine) may follow suit, but this displayed greater sensitivity in its guanidine counterpart compound **9**, as did the iridium complex compound **12**.

Closer examination of the data highlights compounds **2**, **3** and **12,** which share similar low dose responses between 0.8-1.5 µM which are not displayed in the other 11 compounds (Figure 23). Alongside the IC50 values, compounds **2** and **3** were some of the few structures which were dosed at a dilution factor of 1:4. This was due to attempts in using a dilution factor of 1:2 causing non-viable cells throughout the MTT plates and cell lines, with an IC50 value unable to be calculated, also suggesting the high potentcy of these compounds. It could be considered that with these compounds exhibiting similar low dose responses with low error repeats, they share a similar mode of action once uptaken by the cell which would require confirmation through further analysis.

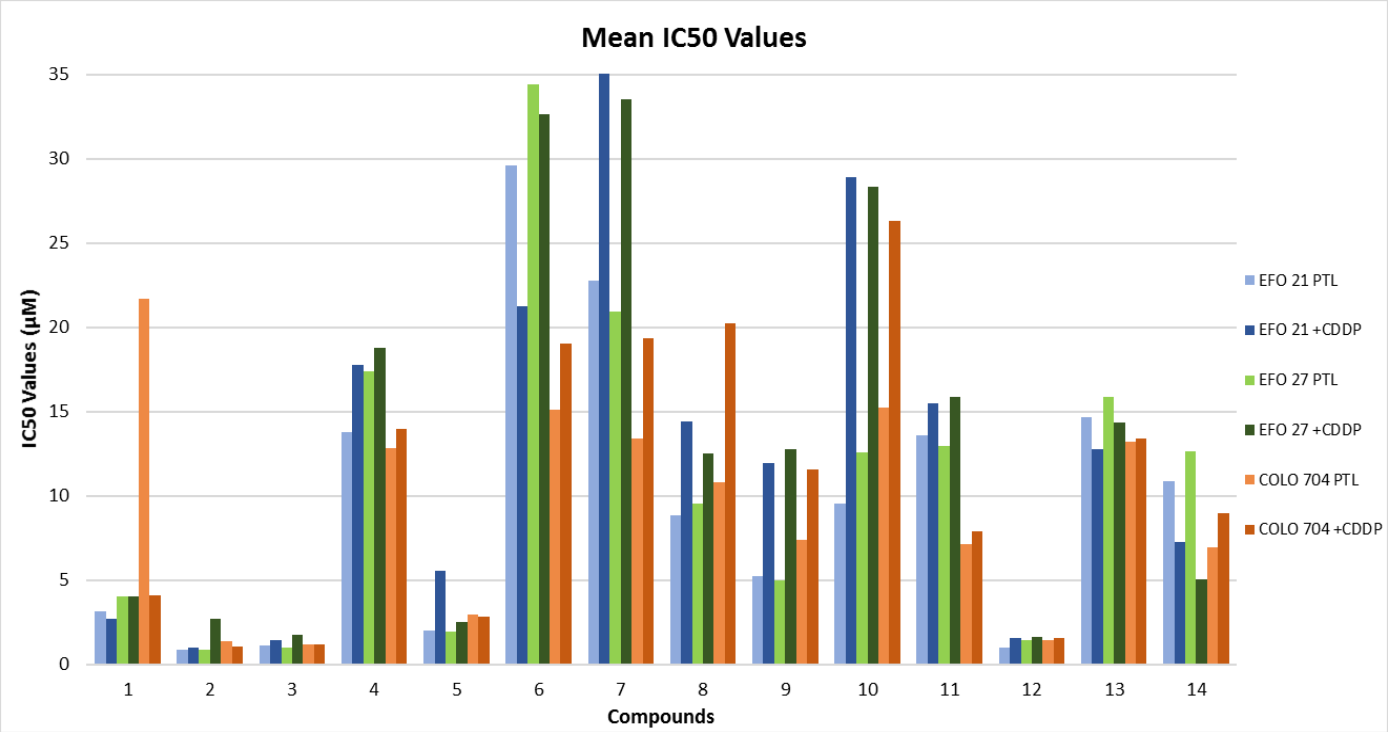

Figure 23. Bar chart displaying the mean IC50 values of the 3 MTT repeats for each compound and cell lines.

Compounds	Mean IC50 Values (μM)					
	EFO 21 PTL	EFO 21 +CDDP	EFO 27 PTL	EFO 27 +CDDP	COLO 704 PTL	COLO 704 +CDDP
1	3.1	2.7	4.0	4.0	21.7	4.1
2	0.8	1.0	0.9	2.7	1.4	1.0
3	1.1	1.4	1.0	1.7	1.2	1.1
4	13.8	17.8	17.4	18.8	12.8	14.0
5	2.0	5.5	1.9	2.5	2.9	2.8
6	29.6	21.3	34.4	32.6	15.1	19.0
7	22.7	35.4	20.9	33.5	13.4	19.3
8	8.9	14.4	9.5	12.5	10.8	20.3
9	5.2	11.9	5.0	12.8	7.4	11.6
10	9.5	28.9	12.6	28.3	15.2	26.3
11	13.6	15.5	13.0	15.9	7.1	7.9
12	1.0	1.6	1.5	1.6	1.4	1.6
13	14.7	12.8	15.9	14.3	13.2	13.4
14	10.8	7.2	12.7	5.1	6.9	8.9

Table 1. Table displaying the mean IC50 values of the 3 MTT repeats for each compound and cell line.

While these low dose similarities may be expected between compounds **2** and **3** due to the small structural difference between them (Figure 24), it would be expected that compound **12** may also be structurally similar. This is not the case as displayed in Figure 24, whilst compound **12** bears the same butylamine chain as compound **3** the rest of the structure is significanty different being one of the two iridium complexes. Compound **12** incorporates the guanidine derivatve compound **8**, yet there is a 3 fold increase in the effectiveness of compound **12** when comparing to compound **8** suggesting the irdium complex increases toxicity. When comparing to the first iridium complex Compound **11**, this incorporates the thiourea derivative compound **3**, yet an opposite effect is observed being that compound **3** exhibits greater sensetivity then compound **11**. This MTT data would suggest that it only requires a small change between a sulfur ion to an NH group to drastically increase the sensitivity and success of the iridium complexes.

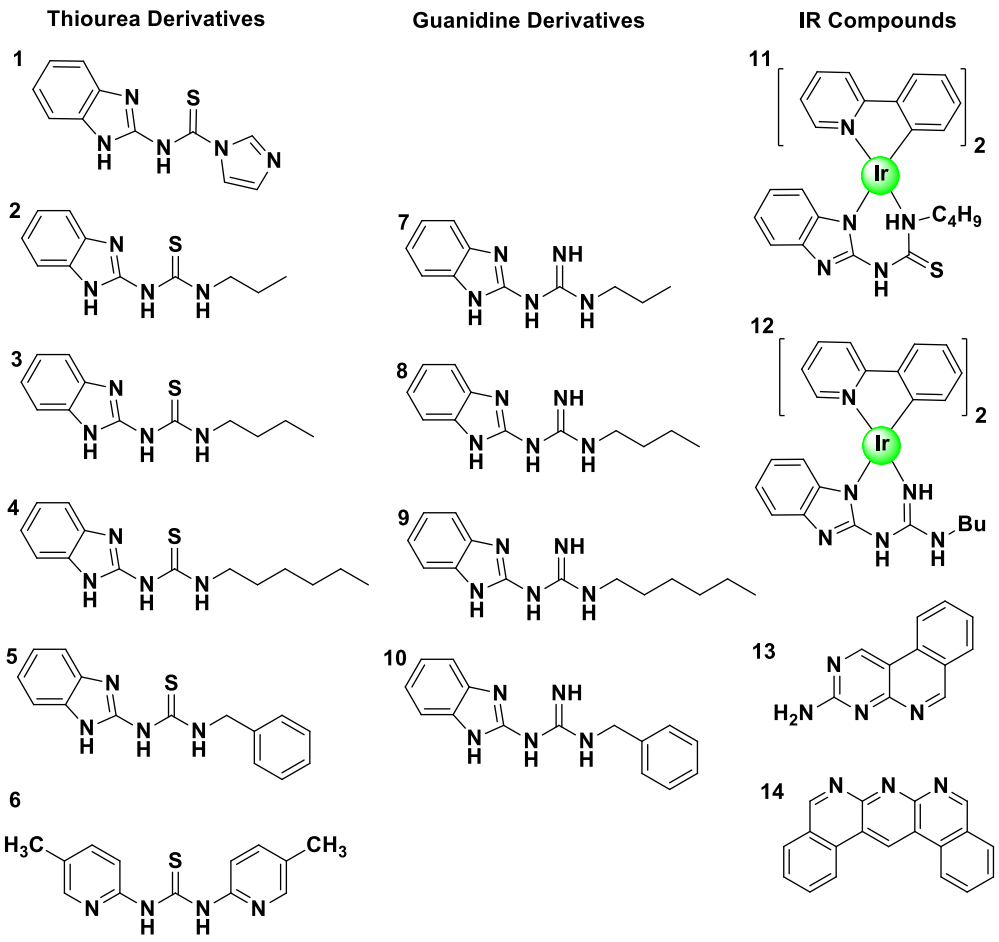

Figure 24. Structures of compounds 1-14.

Compounds **1**, **5** and **10** express the highest error margins in comparison to the remaining compounds. There are similar patterns observed in compound **1** through all repeats although these carry unacceptable error margins, whilst COLO-704 parental line has a far higher dose response and EFO-21 resistant subline exhibits consistant low dose data. The inconsistencies in compound **1** may indicate several causes including the compound having no specific target, causing cytostatic growth effects of the cell lines or there may be a potetntial stability issue of the compound itself. Both benzylamine derivatives display some high error margins, compound **5** displays a high level of error in the EFO-27 reistant subline, whilst it is observed in compound **10** to be in both EFO-21 and EFO-27 resistant sublines. As these error margins are only recognised in the sublines it may be that these compounds struggle to subdue the mechanisms of these resistant sublines, rather then an issue with the compounds stability.

The importance of IC50 values between parental cell lines and cisplatin-adapted sublines must be considered when reviewing the MTT data. Compounds **2**, **3**, **4**, **5**, **12**, **13** and **14** all shared similarities in IC50 values between the three parental cell lines and their cisplatin resistant sublines, whilst compounds **13** and **14** are observed to have a slightly higher activity in EFO-21 and EFO-27 cisplatin resistant sublines, seen throughout all the repeats. The similaraties indicate that these compounds are not susceptible to the restant mechanisms presented by the cisplatin reistant sublines, thus achieving the same sensitivity as within the parental cell lines. Greater sensitivity in compound **13** and **14** is displayed in the cisplatin resistant sublines, initially suggesting these two compounds are more effective in treating the resistant cell lines then the parental cell lines, and have potentially overcome the resistant mechanisms. While this is a promising assement, on closer inspection of the data there is not a significant enough difference to come to a firm conclusion when comparing to the whole dataset, although these compounds were the only two to display such results. Treating resistant cells is a crucial challenge in cancer therapies,[83] but these compounds have shown promise in being able to tackle the mechanisms presented by these resistant overian cancer sublines.

While keeping in mind the range of the IC50 values achieved through these assays, it has been suggested that an IC50 figure which is between 10-100 µM may not nessessarily be an ideal candidate for *in vivo* studies, due to the quantities of compound which would be required to upscale into the human body to observe the same desired effect.[55] In this instance compounds **2**, **3**, **5**, **12** and **14** achieved successful IC50 concentrations below a 10 µM dose in both parental lines and cisplatin resistant sublines, and should be considered for further studies.

Whilst the MTT technique remains an ever popular and confident cell viability assay throughout literature, limitations must be considered when studying the data.[80] It has been highlighted that in some cases, results can be influenced due to compound modifications causing cellular metabolism changes,[79] but also compound interactions with the MTT dye itself effecting the expression when analysing via a plate reader are possible.[81]

Chapter 4: Confocal microscopy of iridium complex compounds

4.1 Introduction

Confocal microscopy was used for qualitative assessment of EFO-21 and EFO-27 parental and cisplatin resistant sublines when dosed with compound **11** and compound **12**, to potentially observe expression differences in cellular uptake between the two iridium complexes. As differences were noted between compound **11** and compound **12** during MTT viability assays, it would be expected that there are uptake differences between the thiourea and guanidine complexes and this may be seen through confocal microscopy assays. The Colo-704 cell lines could not be used in this assay due to poor adhesion to the cover slips even when using an adhesion activator Poly-l-lysine.

4.2 Materials and Methods

Materials

Iridium complex compounds **11** and compound **12** tested were dissolved in DMSO and stored at room temperature prior to the assay.

The cell lines EFO-21, EFO-27 and COLO-704 were purchased from DSMZ (Braunschweig, Germany). The cisplatin-resistant sublines EFO-21^{r}CDDP^{2000} (adapted to 2,000 ng/mL cisplatin), EFO-27^{r}CDDP^{2000}, COLO-704^{r}CDDP^{1000} were obtained from the Resistant Cancer Cell Line (RCCL) collection (https://research.kent.ac.uk/ibc/the-resistant-cancer-cell-line-rccl-collection). All cell lines were cultured in IMDM (Gibco™ Life Technologies) which was supplemented with 10% (v/v) foetal bovine serum (FBS) (Sigma-Aldrich), 100 IU/mL penicillin (Sigma-Aldrich) and 100 mg/mL streptomycin (Sigma-Aldrich). PBS tablets (Oxoid Limited) were used to wash all cell lines prior to dissociation. Trypsin (0.25% w/v) (Gibco Life Technologies) was used for dissociation of all adherent cell lines cultured in T25 flasks. 24 well plates used during the confocal assays were purchased from Greiner Bio-one. Sterile reservoirs, cover slips, and forceps were used from lab supplies and autoclaved prior to each use.

Methods

Cells were cultured following methods seen in chapter 3.3.1. Sterile cover slips were added to each of the 5 test wells per 24 well plate, with one plate per cell line to minimise contamination. From this each cell line was split as following methods from chapter 3.3.1 and were seeded at $5x10^{-4}$ cells per well, with a total well volume of cells/medium at 2ml. Once seeded the cell lines were then dosed with compound **11** besides compound **12**, with the dose calculated by the average result of IC50 value repeats obtained from the MTT assays seen in chapter 3.4 with the averages displayed in Table 2.

	EFO-21 PTL	**EFO-21 +CDDP**	**EFO-27 PTL**	**EFO-21 +CDDP**
Compound 11	13.60uM	15.50uM	12.97uM	15.85uM
Compound 12	1.00uM	1.55uM	1.45uM	1.58uM

Table 2. Table showing the average IC50 values of compound 11 and 12 against the 4 cell lines used.

3 controls were also set up per cell line. This included control 1 being a negative control with only cells and no drug or DMSO. Control 2 being just cells with an addition of DMSO which was comparable to the amount of drug dosed in compound **11**. Whilst the final control 3 being just cells and an addition of DMSO which was comparable to the amount of drug dosed in compound **12**, with the plate layout observed in Table 3. The DMSO controls 2 and 3 were included to observe whether the solvent may impact cell growth when comparing to the 'just cells' control 1. Once the plate setup was complete the samples were then left to incubate at 37°C/5% CO_2 for 24hrs.

	1	**2**	**3**	**4**	**5**	**6**
A	Comp 11 *IC50 dose*	Comp 12 *IC50 dose*	Control 1 *Just cells*	Control 2 *DMSO (comp 11)*	Control 3 *DMSO (comp 12)*	
B						
C						
D						

Table 3. Example of the 24 well plate layout for the 4 cell lines.

After incubation the cells were assessed for a confluency of at least 40% before use. The medium in each well was aspirated followed by washing the cells with 0.5 mL PBS twice. After the PBS wash, the cells were then fixed with 0.3 mL of 4% paraformaldehyde in PBS solution and left to sit at room temperature for 15-20 minutes followed by a further PBS wash repeated 3 times. The slides were then removed from the 24 well plates and mounted on microscope slides cell side face down with Prolong Diamond Antifade Mountant and DAPI (4',6-Diamidine-2'-phenylindole dihydrochloride) between the two slides. The samples were then left to dry for 10 hours in a light protected box prior to imaging on a Zeiss Leica LSM880 confocal microscope using x63 magnification and an oil immersion lens.

4.3 Results

The brightness, gain and excitation of the confocal microscopes laser for compound expression was kept consistent throughout the assays, although slight adjustments were made to the brightness of the DAPI stain to achieve a clear nuclei mapping image. The DMSO control images for all cell lines and compounds were taken whilst the blue (DAPI) and green (Compound **11** + **12**) spectra were highlighted, with only the nuclei DAPI stain fluorescing in the images this suggests that any green fluorescence seen in the compound additions will only be from the uptake of either compound.

Figure 25 depicts results from 'control 1 - Just cells', the nuclei expression for all four cell lines grown in standard conditions as seen throughout the MTT assays with no additions of either compounds or DMSO. The slight difference in the distribution of cells seen between EFO-21 PTL and the rest of the cell lines was due to slight confluency differences of the plate wells. These images resemble expected cell morphology and are a secure negative control to refer to.

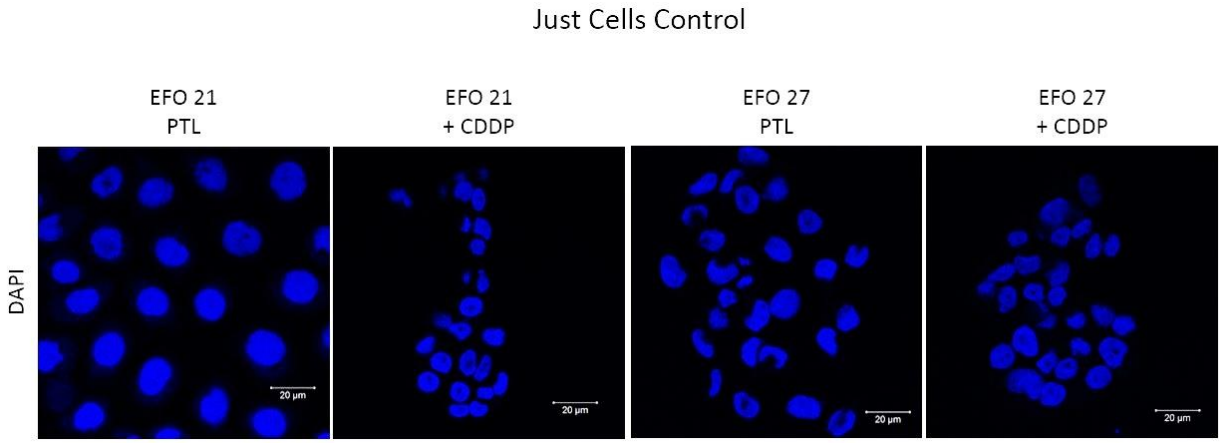

Figure 25. Control 1- Just cells control grown in normal conditions with no addition of DMSO or compound.

Figure 26 highlights EFO-21 PTL when dosed with compounds **11** and **12** using the IC50 value achieved during MTT viability assays. The DMSO control suggests this cell line is not affected by the volume of solvent used in the addition of compound and the nucleus share the same morphology seen in control 1. The expression of both compounds observes uptake into the cells being clear in the overlay of compound/DAPI being a complete cell. Whilst a qualitative assessment of these images would suggest that compound **12** has a higher uptake into the cell cytoplasm when comparing to compound **11**.

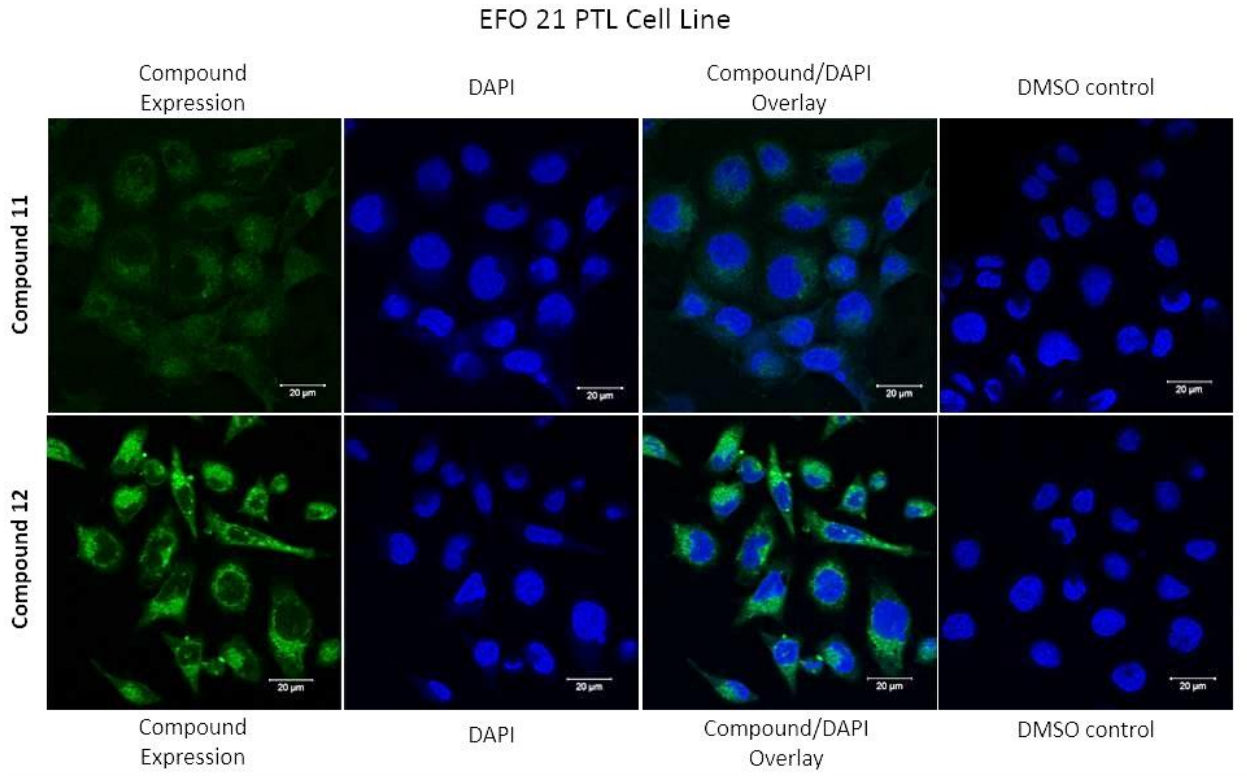

Figure 26. EFO-21 PTL cell line subject to compound 11 and compound 12 dosed at the IC50 concentrations achieved via MTT assays.

Figure 27 depicts EFO-21 +CDDP subline when dosed with compounds **11** and **12** using the IC50 value achieved during MTT viability assays. The DMSO control is consistent with control 1 suggesting this resistant subline is not affected by the volume of solvent applied in the addition of compound. A qualitative assessment of Figure 27 suggests similarities seen in the EFO-21 parental line, whereby compound **12** has a higher uptake into the cell in comparison to compound **11**.

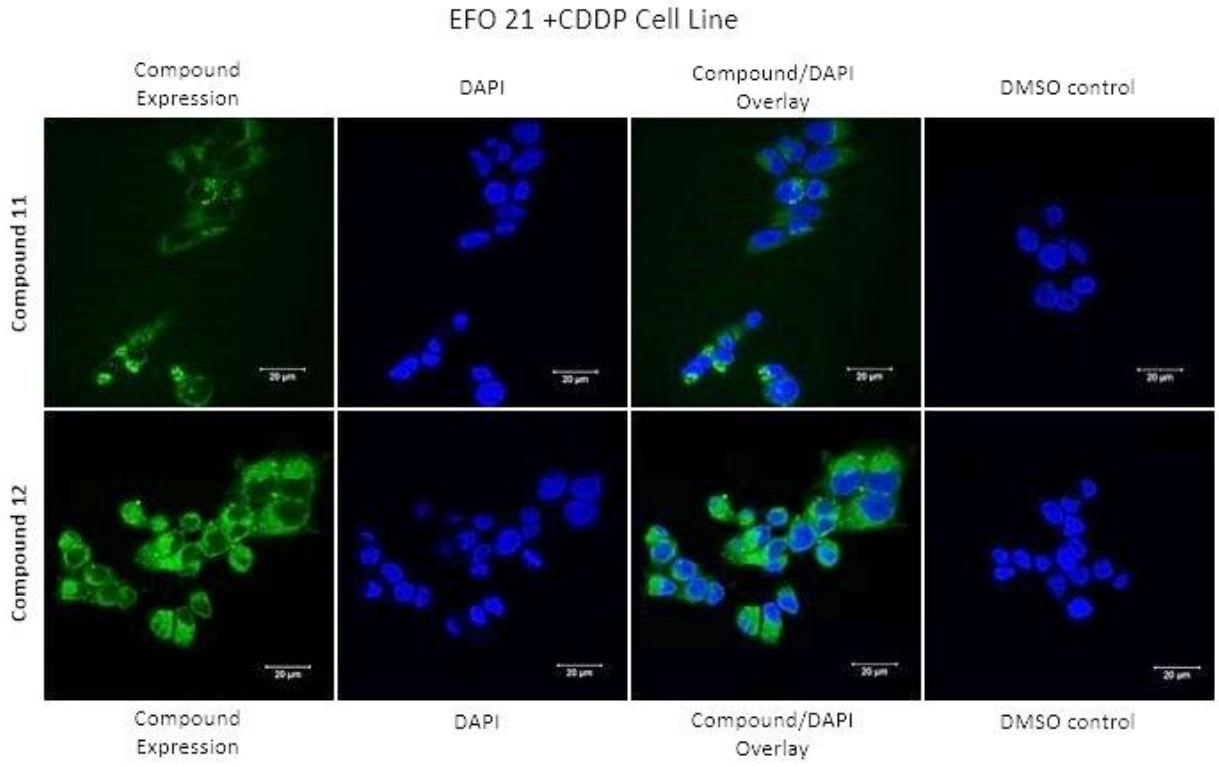

Figure 27. EFO-21 +CDDP subline subject to compound 11 and compound 12 dosed at the IC50 concentrations achieved via MTT assays.

Figure 28 illustrates EFO-27 PTL when dosed with compounds **11** and **12** at the IC50 value achieved during MTT viability assays. When comparing the DMSO control and 'just cells' control 1 the similarities in nuclei morphology would suggest this parental line is unaffected by the volume of solvent used in the addition of compounds. A qualitative assessment of this parental line shares similarities with both EFO 21 cell lines seen in Figure 26 and Figure 27, where by a greater uptake of compound is seen in compound **12** in comparison to compound **11**.

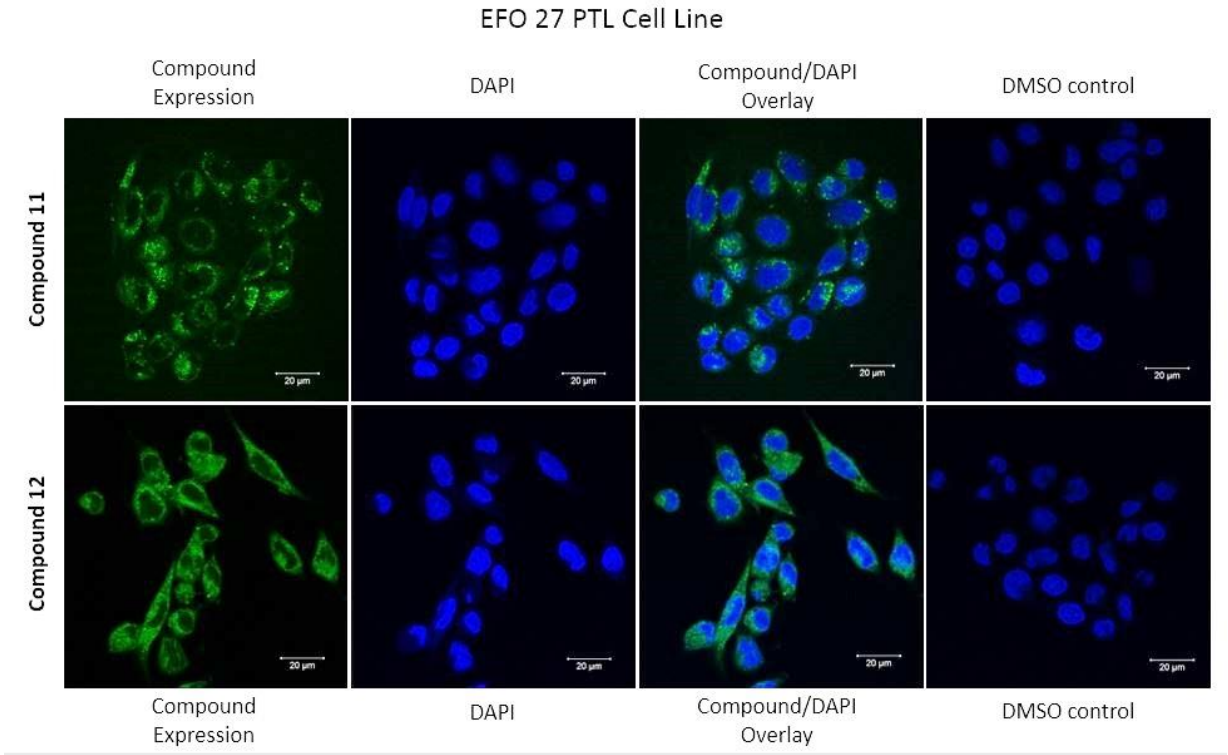

Figure 28. EFO-27 PTL cell line subject to compound 11 and compound 12 dosed at the IC50 concentrations achieved via MTT assays.

Figure 29 presents the confocal images from EFO-27 + CDDP subline when dosed with compounds **11** and **12** at the IC50 value acquired during MTT viability assay. As seen in all other cells lines the DMSO control conforms to morphology similarities displayed in control 1, suggesting this resistant subline is not affected by the volume of solvent used in the addition of compound. The qualitative assessment of this resistant subline observes an increase in uptake of compound **11** when comparing to the previous cell/sublines, although overall the confocal image would suggest there is greater uptake seen in compound **12**.

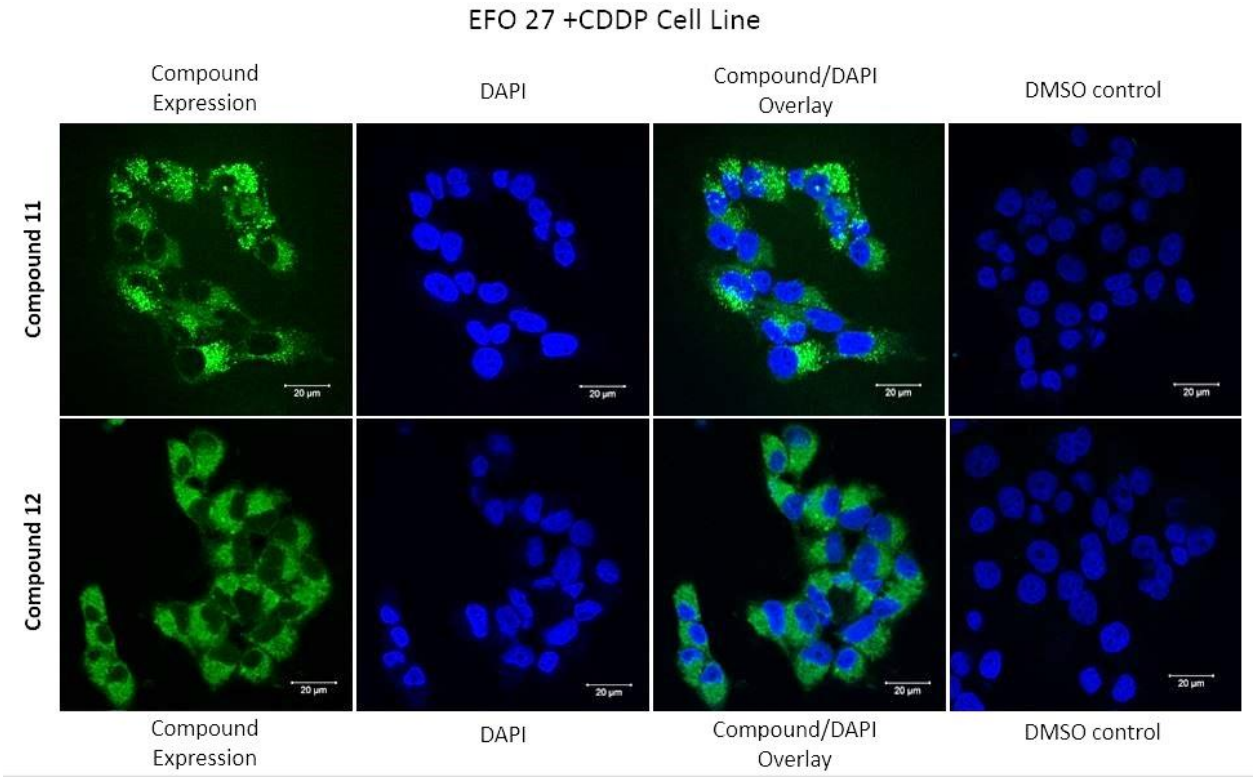

Figure 29. EFO-27 +CDDP subline subject to compound 11 and compound 12 dosed at the IC50 concentrations achieved via MTT assays.

4.4 Discussion

Evaluation of the iridium complexes **11** and **12** through 2D confocal microscopy achieved the unveiling of additional qualitative data to complement chapter 3. Throughout the images in chapter 4.3, all negative controls confirm that the fluorescence observed in the complete cell images were true to the compounds excitation and not due to non-specific staining. These images also imply both compound **11** and **12** to be primarily localised to the cytoplasm, suggesting either compound has not passed the outer nuclear membrane in all parental and resistant cell lines. Although we must consider that due to the fact these images are 2D we cannot guarantee there may not be small localised areas of either compound within the nucleus. This would require further analysis of the cells through methods involving 3D imaging to observe in-depth analysis into the nuclei compartments.[76]

When relating the intensity of fluorescence in the confocal images to the MTT data collected in chapter 3.5.1 similarities can be observed and considered as a qualitative tool. Whilst comparing IC50 values between the iridium complexes against all parental and resistant cell lines, it is noted that the guanidine variant compound **12** has greater dose sensitivity when comparing to the thiourea bearing compound **11**. The confocal images somewhat support the higher dose sensitivity, with an increase of fluorescence emission and greater distribution of compound **12** within all cell lines suggesting this iridium derivative has greater efficiency/potency.

Observed mainly in both EFO-27 parental cell line and cisplatin resistant subline dosed with compound **11**, are localised areas of compound appearing as intense fluorescent dots. Whilst further analysis would be required to depict what may cause these areas, it may be possible the cells are potentially preparing/packaging the compound for further use.

Confocal microscopy was a useful tool in which we could observe the uptake of the iridium complexes within the cell lines and make comparisons to MTT data, but it must be considered that prolonged exposure to the confocal microscopes laser can cause potential photobleaching, and fluorescence saturation, altering the exposure rates of the iridium complexes.[77,78]

Chapter 5: General Discussions and Outlook

5.1 General discussion and conclusions

Firstly, within chapter 2 14 compounds were successfully synthesised some of which being novel structures to be screened against a panel of ovarian cancer cell lines. This included 6 derivatives of thiourea, 4 derivatives of guanidine, and an additional 4 compounds supplied by Barbora Balonova as part of her research towards OLED technology,[82] 2 compounds of which being iridium complexes. Due to time pressures the synthesis methods could not be optimised with some thiourea and guanidine derivatives achieving yields as low as 15% during their final synthesis steps. Although some low yields were collected, both sets of derivatives were successfully characterised through ^{1}H NMR (400MHz), ^{13}C NMR (125MHz), Mass Spectrometry, Elemental Analysis and Melting Point analysis.

In Chapter 3, the compounds synthesised within the previous chapter were screened via an MTT cell viability assay against a panel of human ovarian cancer cell lines; EFO-21, EFO-27 and COLO-704 were all examined in their parental cell line and cisplatin resistance subline variants. Apart from the starting compound (**1**) which displayed high error margins, all the compounds displayed promising results from the viability assay with low error margins and dose strengths required to achieve IC50 values ranging from 0.8-35µM. The most efficient data was achieved in a mix of thiourea and guanidine derivatives including compounds **2**, **3**, **5**, **12** and **14** achieving successful IC50 concentrations below a 10 µM dose in both parental lines and cisplatin resistant sublines and should be considered for further studies.

Chapter 4 allowed us to observe the uptake of both iridium complexes (compound **11** and **12**) within the parental lines and cisplatin resistant sublines of EFO-21 and EFO-27. We were able to harness the fluorescence properties of each complex whilst also collecting qualitative data which complemented the MTT analysis in the previous chapter. It was found that the compounds were primarily localised to the cytoplasm of all cell lines, whilst also noting a higher fluorescence activity of compound **12** which also had a more successful low dose response within the cell viability assay when comparing to compound **11**.

To conclude, the investigated thiourea and guanidine derivatives uncovered promising low dose responses in the early research stages of human *in vitro* cell assays, with the data collected providing a start to new potential therapeutic pathways in the battle against cancer resistant ovarian cell lines.

5.2 Future Work

Due to time constraints within this project we were unable to optimise the synthesis of our derivatives resulting in low yields of some thioureas and guanidines, being an area to improve to maximise purity and efficiency of the synthesis methods. To further understand the effects that these compounds have on human ovarian cancer cells, carrying out an assay such as a Western Blot pre and post dosing the cells with each compound, may reveal possible protein targeting and assist in understanding the mechanism of action for these structures. Furthering from this, pharmacokinetic and pharmacodynamics studies of our compounds would give an insight into the possible *in vivo* impact these structures may have and potential barriers they may be presented with.

To further the confocal analysis of cell lines EFO-21 PTL and EFO-27 PTL dosed with both iridium complexes, it would be beneficial to include observations of the uptake difference between various compound concentrations. Alongside the IC50 value it would be constructive to include the IC90 values which would select for the more resistant cells, but also the IC10 concentration to select for those cells which would be under less stress. Additionally, 3D imaging methods would complement the 2D imaging to observe the spread of compound throughout the cell, and differentiate between any variations in compound density throughout all regions of the cell.

In the final weeks of this project, we conducted antibiotic susceptibility assays using wild type E. coli cells dosed with all 14 compounds to determine potential antimicrobial effects. Unfortunately, the data was inconclusive but should be considered for retesting with an optimised method to compliment the research so far.

5.3 References:

1. Schroeder, D,C. (1954) 'Thioureas', Research Department, Ciba Pharmaceutical Products, Inc., Summit, New Jersey, pp. 181-221.

2. GIP, L. (1975) 'Urea Creams in the Treatment of Dry Skin and Hand Dermatitis', *International Journal of Dermatology*, 14(6), pp. 442–444.

3. Vig, R., Mao, C., Venkatachalam, T. K., Tuel-Ahlgren, L., Sudbeck, E. A., & Uckun, F. M. (1998) 'Rational design and synthesis of phenethyl-5-bromopyridyl thiourea derivatives as potent non-nucleoside inhibitors of HIV reverse transcriptase', *Bioorganic & Medicinal Chemistry*, 6(10), pp. 1789–1797.

4. Gupta, D., Soman, R. and Dev, S. (1982) 'Thiourea, A convenient reagent for the reductive cleavage of olefin ozonolysis products', *Tetrahedron*, 38(20), pp. 3013–3018.

5. Press, C. (2011) 'Invited in Physiological Perspectives Zoology Roles of Urea in Vertebrates Functional', *Synthesis*, 65(2), pp. 243–267.

6. Li, H-Q., Lv, P-C., Yan, T., Zhu, H-L. (2009) 'Urea Derivatives as Anticancer Agents', *Anti-Cancer Agents in Medicinal Chemistry*, 9(4), pp. 471–480.

7. Shakeel, A. (2016) 'Thiourea Derivatives in Drug Design and Medicinal Chemistry: A Short Review', *Journal of Drug Design and Medicinal Chemistry*, 2(1), p. 10.

8. Liu, W., Zhou, J., Zhang, T., Zhu, H., Qian, H., Zhang, H., Huang, W., Gust, G. (2012) 'Design and synthesis of thiourea derivatives containing a benzo[5,6]cyclohepta[1,2-b]pyridine moiety as potential antitumor and anti-inflammatory agents', *Bioorganic and Medicinal Chemistry Letters*. Elsevier Ltd, 22(8), pp. 2701–2704.

9. Taylor, C, W., Alberts, D, S., Peng, Y-M., McCloskey, T, M., Matzner, M., Roe, D, J., Plezia, P, M., Grindey, G, B., Hamilton, M., Seitz, D. (1992) 'Antitumor Activity and Clinical Pharmacology of Sulofenur in Ovarian Cancer', *Journal of the National Cancer Institute*, 84 (23), pp. 1798-1802.

10. O'Brien, M. E., Hardy, J., Tan, S., Walling, J., Peters, B., Hatty, S., Wiltshaw, E. (1992) 'A phase II study of sulofenur, a novel sulfonylurea, in recurrent epithelial ovarian cancer.', *Cancer chemotherapy and pharmacology*, 30(3), pp. 245–248.

11. Gonzalez, V. M., Fuertes, M, A., Alonso, C., Perez, J, M. (2001) 'Is cisplatin-induced cell death always produced by apoptosis?', *Molecular pharmacology*, 59(4), pp. 657–663.

12. Alderden, R. A., Hall, M. D., Hambley, T. W. (2006) 'The Discovery and Development of Cisplatin', *Journal of Chemical Education*, 83(5), p. 728.

13. Dasari, S., Tchounwou, P, B. (2015) 'Cisplatin in cancer therapy: molecular mechanisms of action', *Eur J Pharmacol*, 5(0), pp. 364–378.

14. De Jongh, F. E., Van Veen, R, N., Veltman, S, J., De Wit, R., Can Der Burg, M, E, L., van Den Bent, M, J., Planting, A, S., Graveland, W, J., Stoter, G., Verweij, J. (2003) 'Weekly high-dose cisplatin is a feasible treatment option: Analysis on prognostic factors for toxicity in 400 patients', *British Journal of Cancer*, 88(8), pp. 1199–1206.

15. Florea, A-M., Büsselberg, D. (2011) 'Cisplatin as an Anti-Tumor Drug: Cellular Mechanisms of Activity, Drug Resistance and Induced Side Effects', *Cancers*, 3(4), pp. 1351–1371.

16. Godwin, A. K., Meister, A., O'Dwyer, P, J., Huang, C, S., Hamilton, T, C., Anderson, M, E. (1992) 'High resistance to cisplatin in human ovarian cancer cell lines is associated with marked increase of glutathione synthesis.', *Proceedings of the National Academy of Sciences of the United States of America*, 89(7), pp. 3070–3074.

17. Lai, G-M., Ozols, R, F., Smyth, J, F., Young, R, C., Hamilton, T, C. (1988) 'Enhanced DNA repair and resistance to Cisplatin in human ovarian cancer', *Biochemical Pharmacology*, 37(24), pp. 4597–1600.

18. Cepeda, V., Fuertes, M, A., Castilla, J., Alonso, C., Quevedo, C., Perez, J, M. (2007) 'Biochemical Mechanisms of Cisplatin Cytotoxicity', *Anti-Cancer Agents in Medicinal Chemistry*, 7(1), pp. 3–18.

19. Riman, T., Persson, I., Nilsson, S. (1998) 'Hormonal aspects of epithelial ovarian cancer: review of epidemiological evidence', *Clin.Endocrinol.(Oxf)*, 49(6), pp. 695–707.

20. Moyer, V, A. (2012) 'Screening for Ovarian Cancer: U.S. Preventive Services Task Force Reaffirmation Recommendation Statement', *Annals of Internal Medicine*, 157(12), pp. 1–6.

21. Jelovac, D., Armstrong, D, K. (2011) 'Recent progress in the diagnosis and treatment of ovarian cancer', *CA Cancer J Clin*, 61(3), pp. 183–203.

22. Gras, M., Therrien, B., Suss-Fink, G., Casini, A., Edafe, F., Dyson, P, J. (2010) 'Anticancer activity of new organo-ruthenium, rhodium and iridium complexes containing the 2-(pyridine-2-yl)thiazole N,N-chelating ligand', *Journal of Organometallic Chemistry*. Elsevier B.V., 695(8), pp. 1119–1125.

23. Liu, Z., Salassa, L., Habtemarim, A., Pizarro, A, M., Clarkson, G, J., Sadler, P, J. (2011) 'Contrasting reactivity and cancer cell cytotoxicity of isoelectronic organometallic iridium(III) complexes', *Inorganic Chemistry*, 50(12), pp. 5777–5783.

24. Liu, Z., Romero-Canelon, I., Habtemariam, A., Clarkson, G, J., Sadler, P, J. (2014) 'Potent half-sandwich iridium(III) anticancer complexes containing C^N-chelated and pyridine ligands', *Organometallics*, 33(19), pp. 5324–5333.

25. Frezza, M., Hindo, S., Chen, D., Davenport, A., Schmitt., Tomco, D., Dou, Q, P. (2010) 'Novel Metals and Metal Complexes as Platforms for Cancer Therapy', *Current Pharmaceutical Design*, 16(16), pp. 1813–1825.

26. Said, M., Badshah, A., Shah, N. A., Khan, H., Murtaza, G., Vabre, B., Zargarian, D., Khan, M. R. (2013). 'Antitumor, antioxidant and antimicrobial studies of substituted pyridylguanidines', *Molecules*, 18(9), pp. 10378–10396.

27. Van Pilsum, J. F. and Wolin, E. A. (1958) 'Guanidinium compounds in blood and urine of patients suffering from muscle disorders', *The Journal of Laboratory and Clinical Medicine*. Elsevier, 51(2), pp. 219–223.

28. Weber, C. J. (1928) 'Guanidine Bases in Urine', *The Journal of Biological Chemistry*. 78, pp. 465-473.

29. Ishikawa, T., Isobe, T. (2002) 'Modified guanidines as chiral auxiliaries.', *Chemistry (Weinheim an der Bergstrasse, Germany)*, 8(3), pp. 552–557.

30. Rightsel, W. A., Dice. J. R., McAlpine. R. J., Timm. E. A., McLean Jr. I. W., Dixon. G. J., Schabel Jr. F. M. (1961) 'Antiviral Effect of Guanidine', *Science*, 134(3478), pp. 558-559.

31. Huang, W., Sun, X. (2000) 'Adhesive properties of soy proteins modified by urea and guanidine hydrochloride', *Journal of the American Oil Chemists' Society*, 77(1), pp. 101–104.

32. Sączewski, F., Balewski, Ł. (2013) 'Biological activities of guanidine compounds, 2008 – 2012 update', *Expert Opinion on Therapeutic Patents*, 23(8), pp. 965–995.

33. Editorial, N. (2006) 'Biology and brimstone' (2006) *Nature Chemical Biology*, 2(4), p. 169.

34. Huxtable, R. J. (1986) 'The Chemistry of Sulfur', in *Biochemistry of Sulfur*. Boston, MA: Springer US, pp. 1–9.

35. Kice, J. L. (1968) 'Electrophilic and Nucleophilic Catalysis of the Scission of the Sulfur-Sulfur Bond', *Accounts of Chemical Research*, 1(2), pp. 58–64.

36. Sawant, S., Youssef, D., Mayer, A., Sylvester, P., Wali, V., Arant, M., El Sayed, K. (2006) 'Anticancer and anti-inflammatory sulfur-containing semisynthetic derivatives of sarcophine.', *Chemical & pharmaceutical bulletin*, 54(8), pp. 1119–23.

37. Tokala, R., Bale, S., Janrao, I. P., Vennela, A., Kumar, N. P., Senwar, K. R., Shankaraiah, N. (2018) 'Synthesis of 1,2,4-triazole-linked urea/thiourea conjugates as cytotoxic and apoptosis inducing agents', *Bioorganic and Medicinal Chemistry Letters*. Elsevier Ltd, 28(10), pp. 1919–1924.

38. Gonçalves, I., Azambuja, G., Kawano, D., Eifler-lima, V. (2017) Thioureas as Building Blocks for Generation of Heterocycles and Compounds with Pharmacological Activity: a mini review, *Mini-Reviews in Organic Chemistry*, 15(1), pp. 28-35.

39. Liao, P., Hu, S-Q., Zhang, H., Xu, L-B., Liu, J. Z., He, B., Liao, S, G., Li, Y. J. (2018) 'Study on anti-proliferative activity in cancer cells and preliminary structure–activity relationship of pseudo-peptide chiral thioureas', *Bulletin of the Korean Chemical Society*, 39(3), pp. 300–304.

40. Pingaew, R., Sinthupoom, N., Mandi, P., Prachayasittikul, V., Cherdtrakulkiat, R., Prachayasittikul, S., Ruchirawat, S., Prachayasittikul, V. (2017) 'Synthesis, biological evaluation and in silico study of bis-thiourea derivatives as anticancer, antimalarial and antimicrobial agents', *Medicinal Chemistry Research*. Springer US, 26(12), pp. 3136–3148.

41. Hu, H., Lin, C., Ao, M., Ji, Y., Tang, B., Zhou, X., Fang, M., Zeng, J., Wu, Z. (2017) 'Synthesis and biological evaluation of 1-(2-(adamantane-1-yl)-1: H -indol-5-yl)-3-substituted urea/thiourea derivatives as anticancer agents', *RSC Advances*. Royal Society of Chemistry, 7(81), pp. 51640–51651.

42. Durant, G. J. (1985) 'Guanidine derivatives acting at histaminergic receptors', *Chemical Society Reviews*, 14(4), pp. 375–398.

43. Blessing, T., Remy, J. S., Behr, J. P., Ehr, B. (1998) 'Monomolecular collapse of plasmid DNA into stable virus-like particles.', *Proceedings of the National Academy of Sciences of the United States of America*, 95(4), pp. 1427–31.

44. Blanco, F., Kelly, B., Sánchez-Sanz, G., Trujillo, C., Alkorta, I., Elguero, J., Rozas, I. (2013) 'Non-covalent interactions: Complexes of guanidinium with DNA and RNA nucleobases', *Journal of Physical Chemistry B*, 117(39), pp. 11608–11616.

45. Berlinck, R. G. S., Burtoloso, A, C, B., Kossuga, M, H. (2008) 'The chemistry and biology of organic guanidine derivatives', *Natural Product Reports*, 29(12), pp. 1382–1406.

46. Qian, Y., Zhang, H-J., Lv, P-C., Zhu, H-L. (2017) 'Synthesis, molecular modelling and biological evaluation of guanidine derivatives as novel antitubulin agents', *Bioorganic and Medicinal Chemistry*. Elsevier Ltd, 25(15), pp. 4088–4099.

47. Legin, A. A., Jakupec, M. A., Bokach, N. A., Tyan, M. R., Kukushkin, V. Y., & Keppler, B. K. (2014) 'Guanidine platinum(II) complexes: Synthesis, in vitro antitumor activity, and DNA interactions', *Journal of Inorganic Biochemistry*. The Authors, 133, pp. 33–39.

48. Thériault, B. L., Nachtigal, M. W. (2011) 'Human ovarian cancer cell morphology, motility, and proliferation are differentially influenced by autocrine TGFβ superfamily signalling', *Cancer Letters*, 313(1), pp. 108–121.

49. Cross. S. E., Jin. Y-S., Rao. J., Gimzewski. J. K. (2007) 'Nanomechanical analysis of cells from cancer patients', *Nature Nanotechnology*, 2, pp. 780-783.

50. Bhadriraju, K., Hansen, L. K. (2002) 'Extracellular matrix- and cytoskeleton-dependent changes in cell shape and stiffness', *Experimental Cell Research*, 278(1), pp. 92–100.

51. Kelderman, S., Schumacher, T, N, M., Haanen, J, B, A, G. (2014) 'Acquired and intrinsic resistance in cancer immunotherapy', *Molecular Oncology*. Elsevier B.V, 8(6), pp. 1132–1139.

52. Agarwal, R., Kaye, S. B. (2003) 'Ovarian cancer: Strategies for overcoming resistance to chemotherapy', *Nature Reviews Cancer*, 3(7), pp. 502–516.

53. Ai, Z., Lu, Y., Qiu, S., Fan, Z. (2016) 'Overcoming cisplatin resistance of ovarian cancer cells by targeting HIF-1-regulated cancer metabolism', *Cancer Letters*. Elsevier Ireland Ltd, 373(1), pp. 36–44.

54. Krieger, M. L., Eckstein, N., Schneider, V., Koch, M., Royer, H. D., Jaehde, U., Bendas, G. (2010) 'Overcoming cisplatin resistance of ovarian cancer cells by targeted liposomes in vitro', *International Journal of Pharmaceutics*. Elsevier B.V., 389(1–2), pp. 10–17.

55. Weinburg, R. A. (2014) The Biology of Cancer. 2nd Edition. New York: Garland Science.

56. Cao, Y., Depinho, R. A., Ernst, M., Vousden, K. (2011) 'Cancer research: Past, present and future', *Nature Reviews Cancer*. Nature Publishing Group, 11(10), pp. 749–754.

57. Lawrence, W., Lopez, M. J. (2005) 'Radical surgery for cancer: A historical perspective', *Surgical Oncology Clinics of North America*, 14(3 SPEC. ISS.), pp. 441–446.

58. Zhang, J., Campbell, R. E., Ting, A. Y., Tsien, R. Y. (2002) 'Creating new fluorescent probes for cell biology', *Nature Reviews Molecular Cell Biology*, 3(12), pp. 906–918.

59. Valeur, B., Berberan-Santos, M. N. (2012) *Molecular Fluorescence: Principles and Applications.* 2nd Edn. Weinheim Germany: Wiley-VCH Verlay & Co. KGaA.

60. Ulrich, G., Ziessel, R., Harriman, A. (2008) 'The chemistry of fluorescent bodipy dyes: Versatility unsurpassed', *Angewandte Chemie - International Edition*, 47(7), pp. 1184–1201.

61. Loudet, A., Burgess, K. (2007) 'BODIPY dyes and their derivatives', *Chemical Reviews*, 107(11), pp. 4891–4932.

62. Wang, F., Zhu, Y., Zhou, L., Pan, L., Cui, Z., Fei, Q., Luo, S., Pan, D., Huang, Q., Wang, R., Zhao, C., Tian, H., Fan, C. (2015) 'Fluorescent in Situ Targeting Probes for Rapid Imaging of Ovarian-Cancer-Specific γ-Glutamyltranspeptidase', *Angewandte Chemie - International Edition*, 54(25), pp. 7349–7353.

63. Boens, N., Leen, V., Dehaen, W. (2012) 'Fluorescent indicators based on BODIPY', *Chemical Society Reviews*, 41(3), pp. 1130–1172.

64. Zheng, Y., He, L., Zhang, D. Y., Tan, C. P., Ji, L. N., Mao, Z. W. (2017) 'Mixed-ligand iridium(III) complexes as photodynamic anticancer agents', *Dalton Transactions*. Royal Society of Chemistry, 46(34), pp. 11395–11407.
65. Gerlier, D., Thomasset, N. (1986) 'Use of MTT colorimetric assay to measure cell activation', *Journal of Immunological Methods*, 94(1–2), pp. 57–63.

66. Zhang, P., Chiu, C. K. C., Huang, H., Lam, Y. P. Y., Habtemariam, A., Malcomson, T., Sadler, P. J. (2017) 'Organoiridium Photosensitizers Induce Specific Oxidative Attack on Proteins within Cancer Cells', *Angewandte Chemie - International Edition*, 56(47), pp. 14898–14902.

67. Ren, X., Deaton, J. C. (2009) *Phosphorescent Iridium Complexes*. United States Patent and Trademark Office. Patent No. 7473477B2. Available at: https://patents.google.com/patent/US7473477B2/en (Accessed: 09-OCT-18).

68. Ulbricht, C., Beyer, B., Friebe, C., Winter, A., & Schubert, U. S. (2009) 'Recent developments in the application of phosphorescent iridium(III) complex systems', *Advanced Materials*, 21(44), pp. 4418–4441.

69. Dobrucki, J. W., Kubitscheck, U. (2017) 'Fluorescence Microscopy', *Fluorescence Microscopy: From Principles to Biological Applications: Second Edition*, 2(12), pp. 85–132.

70. Mukherjee, T., Ganzmann, C., Bhuvanesh, N., Gladysz, J. A. (2014) 'Syntheses of enantiopure bifunctional 2-guanidinobenzimidazole cyclopentadienyl ruthenium complexes: Highly enantioselective organometallic hydrogen bond donor catalysts for carbon-carbon bond forming reactions', *Organometallics*, 33(23), pp. 6723–6737.

71. Blight, B. A., Hunter, C. A., Leigh, D. A., McNab, H., Thomson, P. I. T. (2011) 'An AAAA-DDDD quadruple hydrogen-bond array', *Nature Chemistry*, 3(3), pp. 244–248.

72. Walker, J.M. (2013) Mammalian Cell Viability, Methods and Protocol, *Journal of Chemical Information and Modelling*, 53.

73. Meerloo, J. V, Kaspers, G. J. L., Cloos, J. (2011) 'Cell Sensitivity Assays: The MTT Assay Johan', *Cancer Cell Culture: Methods in Molecular Biology*, 731(3), pp. 237–245.

74. Morgan, D. M. (1998) 'Tetrazolium (MTT) assay for cellular viability and activity.', *Methods in molecular biology (Clifton, N.J.)*, 79(4), pp. 179–183.

75. Mossman, T. (1983) 'Rapid colorimetric assay for cellular growth and survival: Application to proliferation and cytotoxicity assays', *Journal of Immunological Methods1983*, 65, pp. 55–63.

76. Shiels, C., Adams, N. M., Islam, S. A., Stephens, D. A., Freemont, P. S. (2007) 'Quantitative analysis of cell nucleus organisation', *PLoS Computational Biology*, 3(7), pp. 1161–1168.

77. Pawley, J. B. (2006) *Handbook of Biological Confocal Microscopy*. 3rd Edn. New York: Springer Science & Business Media.

78. Ghauharali, R. I., Brakenhoff, G. J. (2000) 'Fluorescence photobleaching-based image standardization for fluorescence microscopy', *Journal of Microscopy*, 198(2), pp. 88–100.

79. Lidia, Ś., Wiktorska, K., Suchocki, P. (2016) 'The comparison of MTT and CVS assays for the assessment of anticancer agent interactions', *PLoS ONE*, 11(5), pp. 1–17.

80. Riss, T. L., Moravec, R. A., Niles, A. L., Duellman, S., Benink, H. A., Worzella, T. J., & Minor, L. (2013) 'Cell Viability Assays', *Assay Guidance Manual*, 114(8), pp. 785–796.

81. Jaszczyszyn, A. and Gasiorowski, K. (2008) 'Limitations of the MTT Assay in Cell Viability Testing', *Adv Clin Exp Med*, 17(5), pp. 525–529.

82. Balónová, B., Martir, D. R., Clark, E. R., Shepherd, H. J., Zysman-Colman, Eli., Blight, B. A. (2018) 'Influencing the Optoelectronic Properties of a Heteroleptic Iridium Complex by Second-Sphere H-Bonding Interactions', *Inorganic Chemistry*, 57(14), pp. 8581–8587.

83. Chabner, B. A., Roberts, T. G. (2005) 'Chemotherapy and the war on cancer', *Nature Reviews Cancer*, 5(1), pp. 65-72.

84. Bruijnincx, P. C. A., Sadler, P. J. (2008) 'New trends for metal complexes with anticancer activity', '*Current Opinion in Chemical Biology*', 12, pp. 197-206.

85. Raut. S., Kimball. J., Fudala. R., Doan. H., Maliwal. B., Sabnis. N., Lacko. A., Gryczynski. I., Dzyuba. S. V., Gryczynski. Z. (2014) 'A homodimeric BODIPY rotor as a fluorescent viscosity sensor for membrane-mimicking and cellular environments', *Physical Chemistry Chemical Physics*. Royal Society of Chemistry, 16(48), pp. 27037–27042.

86. Rottenfusser. R., Wilson. E. E., Davidson. M. W. (ND) *Education in Microscopy and Digital Imaging*. Available at: http://zeiss-campus.magnet.fsu.edu/articles/basics/fluorescence.html (Accessed: 12 December 2018).

Appendix: Supplementary Information

1H NMR's:

Figure S1. Compound 1:

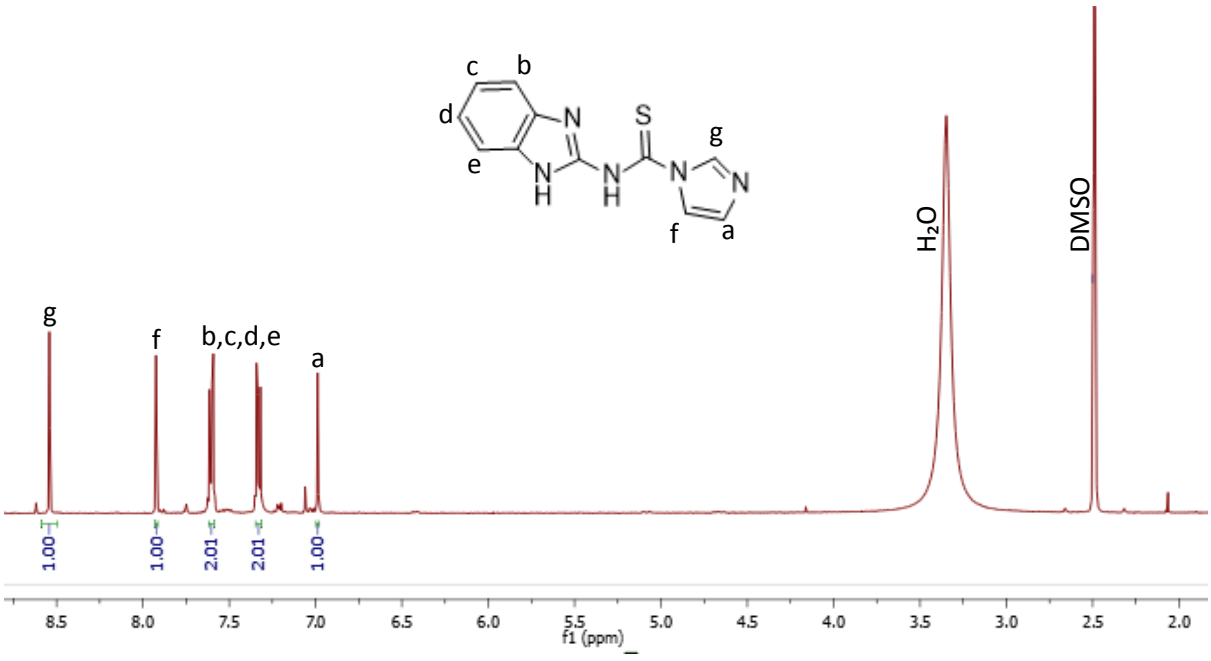

Figure S2. Compound 2:

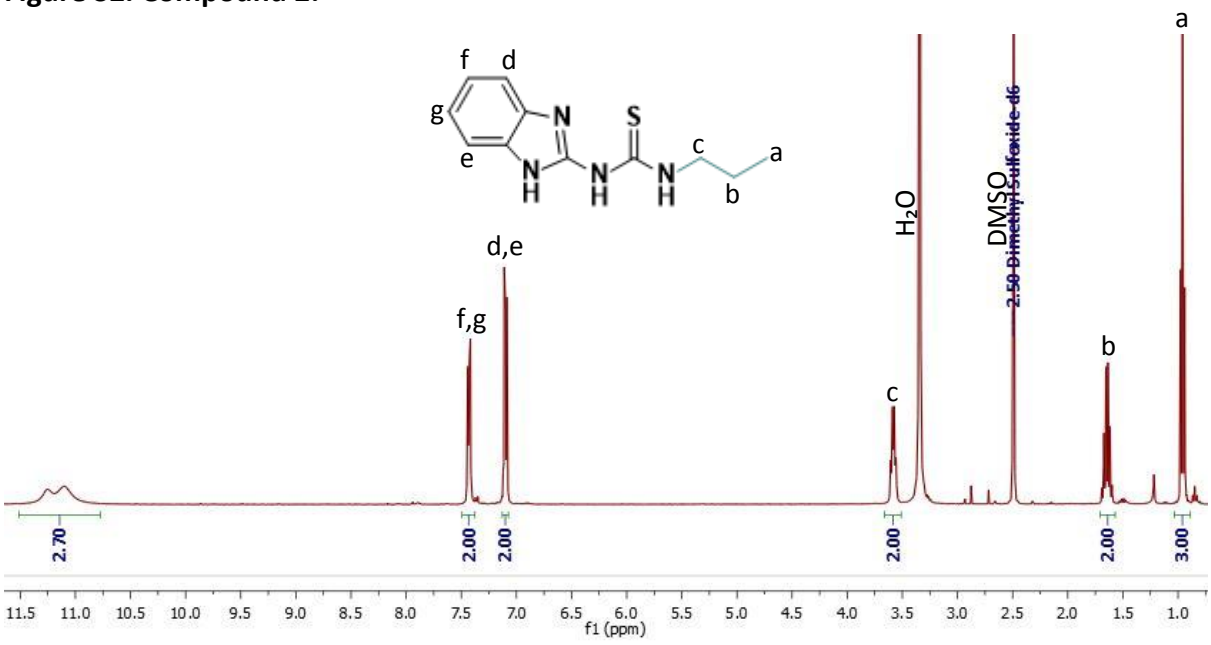

Figure S3. Compound 3:

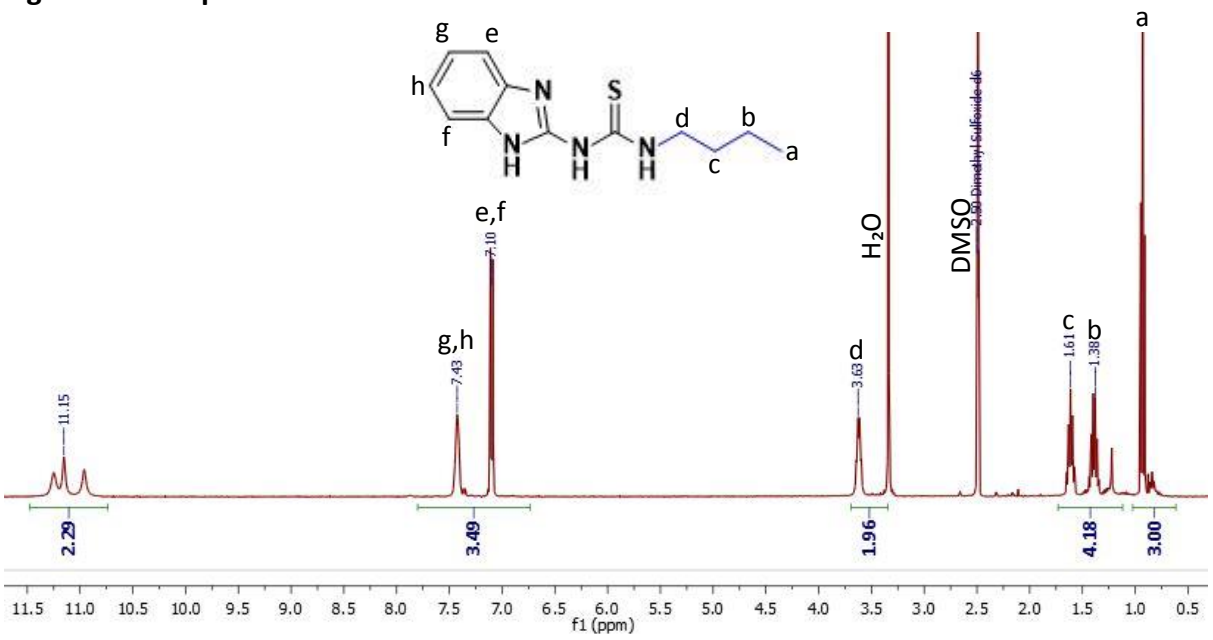

Figure S4. Compound 4:

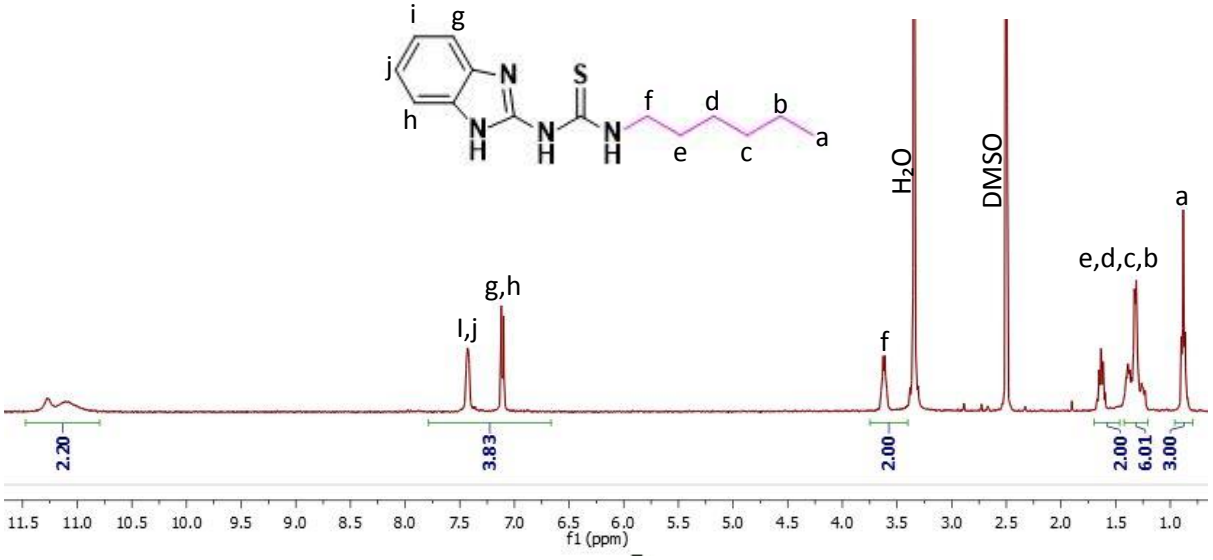

Figure S5. Compound 5:

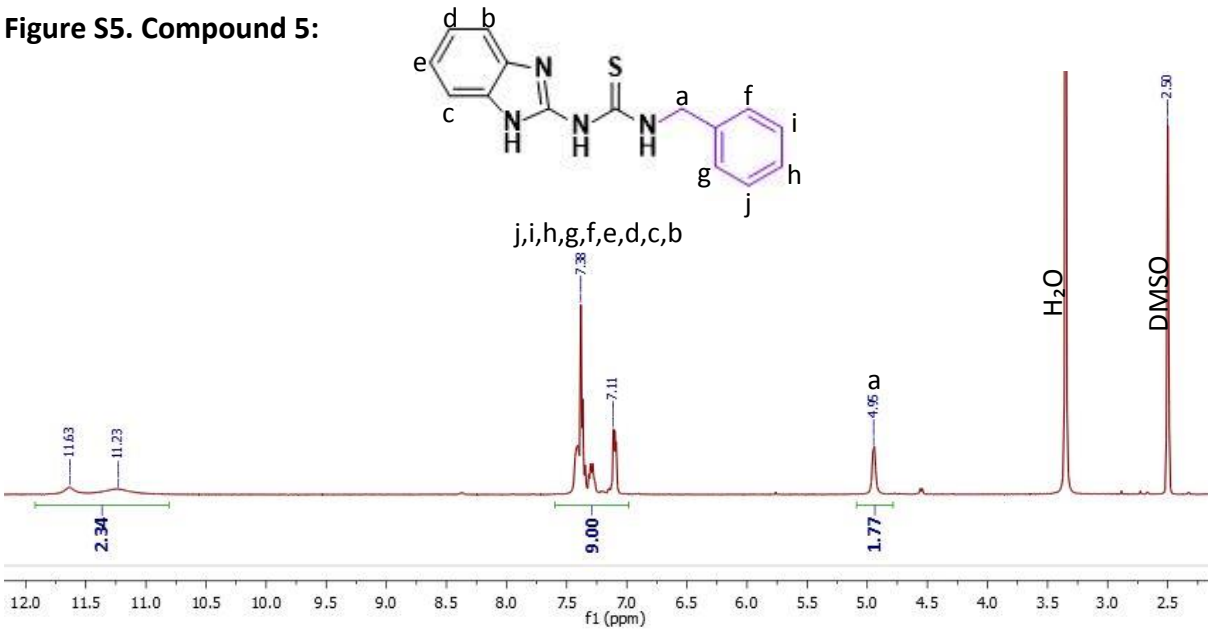

Figure S6. Compound 6:

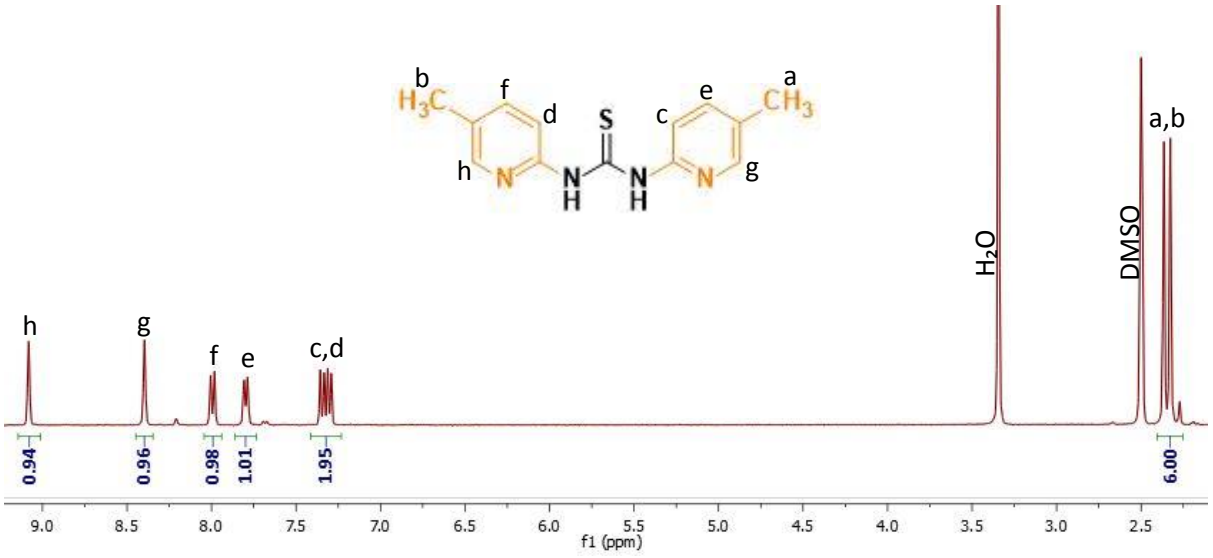

Figure S7. Compound 7:

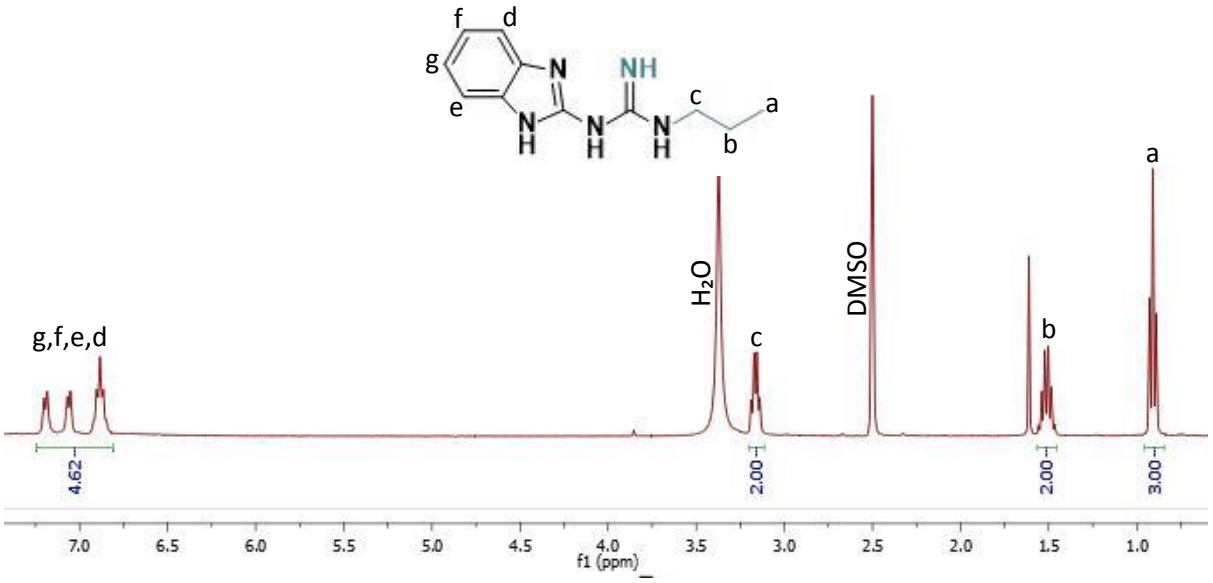

Figure S8. Compound 8:

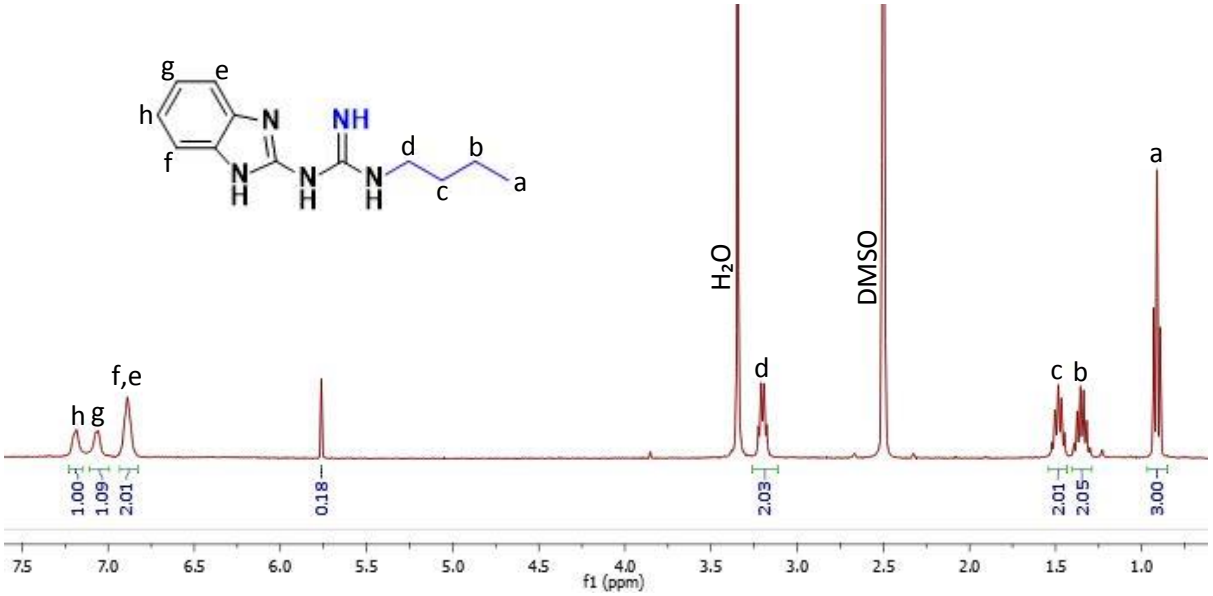

Figure S9. Compound 9:

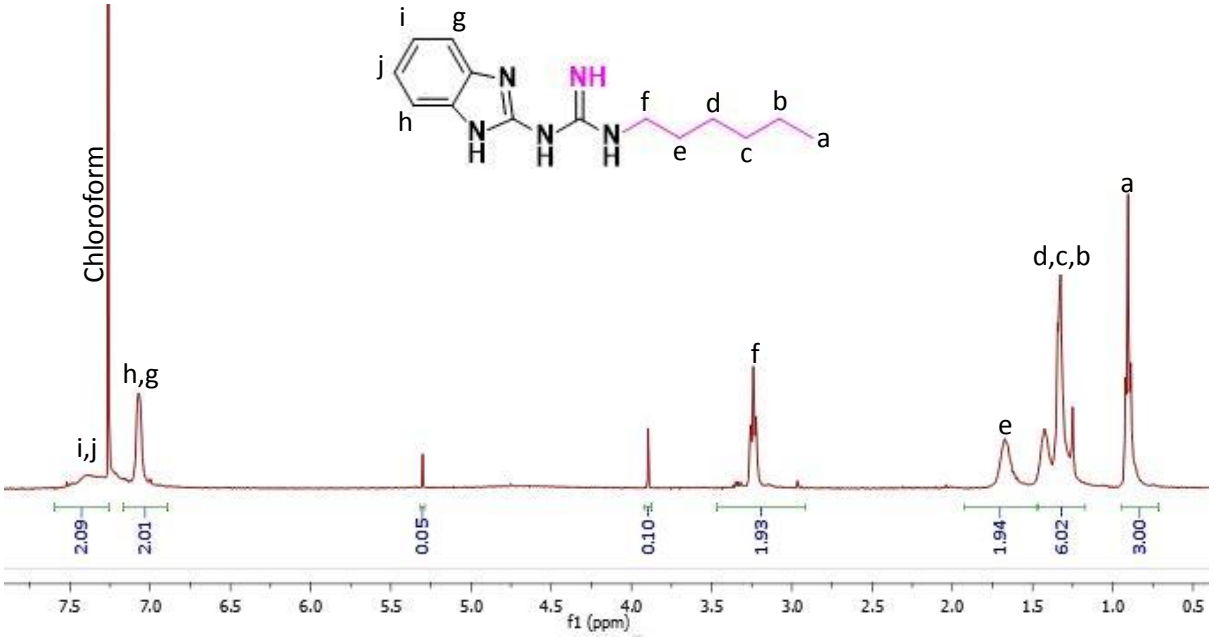

Figure S10. Compound 10:

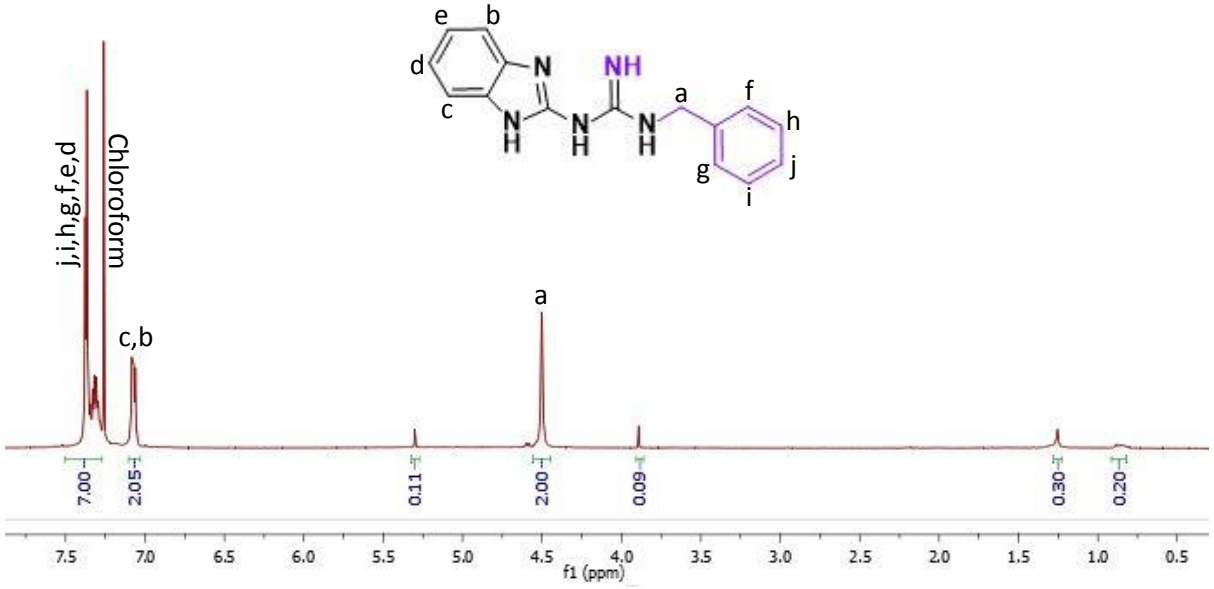

C_{13} NMR:

Figure S11. Compound 1:

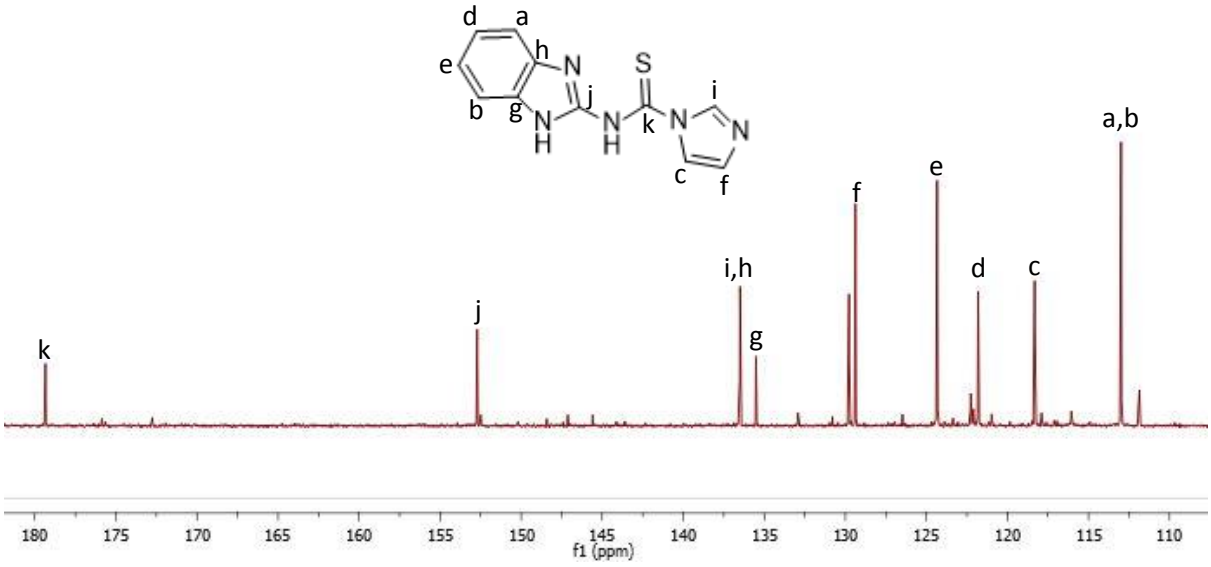

Figure S12. Compound 2:

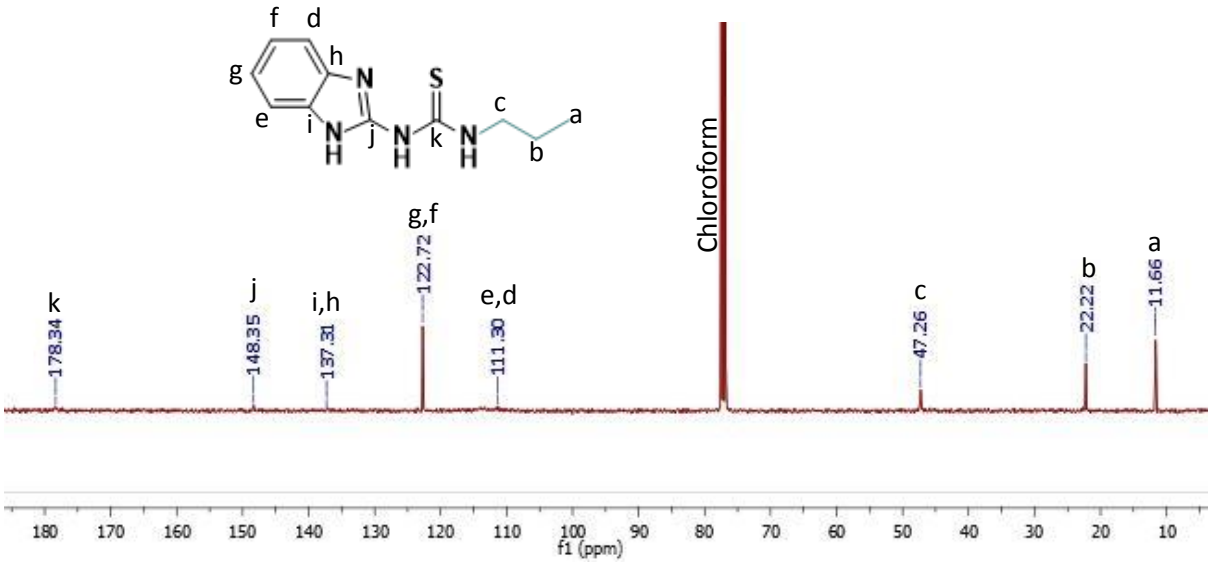

Figure S13. Compound 4:

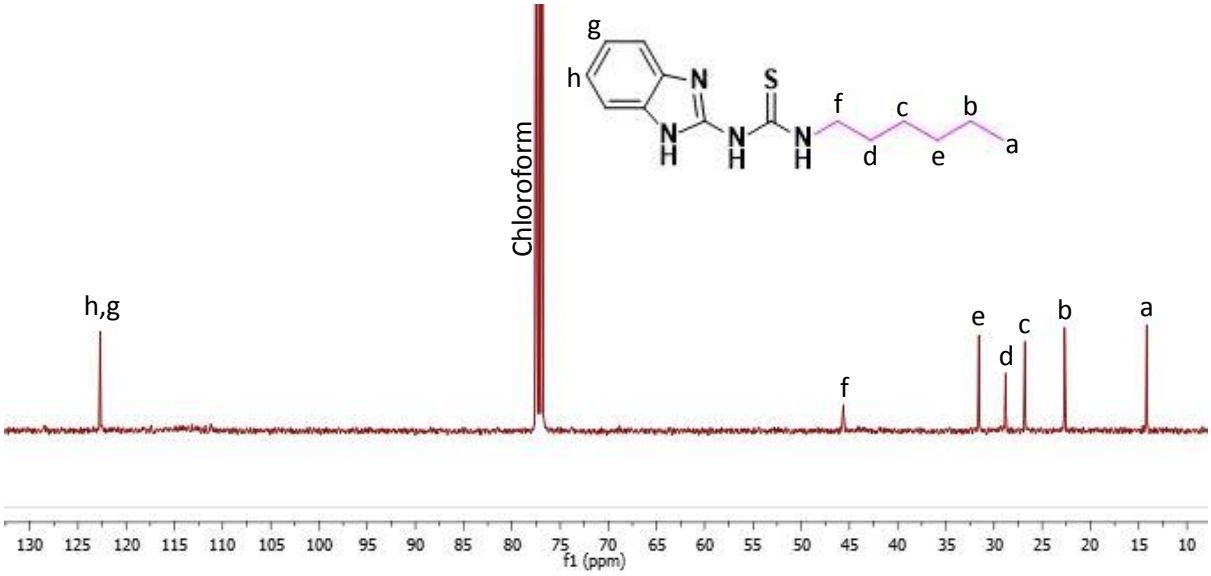

Figure S14. Compound 5:

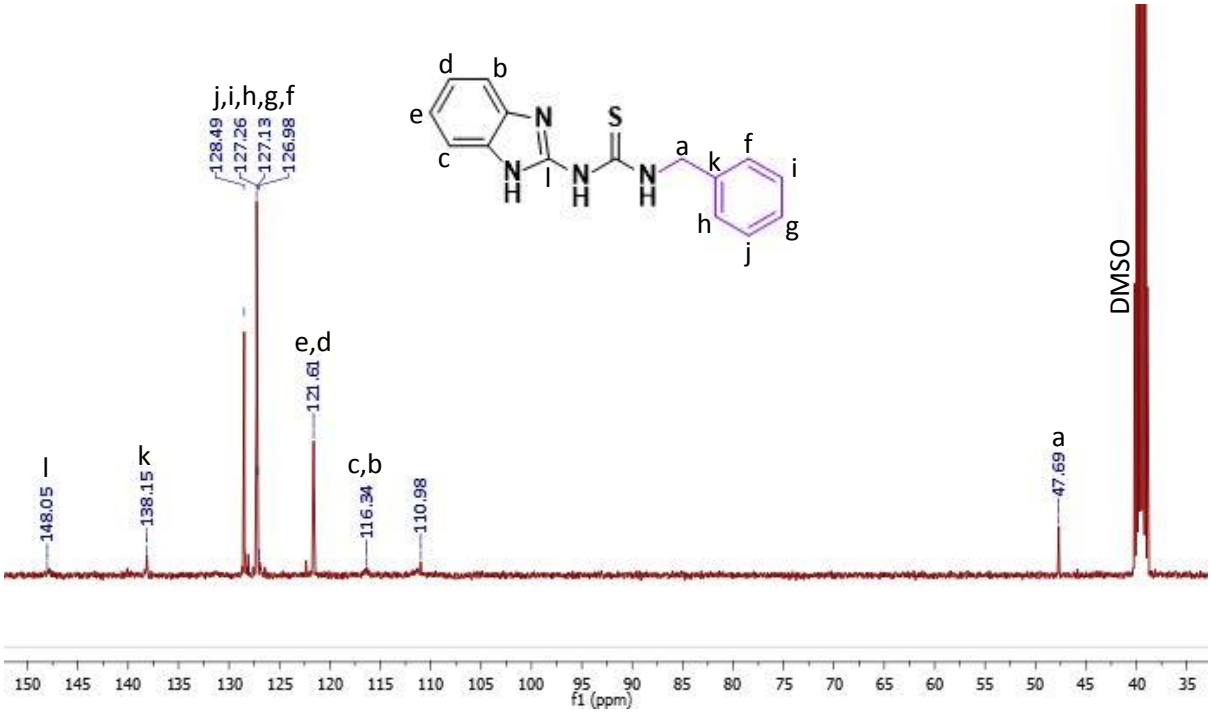

Figure S15. Compound 6:

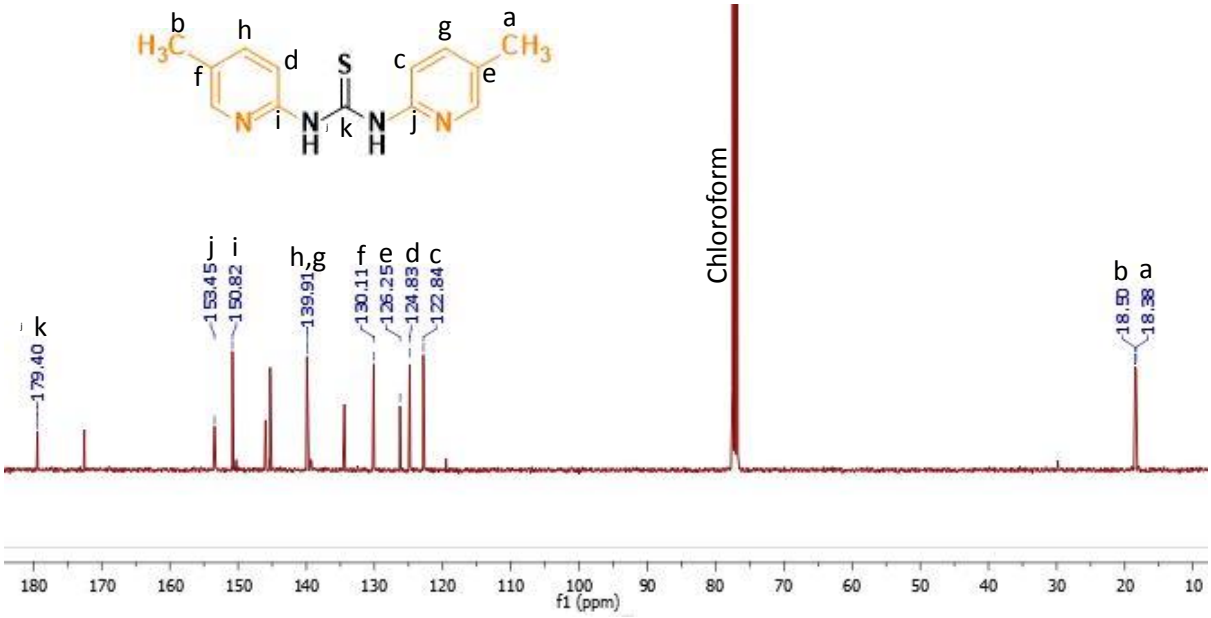

Figure S16. Compound 7:

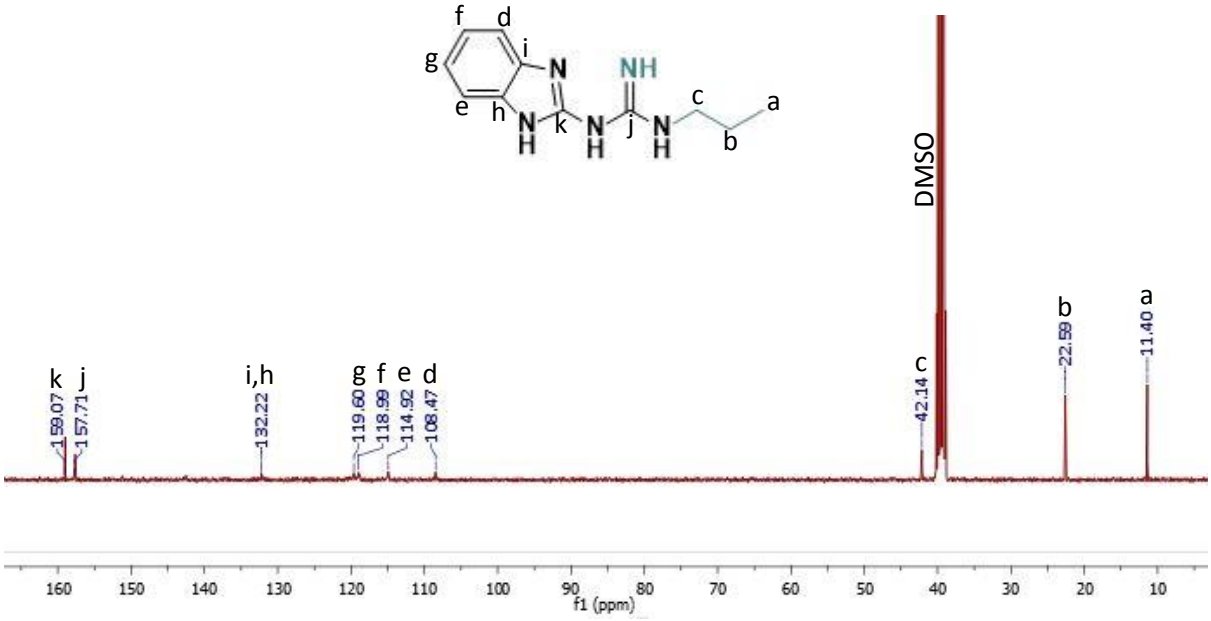

Figure S17. Compound 8:

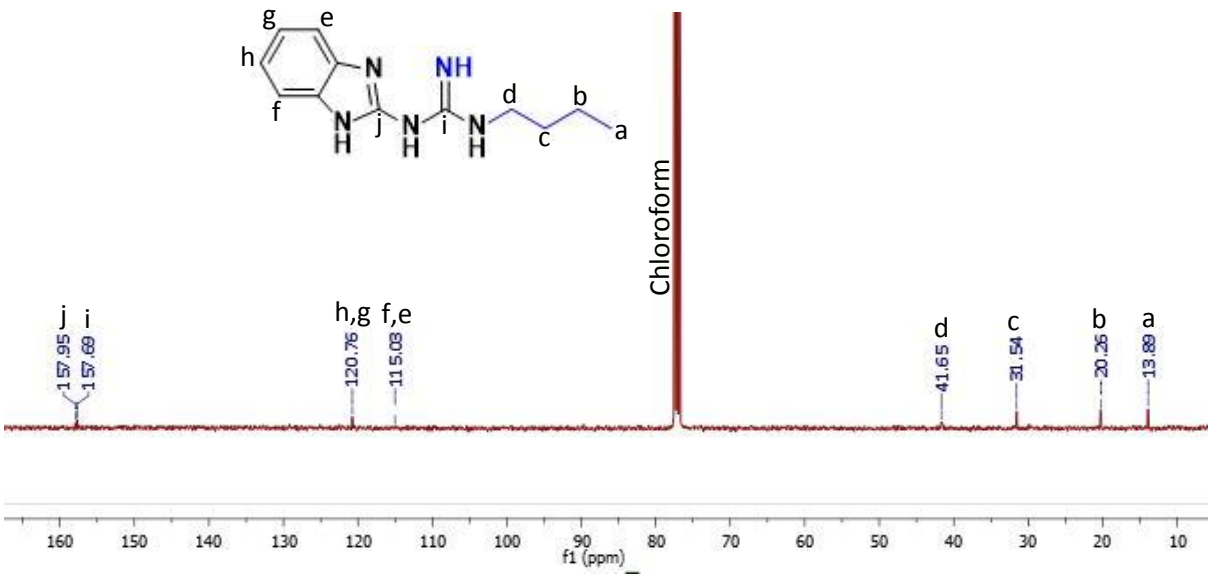

Figure S18. Compound 9:

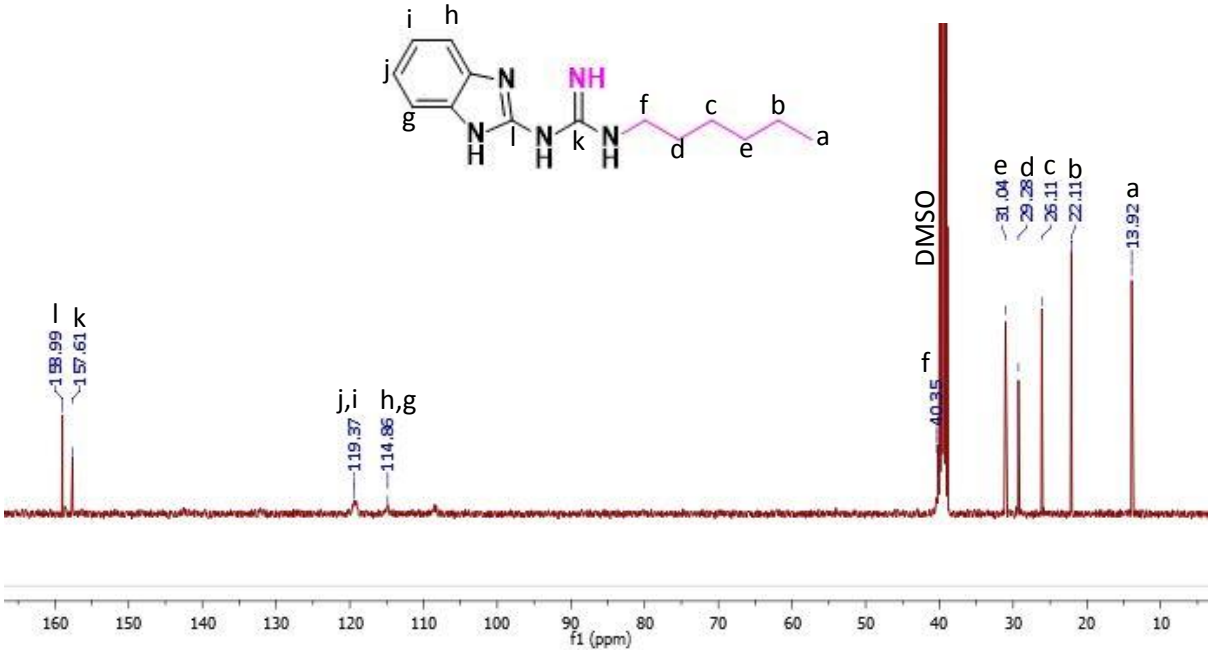

Figure S19. Compound 10: